Top Chain Length for Hook-Up Operations of Floating Offshore Wind Turbines

B.H. Kurstjens

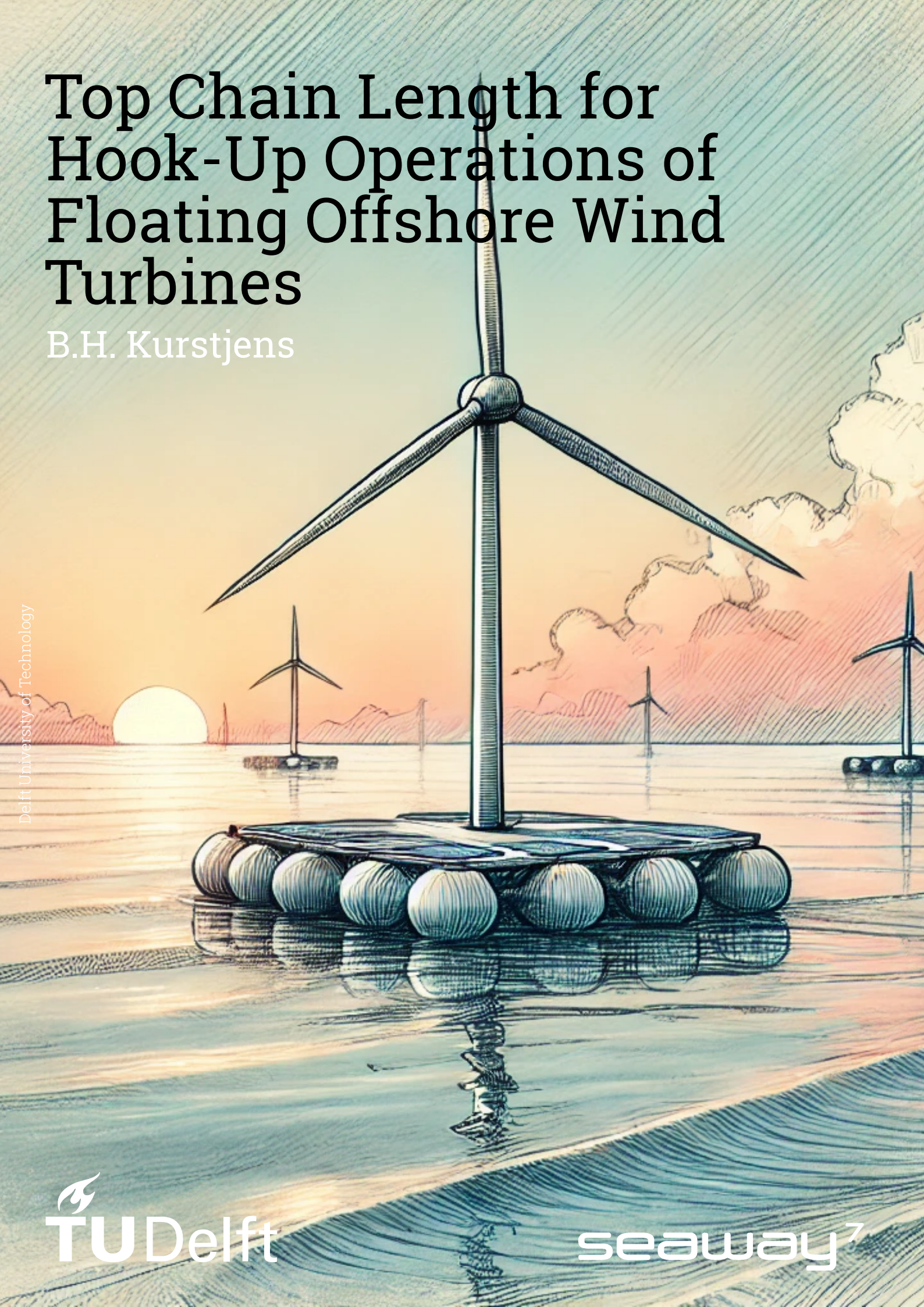

Delft University of Technology

TU Delft

seaway 7

Top Chain Length for Hook-Up Operations of Floating Offshore Wind Turbines

by

B.H. Kurstjens

Student number:	4953584	
Project duration:	April, 2024 – January, 2025	
Faculty:	Faculty of Civil Engineering	
Company:	Seaway7	
Thesis committee:	Dr. Ir. J. O. Colomes,	TU Delft, chair
	Ir. F. C. Lange,	TU Delft, supervisor
	Dr. -Ing. S. Schreier,	TU Delft, supervisor
	BSs. F. van der Heij,	Seaway7, supervisor
	MSc. G.P.A. Smit,	Seaway7, supervisor

TU Delft seaway 7

Preface

This thesis marks the end of my time as a master's student at the Faculty of Civil Engineering and Geosciences at TU Delft. I would like to express my gratitude to my supervisors for their guidance and support throughout this journey, and for giving me the freedom to set my own path during my thesis. Although I initially found myself navigating between the differing interests of TU Delft and Seaway7, the entire process has been an invaluable learning experience.

I would like to thank Frank, Oriol, and Sebastian for their invaluable support and insight. Regular meetings with Frank were particularly helpful in gaining perspective on my work and keeping me sharp whilst I was inside the bubble of my own research. Additionally, the thorough feedback during and after progress meetings encouraged me to adopt a more critical and reflective approach to my thesis.

I would also like to thank Seaway7, as well as Frans and Gerben, for providing me with the opportunity to conduct this research as an internship. My time at Seaway7 offered me new insights into the offshore and wind energy industries, particularly regarding installation operations. I always felt supported, and you were always willing to help with any questions I had. I enjoyed our discussions, which were always insightful and full of learning.

Lastly, I would like to thank my family and girlfriend for their support throughout my journey at TU Delft. They consistently reminded me that, despite the challenges, my efforts are meaningful and worthwhile.

B.H. Kurstjens
Delft, January 2025

Abstract

The growing demand for renewable energy has positioned Floating Offshore Wind Turbines (FOWTs) as a promising solution for harnessing wind energy in deeper waters. Unlike fixed foundation turbines, which are limited to depths of around 50 metres, FOWTs can operate in greater depths. However, this relatively new industry faces numerous challenges, with high costs currently limiting its large-scale deployment. While chains are widely used in mooring systems for the Oil & Gas industry, their required size and supply constraints for floating wind applications have made fibre ropes an attractive alternative. This thesis identifies several factors influencing the use of top chain in a hybrid mooring system, with a primary focus on determining the minimum required length for hook-up operations of semi-submersible FOWTs.

The relationship between the connection height of the top chain to the FOWT and the required top chain length, as well as the relationship between sea state variations and top chain length, were investigated through numerical simulations. Complications related to the depth below the sea surface, fibre elongation behaviour, and the overall performance of hybrid mooring systems were reviewed through existing literature. The dynamic behaviour of the top chain during the hook-up operation was analysed using OrcaFlex, with simulations performed in both frequency and time domains.

Dynamic analyses primarily focused on a dry chain link connection method, revealing that top chain lengths between 61 and 76 metres are required during hook-up operations. These lengths depend on wave conditions, connection height, and the installation vessel. The results showed that the required top chain length increases with wave height and period, while the length itself minimally influences its dynamic behaviour. For the lower segment of the mooring line, at least 10 metres of chain are required to prevent contact between the line and the rudders and thrusters of the installation vessel.

The study concludes that the top chain experiences minimal dynamic tensions relative to the static tension during hook-up, provided it includes sufficient sag and submersion. A bottom connection height offers the most benefits but necessitates a longer top chain during hook-up compared to a middle connection height. While fibre materials show promise as alternatives to chains, further investigation is required for their use in shallow waters. The dry chain link method is considered financially advantageous but it is expected to require the longest top chain length for hook-up operations compared to other methods. An in-depth analysis of applying pre-stretch to a 3-line mooring system is recommended to verify this assumption. These findings contribute to enhancing the economic feasibility of floating wind energy solutions, particularly for large-scale deployment.

Contents

List of Figures

List of Tables

Nomenclature

Abbreviations

Abbreviation	Definition
2D	Two-Dimensional
3D	Three-Dimensional
AHTS	Anchor Handling Tug Supply
DOF	Degrees of Freedom
DNV-ST	Standard for Marine Operations
DP	Dynamic Positioning
EoM	Equation of Motion
Floater	Combination of the semi-submersible platform and the wind turbine
FOW	Floating Offshore Wind
FOWT	Floating Offshore Wind Turbine
HAIN	Hydroacoustic Aided Inertial Navigation
Hs	Significant Wave Height
JONSWAP	Joint North Sea Wave Observation Project
LBL	Long Baseline Acoustic Positioning
MBL	Minimum Breaking Load
MPM	Most Probable Maximum
O&G	Oil and Gas
OVT	Off Vessel Tensioning
PT	Pre-tension
PTC	Pull Through Connector
QTF	Quadratic Transfer Function
RAO	Response Amplitude Operator
ROV	Remotely Operated Vehicle
SSBL	Super Short Baseline Acoustic Positioning
SSP	Semi-Submersible Platform
t	Metric Tonne
TLP	Tension Leg Platform
Tp	Peak Wave Period
UTC	Upper Top Chain

1 Introduction

Renewable energy is becoming an increasingly critical component of global efforts to reduce greenhouse gas emissions and combat climate change. Among the renewable energy sources, wind energy has emerged as a key player. Wind power can be harnessed both onshore and offshore, but offshore wind energy has become particularly attractive in recent years. Land availability for large-scale wind farms is increasingly constrained, while the ocean, with its vast and largely untapped potential, remains significantly underutilised for energy generation. This under exploitation of marine areas represents a major opportunity to address global energy demands sustainably, particularly as advancements in offshore wind technology make it increasingly feasible to harness wind resources even in deeper waters.

Although the majority of offshore wind farms are constructed with fixed foundations designed for shallow waters, approximately up to 50 metres water depth, Floating Offshore Wind Turbines (FOWTs) offer a promising solution for harnessing wind energy in deeper offshore locations where fixed structures are not feasible [28]. FOWTs have the potential to unlock wind resources in areas with stronger and more consistent winds, significantly increasing offshore wind energy production [57]. Despite their potential, the adoption of FOWTs faces considerable challenges, primarily due to their high costs [61].

Moreover, the field of floating wind energy is still in its early stages, with FOWTs representing a relatively new segment of the renewable energy market. As of now, no large-scale commercial projects have been executed yet, and most existing installations are limited to pilot projects and demonstration sites [28]. Extensive research and development efforts are underway to address the challenges associated with FOWTs, focusing on reducing costs and aiming to make Floating Offshore Wind (FOW) more economically viable and attractable.

1.1. Research problem

Floating Offshore Wind Turbines (FOWTs) are secured in place by mooring lines anchored to the seabed. Various combinations of floating platforms and mooring systems exist, with knowledge from the Oil & Gas industry providing a solid foundation. However, FOWTs face unique challenges due to additional aerodynamic loads and the large number of structures in a commercial farm. Chains are widely used in mooring systems, but for FOWT applications, it is expected that great chain sizes are required to provide adequate mooring performance. In a catenary chain mooring system, the restoring capacity is related to the chain's weight, and the study by [30] found that shallower water depths, mainly up to 60 metres, require greater chain weight compared to deeper waters, necessitating a larger chain size. Similarly, the open-source semi-submersible FOWT model developed by UMaine [1] also required large chain sizes, specifically a nominal diameter of 185 mm, in its three-line mooring system at a water depth of 200 metres. This was driven by the need to keep the peak surge and sway offsets under 25 metres, in order to protect the dynamic electric cable.

Fibre ropes can be implemented in taut or semi-taut systems, depending on the stability requirements of the floating platform. This study focuses on a semi-submersible floating platform, secured in place by a three-line hybrid or semi-taut mooring system. These three mooring lines consist of a long polyester section in the middle, with two chain ends. The VolturnUS-S 15MW floating turbine model is used for dynamic analyses [1], with mooring dimensions adapted from a reference application. The configuration of the mooring line is shown in Figure 2.3.

As the chains required in this mooring system are more expensive than polyester and face supply constraints [66], a higher proportion of polyester relative to chain is preferred. The length of the bottom chain is primarily influenced by the need to prevent vertical loads on the anchor, depending on the anchor type used, as its weight aids in maintaining a catenary shape at the bottom [36].

The length of the top chain faces more challenges and uncertainties. The area in the water column below the sea surface introduces several issues for fibre ropes, such as UV exposure and marine growth on mooring lines. Current applications address these challenges by avoiding the use of fibre ropes within the first 100 metres below the sea surface [15, 2], instead relying on chain sections to mitigate the associated risks. Additionally, fibre ropes exhibit a non-linear tension-stretch behaviour, which requires careful consideration in their design and long-term performance management [43]. In the Oil & Gas industry, chain tensioners are commonly employed to manage the behaviour of fibre ropes and address permanent stretch. However, it is anticipated that such equipment will not be present on FOWT platforms [5]. A thorough understanding of how to manage fibre rope behaviour over a FOWT's operational lifetime is therefore crucial to ensuring its performance.

Furthermore, the required length of the top chain is influenced by the installation process and the specific hook-up method employed to connect the FOWT to the mooring system. A clear understanding of the required top chain length for installation is important to avoid over-dimensioning, as even a small increase in the length of the top chain per mooring line can result in a significant cost difference for an entire FOW farm. This study outlines several hook-up methods that could be applied to FOWTs, with a detailed analysis of the required top chain length for a dry chain link connection method. In this method, the upper segment of the mooring line is attached to the FOWT, while the lower segment is pre-laid on the seabed well in advance of the hook-up operation. Both segments are subsequently retrieved onto the deck of the installation vessel, where the connection between the two chain ends is completed. This method is anticipated to offer financial advantages for large-scale deployments, as it eliminates the need for tensioning equipment, unlike alternative approaches. However, comprehensive analysis regarding the required top chain length remain limited.

1.2. Research objectives and scope

This research aims to determine the required top chain length for the hook-up operation of a semi-submersible FOWT. This objective is divided into the following sub-objectives:

- Identify the challenges associated with the depth below the sea surface for fibre ropes.
- Evaluate the extent to which fibre rope stretch management during the installation of a FOWT affects the required top chain length.
- Establish the relationship between the connection height of the top chain to the floater and its length.
- Establish the relationship between the top chain length and the operational design limits of the hook-up operation of a semi-submersible FOWT.

There are numerous combinations of floating platforms, mooring systems, and corresponding hook-up methods. This research focuses primarily on the hook-up operation of a semi-submersible FOWT equipped with a three-line hybrid mooring system. The water depth and mooring system dimensions are adapted from a reference application. The hook-up method for the three-line mooring system is described, with a detailed dynamic analysis conducted on a dry chain link connection method. This analysis aims to identify the relationship between sea states and the corresponding required top chain length during the hook-up, as well as the influence of the connection height of the top chain to the floating platform.

Other factors influencing the required top chain length, such as the water below the sea surface and the tension-stretch behaviour of fibre ropes, are discussed and reviewed through existing literature. While the potential implications of these factors are explored, a comprehensive analysis to definitively determine their impact is beyond the scope of this research. For the depth below the sea surface, the performance of fibre ropes is primarily related to the protection covers and filters developed and applied to the mooring line [15]. The tension-stretch behaviour of fibre ropes introduces numerous variables and methods for managing them. Several studies suggest that the stretch management of the mooring system over its lifetime can be achieved by pre-loading the system to 40% of the Minimum Breaking Load (MBL) of the fibre ropes [3, 43]. This study assumes the feasibility of this pre-loading approach, with the assumption that pulling one of the three lines is sufficient to achieve the required pre-stretch for all three lines. However, further analysis is required to validate this assumption, which is beyond the scope of this study.

1.3. Research questions

The research question follows up from the objective:

What is the minimum length of the top chain required for hook-up operations of a semi-submersible floating offshore wind turbine?

The following sub-questions provide further insights:

- How does the depth below the sea surface influence the need for top chain?
- Does fibre stretch management during the installation of a FOWT affect the required top chain length?
- How does the connection height of the top chain to the floating platform influence its required length?
- How do variations in sea states and weather conditions affect the required length of the top chain?

1.4. Report outline

The report structure is provided along with a brief summary of each chapter.

Chapter 2 Provides an overview of the relevant background, insights into the challenges associated with FOWTs, and an evaluation of fibre ropes versus chains in mooring lines.

Chapter 3 Introduces the FOWT and the reference application, followed by an explanation of the installation sequence of the hook-up method considered in this research.

Chapter 4 Describes the methodology and inputs for the dynamic model of the hook-up operation.

Chapter 5 Explains the distinctions between frequency and time domain simulations. Compares results from both domains and assesses the sensitivity of simulations to time step and duration.

Chapter 6 Presents the results of the top chain length and the dynamic simulations related to the research objectives and questions.

Chapter 7 Summarises the key findings of the research and addresses the research questions outlined earlier.

Chapter 8 Discusses the implications of the results, identifies limitations, and provides recommendations for future research and practical applications.

2
Literature review

This chapter reviews literature relevant to this research, providing insights needed to achieve the study's objectives. It provides an overview of the semi-submersible Floating Offshore Wind Turbine and its mooring system, along with the associated challenges. The mooring performance of hybrid systems is evaluated in comparison to catenary systems, followed by an exploration of the tension-stretch behaviour of fibre materials, with a focus on polyester. The chapter also describes the hook-up operation and various methods for establishing the connection between the FOWT and its mooring system.

2.1. Overview of semi-submersible FOWT and mooring system

This section provides an overview of floating wind turbines, their mooring systems, and the operational aspects of their installation.

This research focuses on semi-submersible Floating Offshore Wind Turbines (FOWTs), which are anchored to the seabed using mooring lines. The FOW industry is converging to hybrid mooring systems, which typically consist of a fibre rope with chain sections at both ends [66]. These systems are discussed in more detail in 2.2. Various designs for semi-submersible platforms (SSPs) exist. This study specifically utilises the University of Maine's (UMaine) VolturnUS-S 15MW reference semi-submersible floating offshore wind turbine [1]. A schematic overview of an SSP, including its turbine and key components, is presented in Figure 2.1. Additionally, Table 2.1 summarises typical dimensions of offshore wind turbines for three different power capacities, as reported by [13]. The exact layout and dimensions of the VolturnUS-S reference turbine are detailed in Section 3.1.

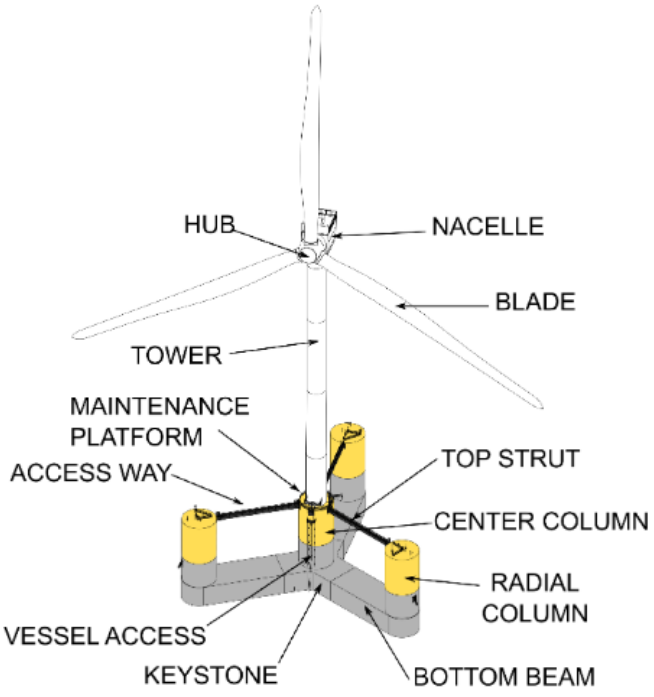

Figure 2.1: An illustration of a semi-submersible FOWT [66]

Properties	Dimensions			Unit
Power of turbine	10	15	20	MW
Blade length	91	109	125	m
Nacelle to waterline	123	150	161	m
Nacelle weight	550	850	1200	t

Table 2.1: Typical dimensions of offshore wind turbines [13]

The installation of FOWTs involves a combination of inshore preparation and offshore operations, ensuring

the turbine is properly secured to the seabed and connected to the power grid. FOWTs are integrated and commissioned inshore before being towed out to sea. The typical offshore installation sequence is as follows:

1. Anchor installation
2. Pre-lay of the mooring lines and cables
3. FOWT tow to field
4. Mooring hook-up and tensioning
5. Fibre rope stretch removal
6. Cable installation, pull-in, and offshore commissioning

Several hook-up methods are discussed in Section 2.5, with a detailed explanation of the installation sequence considered in this research provided in Section 3.2.

2.1.1. Floating platform and mooring system

Different mooring configurations and floating platforms are considered for FOWTs. Figure 2.2 illustrates four distinct platform types and three corresponding mooring systems. While the mooring systems in the figure are shown supporting specific platforms, they are not exclusively applicable to those configurations, except for the Tension Leg Platform (TLP). Instead, the figure provides a clear overview of the range of possibilities.

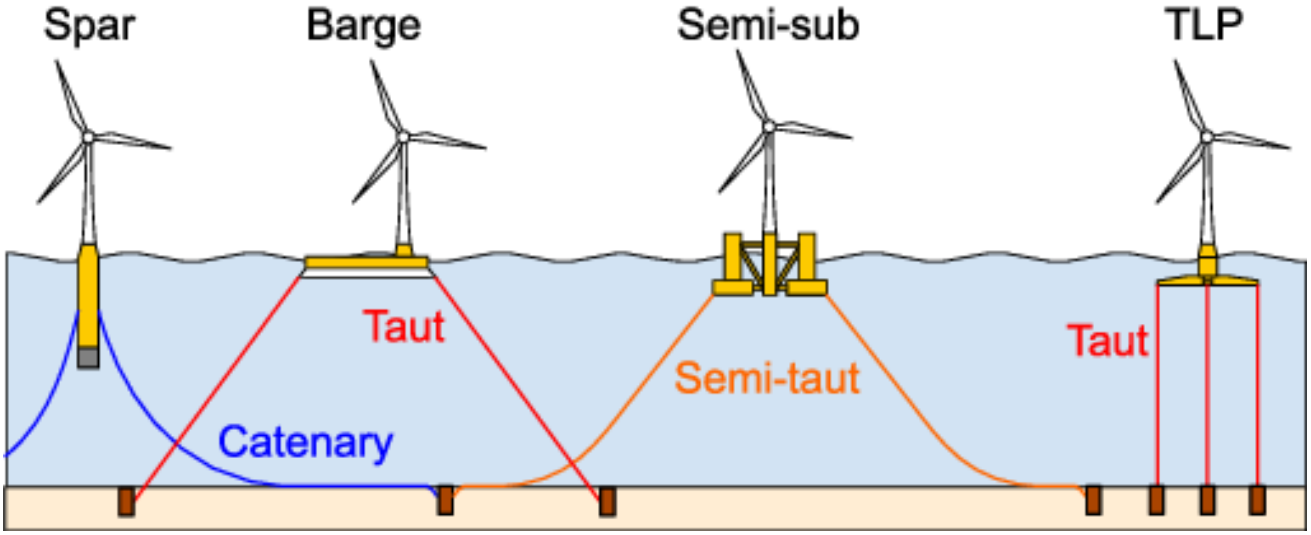

Figure 2.2: Mooring configurations and floating platform types [8]

Catenary mooring systems rely on heavy chains or cables that form a curved shape, known as a catenary, due to their self-weight. The mooring lines rest on the seabed over a portion of their length, and restoring forces are generated by lifting and lowering the weight of the line. These systems are well-suited for shallow to moderate water depths but require substantial space, as adequate length on the seabed is necessary to maintain purely horizontal forces at the anchor [66].

Taut systems use lighter, more elastic lines that remain under tension and extend directly from the anchor to the platform. The restoring forces are generated by the elasticity of the mooring lines, acting both vertically and horizontally. These systems are efficient in deeper water, as they require less seabed space compared to catenary systems. However, a taut system results in higher tensions in both the lines and anchors [6]. In contrast to catenary systems, taut systems also introduce significant vertical forces on the anchor.

Semi-taut systems combine elements of both catenary and taut configurations. The lines have a steeper angle than catenary systems but include a segment that rests on the seabed, allowing for a balance between horizontal and vertical restoring forces. A more detailed review of the trade-offs between catenary and semi-taut mooring systems is provided in Section 2.2. The hybrid mooring design considered in this research is regarded as an example of a semi-taut system. Figure 2.3 illustrates the mooring line and its sections considered in this study. The zoomed-in view distinguishes between the upper segment and the lower segment of the mooring line. The upper segment, up to the H-link, is connected to the floating platform prior to hook-up, while the lower segment is pre-laid on the seabed in advance of the hook-up operation.

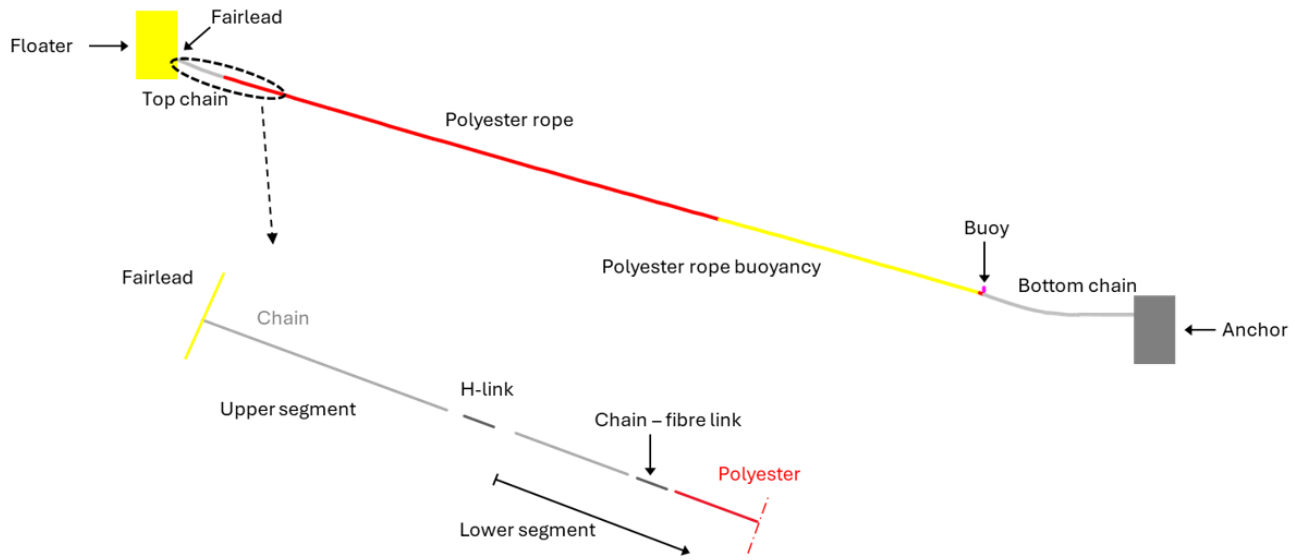

Figure 2.3: Schematic representation of a hybrid mooring line, illustrating its distinct sections.

The buoyancy added to the lower part of the fibre rope ensures the rope avoids contact with the seabed, the same applies to the buoy. Two examples of connectors are shown in Figures 2.4 and 2.5: an H-link for connecting mooring chains and a thimble connector for attaching a polyester rope to a mooring chain. The length of an H-link closely resembles that of a chain link.

Figure 2.4: H-link connector that connects two mooring chain segments [64]

Figure 2.5: Thimble connector that connects mooring chain to polyester rope [65]

Terminology
In this report, the terms "floater" and "vessel" are frequently used. Unless otherwise specified, "floater" refers to the semi-submersible Floating Offshore Wind Turbine, and "vessel" refers to the installation vessel used during the hook-up operation. For the top chain, different sections are distinguished, and the length of each section is determined based on specific criteria applicable to that section. This is further discussed in Section 4.3.2 and illustrated in Figure 4.7.

2.1.2. Learnings oil and gas industry
Much of the literature emphasises that valuable lessons can be drawn from the oil and gas (O&G) industry regarding efficient mooring systems, which can and should be applied to FOWTs. Catenary mooring systems are widely used for anchoring floating structures, such as semi-submersible platforms in the O&G industry and

FOWTs. This system makes use of heavy chains or cables that form a catenary curve from the floating structure down to the seabed anchors. The weight and length of the mooring lines provide horizontal restoring forces that stabilise the platform. These restoring forces counteract the dynamic loads from waves and wind, thereby reducing the motion of the floating platform [24, 5, 38].

A case study presented in [5] highlights the differences and similarities between deeper offshore O&G applications and shallower floating wind turbines. Although the water depths of the O&G industry are often significantly greater, 1200 metres in the case study by [5], the author asserts that the mooring techniques would still be applicable in shallower waters for FOWTs. In fact, these methods have proven to be reliable, meaning FOWT projects can hugely benefit from them. To compare to the water depth of 1200 metres, [14] states that, based on technical limitations, the operational water depths for SSP wind turbines range from 60 to 300 metres, where [20] expects floating wind farms will be suitable for water depths up to 1000 metres.

[5] describes differences and applications that should be implemented in FOWT projects to increase the efficiency and reduce risks, compared to the O&G industry. Although these aspects are outside the scope of this research, they do influence the feasibility of a realistic installation process and should therefore be considered. To increase weather windows, which will be further elaborated upon in Section 2.4.1, no personnel should be on the floating platform during installation. To achieve this, smaller and more manoeuvrable Remotely Operated Vehicles (ROVs) should be designed for mooring operations. Furthermore, a mooring method that allows for hook-up and installation without the need for high bollard pull should be utilised, so vessels containing large chain lockers can be used for pre-laying of mooring lines elsewhere. Lastly, a mooring method that can quickly be disconnected is favoured as it simplifies maintenance. As the number of mooring lines is reduced, compared to oil & gas applications, and higher tensions are expected and farms will include a large number of FOWTS, still many differences and challenges are recognised that need investigation.

The same case study made use of an Off Vessel Tensioning (OVT) mooring method, which turned out to be quite efficient. As for this research, the mooring lines were pre-laid, then gathered at the vessel during installation, hooked up with the top chain, and tensioned as desired. While the study lacks specific information on the length of the top chain, it mentions that the top chain can be reduced to a short section for FOWT applications. Besides project costs reduction, this would decrease the time needed for hook-up and pull through. As discussed earlier, performing tensioning operations off the vessel or floater, rather than using topside tensioning equipment on the floating platform, enhances safety by reducing or eliminating the need for personnel on the structure during operations. This reduction in personnel requirements also allows for increased operational weather windows. More detail on installation methods is provided in Section 2.5.

2.2. Hybrid mooring system

The FOW industry is converging towards a hybrid mooring system. As described before, this entails the mooring system consists of two chain sections at both ends, with a fibre rope in between. Polyester has been widely used in deep water mooring systems in the O&G industry, and has proven performance for many years. Compared to other fibre materials, it has low creep, high resistance against oceanic environmental conditions, very low hydrolytic degradation and it has the lowest costs [7]. Although UHMW-PE (HMPE) is much stronger and stiffer than polyester, it is not favoured yet due to its significantly higher creep and a price per kilo that is ten to fifteen times higher. The following section describes both advantages and disadvantages of the usage of chain and fibre ropes in mooring systems.

2.2.1. Considerations for using fibre ropes versus chains in mooring systems

Footprint of mooring system

As previously mentioned, a hybrid system is favoured over a full chain catenary system or a fully fibre rope mooring design for several reasons. One downside of chain catenary mooring systems is the size of their required footprint. Typically, drag embedment anchors are used, which cannot support vertical loads, leading to a larger required chain part that lays on the sea bottom and hence a larger anchor radius. The chain lying on the seabed also contributes to a horizontal restoring force. When the FOWT moves in one direction, the chain on the opposite side is lifted off the seabed. Its weight then acts to pull the turbine back toward its original position, counteracting the displacement and enhancing the system's stability. A hybrid system is actually considered to be semi-taut, which can significantly reduce the footprint of the mooring system. The footprint, or anchor radius, refers to the area on the seabed occupied by the anchors and mooring lines used for a, in this case, FOWT. Different anchor types, like suction anchors, might be required to support vertical loads coming from the semi-taut system.

In the research by [66], a comparison was made between two mooring designs of a 10MW FOWT: a chain catenary system and a hybrid system. The results showed that the total required length of a mooring line for a hybrid

system was almost half the length of a chain catenary system. Although these results could vary for different water depths (only 60-110 m in this example) or environments, it is clear that the footprint can be significantly reduced. This brings huge benefits when installing floating wind farms and allows other ocean users, such as fishers, to operate closer to installed floating turbines. Large and long anchor chains have also been shown to cause significant environmental damage to seabed habitats [16]. Reduced peak loads due to hybrid systems offer an opportunity to reduce the size of anchor chains and thereby environmental damage caused by the mooring system. These reduced loads are described below. However, sufficient anchor chain length is necessary to prevent vertical forces on the anchor, which is critical when using drag anchors. Conversely, other types of anchors, such as suction piles, can withstand vertical loads but are generally more expensive. This creates a trade-off between increased costs due to chain length and the choice of anchor type [36].

Costs and supply

Moreover, fibre ropes, especially polyester, are cheaper per unit break strength compared to chains of the same strength. Based on prices per tonne provided by Seaway7, calculated for the dimensions of the reference application, the chain was found to be approximately 8 times more expensive than polyester per metre. As turbines and platforms become larger, longer and larger chains are needed to withstand increasing environmental forces. This leads to a significant supply issue. The current manufacturing capacity is insufficient to deliver the large chains needed for commercial FOW farms [66]. Additionally, the number of vessels capable of handling such large chains is limited. These specialised vessels are not only scarce but also expensive to operate, adding to the logistical challenges. Fibre ropes, being lighter and storable on spools, require smaller installation vessels, especially given the reduced length needed for a robust mooring system. The production of fibre ropes can also be rapidly increased to meet the demands of large-scale FOW projects [66].

Mooring loads and platform excursions

Multiple studies, discussed below, have compared the behaviour of full chain versus hybrid mooring systems for floating offshore wind turbines. Two main conclusions can be drawn: for mooring systems containing fibre ropes, the mooring loads are significantly reduced, but the excursions of the floating turbine become larger. These studies and their findings are discussed in detail below.

[54] compared a hybrid mooring system with a catenary chain system for a semi-submersible FOWT across three different anchor radii, considering both polyester and exeter tethers, a novel mooring rope material. The research emphasises the importance of optimising both mooring system weight and compliance. Finding the right balance between the two would lead to reduced loads and limited seabed disruption, while keeping platform excursions within acceptable limits. For the reference turbine and floating platform considered in this research, the maximum surge and sway offset are limited to 25 metres, which is related to meeting the design constraints of the power cable. In general, heavy mooring systems lead to lower excursions due to the self-weight of the mooring lines, while compliant mooring systems are designed to absorb energy from environmental loads, which leads to load reduction [27]. Additionally, reducing the weight in the mooring system decreases the load on the floating platform, allowing further optimisation of the platform design, which can, in turn, reduce its excursions.

The study by [54] focused on peak anchor loads, revealing that the smaller the system footprint, the greater the reduction in anchor loads when using fibre ropes. For the smallest footprint, peak anchor loads were reduced by 84% compared to the chain-only system. Even when comparing the smallest footprint of the hybrid system to the largest footprint of the chain-only system, there was still a significant 55% reduction in peak loads, while the footprint was 12% smaller. These results indicate that hybrid mooring systems can achieve significantly lower loads and, again, reduced footprints. The research also concluded that increasing the anchor radius has a marginal influence on reducing peak loads in hybrid mooring systems, which is a beneficial property for minimising the mooring footprint.

However, the more compliant hybrid mooring system leads to greater excursions of the platform. Excursions of a FOWT are limited in order to protect the dynamic electrical cable. While the chain-only systems stayed within acceptable limits for all radii, the excursions of the hybrid systems were too large. The study's water depth was relatively shallow for floating wind projects, at only 70 metres. Similar findings on loads and excursions were reported in [31], which also indicated that increased water depth could significantly reduce platform excursions in shallow waters (40 m to 100 m). [30] also found reduced excursions at 100 metres water depth compared to 50 metres. The restoring capacity of a catenary mooring system depends on its shape, and the research showed that shallower waters require heavier chains to meet design requirements, while chain weight decreases exponentially with depth up to 60 m and increases linearly between 60 m and 100 m.

The flexibility of fibre ropes causes potential problems to animals as well. [34] found that hybrid mooring systems result in larger swept volumes of the mooring lines, which increases the risk of entanglement for marine mammals.

There are many other factors that affect the excursions of a FOWT, and multiple techniques can be applied to reduce them.

Extra weight may be added to the mooring system by making use of clump weights or floats/buoys, while a combination of these can also decrease extreme line tensions [9, 71, 70]. A numerical study by [72] investigated the effects of buoys and clump weights in the mooring system of a SSP. Buoys were particularly effective in reducing the top tension on the mooring lines, and [70] found beneficial stiffness properties could be achieved with respect to the top end offset. The weight of clump weights can create a catenary end when placed at the lower section of the mooring line. By pulling the segment near the touchdown point towards the seabed, the clump weights increase the length of the mooring line that rests on or closely approaches the seabed. This reduces or completely removes potential vertical loads on the anchor. [9] found that a small spacing between many clump weights, just after the touchdown point, resulted in the lowest tension.

The pre-tension (PT) of the system also significantly influences the excursions of the platform. Generally, an increased PT leads to smaller excursions at the cost of increased line loads. [31] studied the characteristics of a semi-submersible FOWT for different PTs by adjusting the mooring length. For higher PT, surge motions were reduced but for heave little affects were found. Line loads increased for higher PT. In the three cases studied, which varied in PT, the amplitude, defined as the difference between the maximum and minimum relative to the mean, remained the same. Their behaviour across different wave periods was also similar.

Fatigue properties

[4] again emphasises how knowledge gained from the oil and gas industry is hugely beneficial for the application of FOWTs. It mentions that most failures in mooring systems were caused by fatigue, and identifies three main aspects that make FOWT projects even more susceptible to this issue. The wind turbine operations cause increased fatigue loadings on the mooring system. This comes together with a reduction in the number of mooring lines and components as the industry strives to reduce project costs. Furthermore, FOWT platforms with light displacement, moored in relatively shallow water with low to moderate PT, are vulnerable to slack and snap loading of the mooring lines.

Fibre ropes perform significantly better on fatigue life. The study by [66] even showed the fatigue life of the chain sections is increased using a hybrid system, compared to a chain catenary system. Most failures of chains in mooring are associated with fatigue, corrosion and bending stresses or a combination of these. Fatigue and corrosion are not considered as a threat for fibre ropes, as long as contact with sharp objects is prevented, according to [37]. Of the 21 mooring failures that were investigated by [37] between 2001 and 2011, chain segments, connectors and wire ropes were the three main components that caused incidents. However, there are multiple reasons why chain sections are not completely removed from the mooring system.

Splash zone and water below sea surface

The top part of the mooring system is likely to be located within the splash zone, depending on its connection height to the floating platform. The splash zone is the area where a structure is exposed to both air and water due to wave action. This zone and the area close to the water level cause additional challenges. Key aspects that could impact the performance of fibre ropes are UV radiation caused by sunlight, marine growth and fairlead sheaves. Also increased temperatures in shallow waters or even in the air can accelerate the degradation of fibre ropes. The performance of fibre ropes in fairlead sheaves or other deviation elements has not been demonstrated, and chain is mostly used in the upper segment of mooring systems. The knowledge of penetration of UV and marine growth in fibre ropes is therefore limited [15].

DeepStar performed a study to investigate the penetration of UV and marine growth into fibre ropes [15]. The ropes were protected by a filter and a braided cover, combined with a soil ingress protection layer, which are already common practice in mooring applications [68]. They found that very little to no UV reached the fibres of the rope core. Minor damage was found without the use of the cover layer. The ropes were also tested in higher water temperatures. It showed minor effects of hydrolysis, and the results were consistent with the 5% strength loss reported in a previous study [40]. The soil ingress protection was designed against particles larger than 5 microns. After exposure to marine growth for 18 months, no particles larger than 5 microns penetrated into the sub ropes.

Chain also offers better protection against damage caused by vessels or other objects compared to fibre ropes. On the other hand, the splash zone brings more challenges related to fatigue performance. In that perspective, fibre ropes would be more beneficial than chains.

For these reasons, current applications generally use a minimum water depth of 100 metres as a limit for fibre rope deployment [15, 2]. This distance mitigates risks from chafing, UV exposure, and the impact of marine growth.

The exact limit depends on various factors and may be reduced through the implementation of coatings and soil filters, as demonstrated in the study by [15]. Further development and implementation of these protective coatings will be required to enable the use of hybrid mooring systems for FOW applications. From a mooring design perspective, positioning the connection point of the mooring line to the floating platform at a low height is advantageous, as it remains well below the sea surface, mitigating most of the associated risks.

On the bottom part of the mooring system, fibre ropes should not be in contact with the seabed to avoid shaving, which damages the rope [66]. This issue is resolved when using chain. Additionally, laying an adequate amount of chain on the seabed prevents vertical forces from acting on the anchor.

Installation and stretch
Some reasons for the usage of chain are related to the installation or hook-up method. Multiple methods to make the connection between the pre-laid mooring line and the upper segment of the line are described in Section 2.5. In most cases the usage of chain cannot be avoided, but hook-up methods exist that allow for the usage of fibre ropes only. Another aspect is related to the property of fibre ropes that they elongate when tension is applied. When permanent stretch occurs in fibre ropes, the mooring line length increases, leading to a reduction in the system's pre-tension. In systems composed solely of fibre ropes, re-tensioning is not feasible [15]. The behaviour of fibre ropes under tension is described in Section 2.3.

Conclusion
The implementation of hybrid mooring systems containing both fibre and chains, compared to a chain-only system, leads to reduced footprints, peak loads and mean mooring loads but increased excursions [31, 33, 34, 54]. Increased flexibility increases the risks of entanglement for marine mammals, but the usage of buoys and clump weights may decrease platform excursions. Additionally, the costs of the mooring system are reduced, and manufacturing can be easily scaled up. In contrast, chain-only systems face supply constraints [66], which can limit their feasibility for commercial scale FOW parks.

The impact of UV exposure and marine growth penetration in fibre ropes is still uncertain, but soil ingress protection layers have proven to withstand penetration. Sheaving of fibre ropes at both the fairlead and seabed should be prevented. Chain offers a robust solution in these areas.

2.3. Elastic behaviour of fibre ropes

The change in length of fibre ropes in response to a change in applied tension is non-linear. The way this happens is called the tension versus stretch behaviour. Stretch refers to the change in length of the rope under tension, denoted by ΔL. Strain is the amount of change in length divided by the total length L of the rope. The expression is shown in Equation 2.1.

$$\epsilon = \frac{\Delta L}{L} \tag{2.1}$$

Figure 2.6 describes and visualises the typical behaviour of a fibre rope under varying tension conditions.

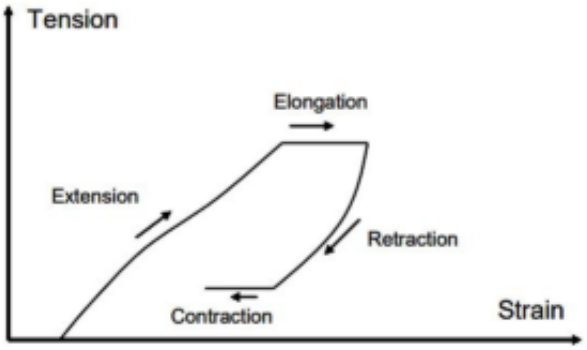

Figure 2.6: Stretch behaviour of a fibre rope under varying tension [60]

The terms in the figure have the following meaning:

- Extension: increase in length of the rope due to an increase in tension.

- Elongation: increase in length of the rope at a constant tension, after an increase in tension.
- Retraction: decrease in length of the rope due to a decreased tension.
- Contraction: decrease in length of the rope at a constant tension, after a decrease in tension.

Figure 2.6 also shows the stiffness of a fibre rope is non-linear, meaning the relation between change in tension and stretch is non-linear. The stiffness depends on the loading history of the rope. Permanent stretch will occur and is usually significant, depending on the kind of fibre used. In Figure 2.6, the permanent stretch is represented by the horizontal distance along the strain axis between the starting point on the left with zero tension and the end point after contraction.

2.3.1. Polyester

This research mainly focusses on the use of polyester as fibre material in the mooring system. The permanent stretch of polyester contains two effects, the polymer-stretch and the construction stretch. The polymer-stretch remains in the rope while construction stretch contracts once the rope is relaxed after applying tension [17, 21].

A typical step during installation is pre-stretching the polyester rope by putting it under tension for a certain amount of time. This is done to remove initial stretch that occurs when the polyester rope experiences its first significant load. It introduces the polymer and visco-elastic stretch in the polyester segments. This tension is called the installation tension [60]. The Syrope model is a tool used for analysing the tension versus stretch behaviour of a polyester mooring line [21]. When tension is applied for the first time, the tension strain relation is described by the original curve. The Syrope model is shown in Figure 2.7. The original working curve represents the original curve, added with the polymer and visco-elastic stretch.

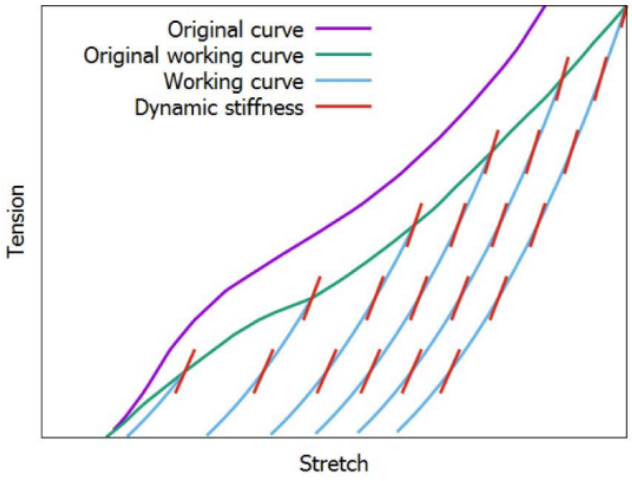

Figure 2.7: The Syrope model, showing the tension versus stretch behaviour of a polyester rope [21]

When the rope is loaded for the first time and the tension is held constant, the rope will stretch until it reaches the original working curve for that tension level. The working point represents a point on the original working curve, representing a highest mean tension. When the mean tension decreases, the working point follows the working curve downwards. When tension is increased again, the rope will follow an upwards working curve, this curve is not shown in Figure 2.7. The upward and downward working curve form a convex shape [17]. When the polyester rope is in a relaxed state, its stretch is represented by a working point on the working curve corresponding to its highest preceding mean tension. Thus, when the preceding highest mean tension is exceeded, an additional permanent stress occurs. The stress-stretch or strain relation will move up and down along the working curve for the highest preceding mean tension, during for example a stationary sea-state.

The stiffness of a rope describes the ratio of the change in tension to the corresponding stretch (Equation 2.2).

$$K = \frac{\Delta T}{\Delta L} \tag{2.2}$$

The dynamic stiffness is also visualised in Figure 2.7, and refers to the rope's resistance to deformation under varying or cyclic loads. This stiffness changes with mean-tension and the amplitude of loading, and it depends

on the loading history of the rope. The dynamic stiffness increases for an increased tension, as well as with the time under loading of the rope.

As described, during installation an installation tension is applied to the polyester mooring line. The pretension describes the tension when all lines are at static equilibrium, excluding environmental factors. Figure 2.8 shows the working curves for three different installation tensions. The horizontal yellow line represents the pre-tension of the mooring system. The first tension, T_1, equals the PT. The other installation tensions are larger, and it can be seen this leads to an increased strain (ϵ) at the same PT. Higher installation loads would be beneficial as additional stretch is already introduced in the polyester rope.

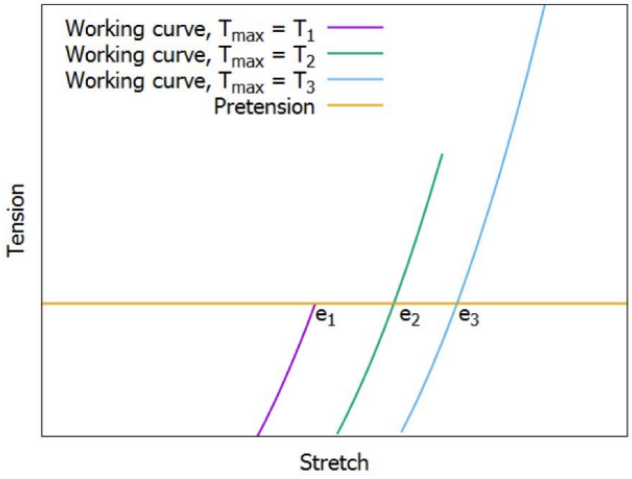

Figure 2.8: Working curves for three different installation tensions [21]

2.3.2. Stretch management

Multiple studies have investigated different methods to manage the tension versus stretch behaviour of polyester ropes. One approach is to re-tension the mooring system at a certain period after installation to regain the desired PT or design tension. This can be achieved by pulling the top chain through the tensioner integrated into the mooring line until the required design tension is reached. This requires sufficient top chain. The spare chain could either be left hanging at sea or it can be cut off. A downside of this method is that it requires sufficient monitoring of the mooring system to identify if the stretch of the polyester rope has become too large to maintain the required design tension.

[43] studied and tested the possibility of eliminating the need to return and re-tension the system after a certain amount of time. The study is focused on a hybrid mooring system containing both chain and polyester. The idea is to pre-stretch the rope to the highest possible tension to induce delayed elastic and plastic elongation and achieve a more predictable rope. Figure 2.9 provides a tension versus elongation curve of polyester with more detailed definitions. The study by [43] applied two different pre-loads on the mooring system, 30% MBL and 40% MBL. These loads were maintained for 100 minutes before returning to the target pre-tension. According to DNV (and other regulatory bodies), the highest load a mooring line may encounter during its design lifetime is 60% MBL. Therefore, a hurricane load of 60% MBL was applied to the polyester rope. The findings showed that ropes subjected to loads of 60% MBL after pre-loading of 30% MBL had an additional elongation of 1%, whereas the ropes pre-loaded to 40% only showed an additional 0.5% elongation after the hurricane load. The response of the rope subjected to 40% MBL pre-load is depicted in Figure 2.10. The results indicate that if a polyester rope, as part of a mooring line, is pre-loaded to 40% MBL, no re-tensioning of the system is required as it can be kept within the design tension. PT or design tension requirements are expected to be within a range of 10-15%.

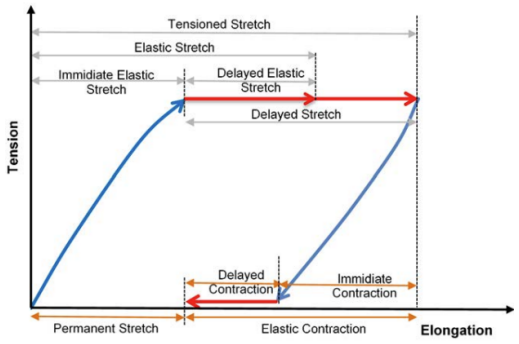

Figure 2.9: Elongation versus tension behaviour of a polyester rope [43]

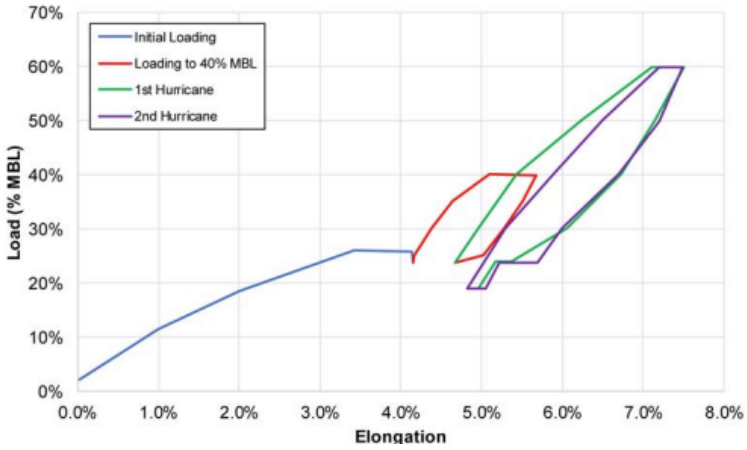

Figure 2.10: Test results of permanent stretch removal of a polyester rope [43]

Another possibility is to introduce a calculated amount of over tension during the installation. The idea is that over time and through environmental load cycles, the elastic strain will convert to plastic strain, causing the tension to drop to the desired design tension. It requires a good understanding of the rope properties and behaviour to accurately calculate how much over tension should be introduced in order to reach the design mooring tension once the ropes have aged. In other words, a higher start-of-life pre-tension is aimed at, which will drop to the desired PT over time due to elongation of the polyester rope. More specifically, this is due to delayed elastic and plastic strain. For all three methods mentioned, a good understanding of the fibre material and its behaviour is crucial. Based on the expected end-of-life stretch of the polyester rope, required pre-loads, over tensions and spare chain lengths for re-tensioning could be calculated.

Bow-string

In oil and gas applications, achieving 40% MBL in the polyester section is relatively straightforward as topside mooring tensioning equipment can be used. These are not present in FOWT applications and reaching 40% MBL will therefore be a challenging task. [43], along with other studies, proposed applying the bow-string method. The polyester ropes are pre-loaded by pulling perpendicular to the mooring line. A line is connected to both the mooring line and the winch on an AHTS vessel. This method should multiply the load applied by the winch in the mooring lines. The pull line leaving the stern roller should be nearly vertical and the pull line is connected around the midpoint of the mooring line. However, for water depth ranges suitable for FOW applications, the feasibility of achieving a tension of 40% MBL using this method needs investigation.

The study by [43] examined the pulling force required to reach both 30% and 40% MBL pre-load in polyester ropes using a winch. Two scenarios were considered: a slack mooring system and a stiff mooring system prior to pre-stretch. In a stiff mooring system, the lines are pre-loaded and tensioned before the final stretch removal. The results indicated that winch capacities slightly exceeding 500 tonnes were necessary to reach 40% MBL, with lower tensions required for the stiff mooring system.

2.4. Hook-up operation

The installation of floating wind turbines is considered as a potential bottleneck as it is sensitive to weather conditions. Floating applications are often in harsh environments, therefore operational limits are crucial to understand to be able to install an entire wind farm within a year. This section describes some of the challenges related to hook-up operations. In Section 2.5, different hook-up methods will be described.

2.4.1. Challenges and variables

The installation brings many challenges that need to be accounted for. There are two primary risks that could lead to failure during installation. Firstly, the installation vessel and the floating turbine could collide, causing damage. Secondly, the tension in the mooring system could become too large during installation, potentially leading to the mooring system snapping or damaging the vessel. These challenges are mainly due to the hazards of the marine environment.

Operational limits

Wave heights, wind speeds, and current speeds all influence the loads on and the behaviour of the floating turbine and the installation vessel. It is therefore crucial to investigate the limits of these variables to determine the

conditions under which installation is feasible. A table is created by [10], indicating the limits of the significant wave heights and maximum wind speeds for various vessels used in marine operations. The values are depicted in Figure 2.11. It is important to distinguish between operational limits and operational design limits. The design limits are found based on models and simulations, these are multiplied by an alpha factor, smaller than 1, to find the operational limits specifically related to the project location and environmental conditions. While the article refers to the values as operational limits, they are based on general applications, suggesting they are more closely aligned with design limits.

[26] performed a similar study and also emphasised that these limits are crucial for identifying weather windows for which the installation is possible. This aspect is important to keep in mind when optimising the length of the top chain. The design of the mooring system may influence the limits of certain sea conditions for which the installation is possible. [10] also stated that raising the values listed in 2.11, by designing innovative vessels, could significantly lower the projects costs of a commercial floating wind farm. These values are provided to give an indication, but the limits should be individually investigated for the specific operation and location of a project.

To add to these values, the current installation limits for significant wave height in fixed offshore wind turbines are often around 1.5 m [22]. [5] argued that, as FOWT applications will be in areas with high sea states, for mooring methods this limit should be at least higher than H_s = 2 m, and the current above 1.5 knots, to be able to efficiently implement commercial offshore floating wind farms. In their own case study, the limits used were H_s = 2.3 m, and current = 1.8-1.9 knots. The wave period was mainly around 4 to 6 seconds. In Section 2.5.5, this case study is described in more detail. Another case study, a project in Korea, is dealing with sea states of mainly H_s = 3 m, with dominant T_p in the range of 4 to 10 seconds. In this case, only incident wave headings of less than 20° relative to the bow of the vessel were considered.

For the towing of the semi-submersible floating platform to its location, this limit is around 2.5 m H_s. This process, however, is out of scope for this research, but it should be kept in mind as it influences the installation possibilities. [14] also states that because most of the construction of floating wind turbines can be done onshore, fewer offshore operations will be required. Together with operations having the potential to be conducted in larger sea states, the weather windows will be larger compared to the fixed offshore wind turbines.

Vessel type	Purpose	Max. significant wave height (m)	Max. wind speed ($m\,s^{-1}$)
AHTS	Installation of anchors and moorings	2	20
Tug boats	Towing	1–1.65	14
Cable laying	Installation of cables	3.5	15
Heavy-lift vessel	Mating of spar-type platforms	1.8	15
Offshore supply	O & M	2	11
Monohull	Crew transfer, O & M	1	–
Catamaran	Crew transfer, O & M	1.2	10
SWATH (small-waterplane-area twin hull)	Crew transfer, O & M	1.5	–
Jack-up barge	O & M	1.65	16

Figure 2.11: Limits of significant wave height and wind speed for marine operations vessels [10]

Dynamic positioning

Dynamic Positioning (DP) is a computer-controlled system used by vessels to automatically maintain their position and heading by adjusting thrusters and propellers. This is essential for offshore operations, such as the hook-up of a FOWT, where precise positioning is required despite external forces such as waves, wind, and currents. The accuracy of DP systems depends on the quality of reference systems providing position data and the environmental conditions under which the system operates. Under typical operating conditions, with manageable environmental forces and fully functional onboard systems, DP systems can achieve positioning accuracy within 1-2 metres. According to [32], reference systems with a standard deviation of less than 1 metre and an update rate of at least 1 second are given equal weight within the DP system. This indicates that when such high-precision reference systems are used, DP systems can maintain reliable and accurate positioning.

[56] states typical SSBL-systems (Super Short Base Line) have a standard deviation of around 0.2% of its distance. [32] shows the introduction of the HAIN (Hydroacoustic Aided Inertial Navigation) system can bring the accuracy of SSBL down to 1 metre, while for LBL and GPS this is around 0.5 metres, at a water dept of 1000 metres.

Increased sea states introduce additional difficulties in accurate positioning. The paper by [56] provides further insights into these challenges. For operations involving gangways or access systems, they found that a typical maximum allowable standard deviation of motions at the gangway location is around 1.75 m. This criterion was used to determine the operational limits for different allowable gangway strokes (5.0 m, 7.0 m and 9.0 m). The study considered environmental conditions including significant wave heights up to 3.5 m, associated wind speeds, and current speeds up to 2 knots. These conditions were simulated to determine their impact on DP station-keeping accuracy. The results showed that as environmental conditions worsen, the ability to maintain accurate positioning decreases, necessitating larger allowable strokes for gangway operations.

According to DNV code DNV-ST-0111, for a DP capability level 3, the displacements of the vessel are considered to be less than 5 metres from the setpoint with the heading within 3 degrees from the target. In the hook-up procedure of an FPSO (Floating Production Storage and Offloading unit) described by [41], a DP accuracy of ±1 m was recommended. Translational motions of the FPSO were limited to a maximum of 5 metres from the reference point. For the hook-up operation of floating wind turbines, an accurate DP system is crucial to maintaining a fixed distance between the installation vessel and the floating turbine.

Snap loads

Snap loads are defined by an abrupt switch in tension in a mooring line, occurring when the line was in slack condition and suddenly re-engages and becomes tight again. As a consequence, a shock on the line material may be induced, which significantly decreases its fatigue life. Snap loads are one of the main causes of mooring line failures. Factors as a low pre-tension, lighter displacement platform and shallow water depths increase the chance of slack line events and hence snap loads [29]. During hook-up installations it must be ensured these snap loads do not occur. For marine operations, DNV has defined a criterion to avoid snap conditions, which is the following:

$$F_{\text{dyn}} \leq 0.9 F_{\text{st}} \tag{2.3}$$

With F denoting the force and the subscripts denoting the dynamic and static components, with a 10% factor of safety added. The research of [29] concludes there is a strong correlation between the vertical motion of the fairlead and the tension spike due to snap loads. Slack occurs when the fairlead is at its lowest position, with snap occurring at its highest position. The same counts for the wave motion. During installation, snap loads not only pose a risk of mooring chain failure but also endanger personnel and equipment on the deck of the installation vessel.

2.5. Hook-up and tensioning methods

This research primarily focuses on a mooring system containing three lines. It is considered that two of these lines are of fixed length and lack any tensioning equipment either along the line or at its end, making their length non-adjustable. The third line, however, includes a tensioner, which enables adjustments to the mooring system's pre-tension by reducing the line's length, thereby functioning as an adjustable-length line. Different methods exist to make the connection between the pre-laid mooring line and the top chain, and for the position of the chain tensioner. These methods are explained in the following sections.

2.5.1. Dry chain-link connection

The first method described is creating a dry chain link connection at the deck of an Anchor Handling Tug Supply (AHTS) vessel. Both the lower and upper segment of the mooring line are recovered to the deck of the AHTS and are locked into shark jaws. A shark jaw on an AHTS vessel is a hydraulically-operated device used to secure and unshackle chains and wires on deck. It features interchangeable jaws for wire and chain, which can be raised to support loads or lowered to sit level with the deck surface for stowage [42]. An H-link connection, as in Figure 2.4, is made between the lower and upper segment of the mooring line. Once completed, the mooring line tension is transferred to a work winch, and the mooring line is released from the shark jaws and deployed [41]. A more detailed explanation of this method is provided in Section 3.2.1.

This method leads to a significant cost reduction compared to methods that include a tensioner or pull-through system. There is no need for a line tensioner or tensioning equipment, and there will be no need for tensioning chain overlength. The main downside is that a minimum length is required for the top chain, with criteria coming from both the lower and upper segment of the mooring line. The segments are visualised in Figure 2.3, with both segments containing a certain amount of chain. For the pre-laid mooring line, contact between the polyester rope and the hull or stern roller of the AHTS should be avoided to prevent damage to the fibre. To ensure this, a sufficient chain length is required. Both segments include a specific chain length on the deck of the AHTS. The upper segment also contains a hanging part between the AHTS and the FOWT. This length is determined by the

vessel's offset from the floating turbine during hook-up and the potential for high mean loads or snap loads in the chain.

2.5.2. In-line tensioning

The in-line tensioner (ILT) is installed and deployed in sheltered water onto the top chain before it is towed-out to the field. Both the lower and upper segment of the mooring line are recovered at the AHTS deck. After the work wire or chain is connected to the winch, the lower segment is connected to the work chain. After both the tensioner and mooring segments are deployed and released, the tension is taken on the work wire/chain to pull the lower segment of the mooring line through the tensioner [69]. An example of an ILT system is displayed in Figure 2.12.

The in-line tensioner allows for reduction of topsides equipment, and it does not require personnel to be on the floating platform to operate the tensioning equipment [12]. It also does not impact the platform design, however, the weight of the in-line tensioner must be carried by the floating platform. Its weight causes a clump weight effect on the mooring line as well, and thereby causes local chain fatigue issues, possibly leading to a larger required chain size. While it provides easier access for a ROV by sitting at a larger water depth compared to the fairlead tensioner, which will be discussed in the next section, the mooring line dynamics may make it very hard for the ROV to work and decrease the operational limits.

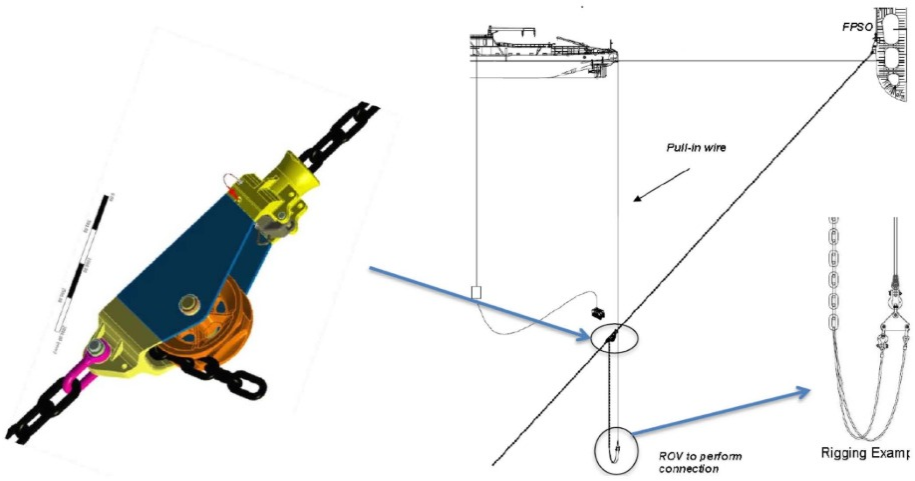

Figure 2.12: Example of an in-line tensioning system [67]

In-line subsea tensioning connectors

These connectors can establish a fixed length connection under tension underwater. After making the connection, they can be recovered and re-used. They are very cheap compared to a pull through connector as they use a chain-link or male-female connection. On the downside, it is a complex method and the time required to establish the connection is uncertain, making it difficult to plan a robust and predictable hook-up operation.

2.5.3. Pull through connector and fairlead chain tensioner

A Pull Through Connector (PTC) enables a relatively quick and efficient connection for hook-up operations. It is typically located on the floating platform and can eliminate the need for the upper segment of the mooring line, including the top chain, as fibre ropes can be connected directly. The installation vessel threads the mooring line through the PTC, which consists of male and female components. Its dual-axis rotational design facilitates flexible movement and allows for efficient disconnection when needed [12]. Unlike the dry chain-link method, the PTC allows connections to be made at a comfortable offset but is comparatively more expensive. An example of a PTC is shown in Figure 2.14.

The floating platform fairlead tensioner or chain stopper is mounted on the hull of the FOWT below the waterline. A benefit compared to the in-line tensioner, described in Section 2.5.2, is that the weight of the tensioner does not sit in the mooring line. However, the floating platform design must account for the tensioner and include sufficient structural support to accommodate its weight. Additionally, its location below the waterline in shallow water makes it challenging for an ROV to operate effectively, a limitation that also applies to a PTC. Figure 2.13 shows an example of a combined fairlead, chain stopper, and tensioner, specifically the Vessel Tensioner from Kongsberg Maritime. The fairlead tensioning method operates in much the same way as the in-line tensioning

method, with the main difference being the placement of the tensioner.

Figure 2.13: Example of a fairlead tensioner installed on the hull of a FOWT platform [39]

Figure 2.14: Example of a pull through connector [62]

2.5.4. Seabed and anchor tensioner

Seabed tensioners are placed in the static part of the chain section at the bottom of the mooring line. This ensures its weight is not carried by the floating platform and it does not impact the design of the platform. However, the FOW industry is not converging towards mooring systems that include a static part at the bottom, meaning this requirement may not be fulfilled. To achieve a static part at the bottom, the chain length has to be significantly increased, leading to higher costs [69, 12].

Anchor tensioners can be attached to gravity-based anchors and suction anchors. Apart from removing the weight from the floating platform, they also eliminate the clump weight effect on the mooring line. For both methods, the excess chain can be left on the seabed, and ROV operations are relatively easy. To make this method feasible, the anchor size and weight must be significantly increased. Both methods also require a long tensioning or work chain pre-installed on each tensioner line to ensure enough slack during the hook-up.

2.5.5. Operation durations and safe conditions

The tow-out and hook-up operation for FOWTs begins with the floating platform securely moored inshore and concludes with the offshore mooring being hooked up and tensioned. The entire operation may extend beyond 72 hours, making it essential to achieve intermediate safe conditions to ensure the predictability and safety of the operation.

The first safe condition, termed "unrestricted holding," is achieved after disconnecting the inshore mooring. This involves ensuring that the tow fleet has sufficient bollard pull to maintain its position under the given environmental conditions, either offshore with ample sea room or at a site sheltered from waves. For inshore holding, weather criteria are determined based on target site conditions agreed upon with the Marine Warranty Surveyor (MWS). Offshore holding weather criteria are defined in DNV-ST-N001 section 11, applying standard conditions unless the site is in a Benign Weather Area, which is currently not the case for most floating wind developments.

The second safe condition is achieved when a minimum number of mooring lines, typically three, are hooked up slack. This stage does not require the power cable to be connected, making the floating turbine offset non-critical, and thus tensioning and stretching are generally not critical for reaching this safe condition. When the tow fleet brings the FOWT into the field to begin the hook-up, it operates in "limited sea room" due to the proximity of other FOWTs and potentially offshore platforms. Design weather criteria for this stage are established based on the selected tow fleet and heading restrictions during hook-up. If bad weather is anticipated, the towed FOWT should be moved out of the field to an area with sufficient free sea room.

There is not an intermediate safe condition between the moment the first line is ready to be connected and the complete connection of all three lines. This means a sufficient weather window must exist so the operation can commit to completing the hook-up of all lines. The operational duration depends on various factors, including the capabilities and experience of the fleet and the equipment used for mooring lines, connectors, and tensioners. It is expected that the first two lines take around 10 hours, with the third hook-up around 14 hours followed by 6

hours of tensioning. These durations show the sensitivity of the operation to weather conditions, and should be kept in mind when defining a required top chain length and its corresponding operational limits.

In the case study of [5], the mooring system contained twelve mooring lines. The thirst three lines were initially hooked up without being tensioned. The hook-up of these lines took 10.75 to 12.75 hours per line. Line four to six were also tensioned, and took 13 to 16.75 hours per line. After the fourth line was hooked up and tensioned, the first three lines were reconnected to tension them as well, which took 5.75 to 7.5 hours per line. At the time of 4 lines connected and tensioned, a storm safe condition had been reached. It was stated that for a FOWT with six lines, three lines installed would be sufficient to arrive at a storm safe condition. The remaining six lines were also tensioned during the same operation as the hook-up, and took around the same amount of time as the sixth line, 13 hours, as the crew gained experience and were up to speed.

Afterwards, all twelve lines were pre-stretched using the bow string method. The stretch removal took 72 hours in total, with an average of two lines per 12 hour shift. It should be noted that the case study took place in very deep waters resulting in very long lines. The water depth was 1200 metres, which is not expected to be near the water depth range of FOWT parks in the near future, as discussed in Section 2.1.2. It was also stated that it is expected to be feasible to tension the mooring system of FOWTs to a higher level than necessary, as permanent stretch of polyester would occur over time, causing the tension to drop to the desired level.

2.6. Research gap

Most literature provides insights into the challenges associated with the installation and overall performance of Floating Offshore Wind Turbines (FOWTs) and their mooring systems. Hybrid, or semi-taut, mooring systems promise to be reliable solutions for FOWTs, as discussed in the literature review, which also identified several factors that require a certain amount of chain usage in hybrid systems. For the water below the sea surface, the performance of fibre ropes is primarily related to the implementation of protective covers and filters [15]. While studies have explored methods and effects of pre-stretching fibre ropes during installation, the relationship between pre-stretching and mooring design is not yet fully addressed. Although this research does not provide a detailed analysis of this aspect, it applies existing theory to the chosen hook-up method and sequence and explores how fibre stretch management could affect the required length of the top chain.

The literature describes numerous hook-up and tensioning methods for FOWTs [12, 69]. However, specific criteria regarding the required top chain length or its connection height to the floating platform are still lacking. This research aims to address these gaps by modelling the hook-up operation and establishing a relationship between the top chain length, connection height, and operational sea states.

3
Floating turbine and hook-up

This chapter introduces the reference floating wind turbine and its mooring system used in this research. The installation sequence and hook-up method considered in this study are explained in Section 3.2.

3.1. Reference application

The FOWT is located at a water depth of 265 metres, and its mooring system contains three hybrid mooring lines with a long middle polyester section and two chain ends. A 2D view of the FOWT and its mooring system is shown in Figure 3.1, highlighting the different components of a single line. Relevant dimensions are summarised in Table 3.1, with line lengths representing the unstretched length, and the pre-tension (PT) is expressed as a percentage of the chain's MBL. Individual dimensions of the semi-submersible platform, turbine and mooring materials are detailed below.

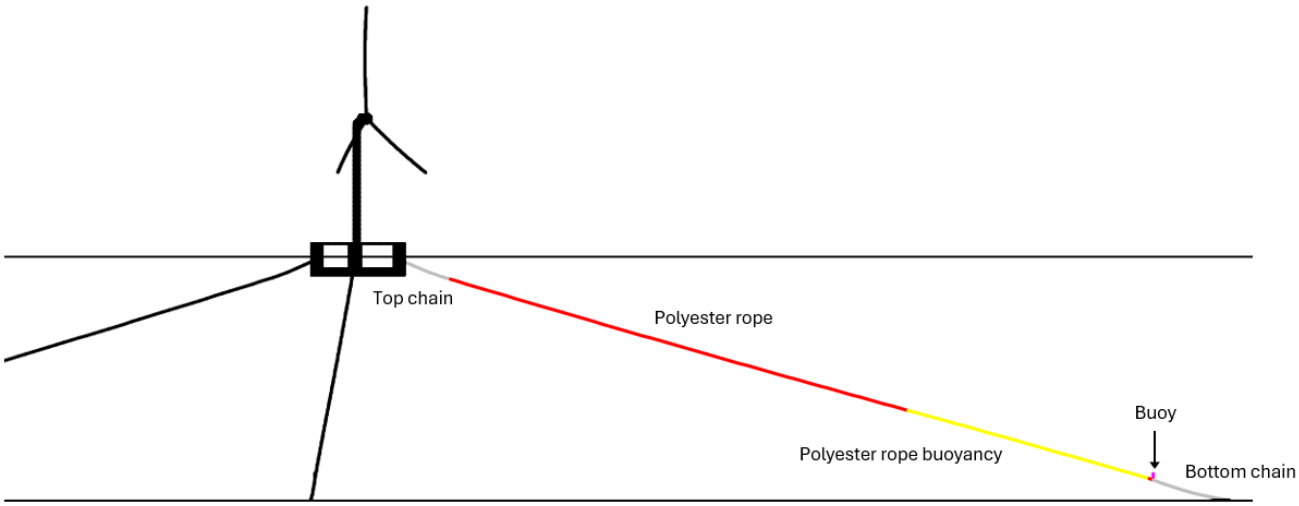

Figure 3.1: Reference FOWT application

Parameter	Dimension	Unit	Parameter	Dimension	Unit
Water depth	265	m	Polyester buoyancy length	300	m
Anchor radius	1,000	m	Bottom chain length	100	m
Top chain length	60	m	Total line length	969	m
Polyester length	508	m	PT	14.5	% MBL

Table 3.1: Dimensions of the reference FOWT application

Floating wind turbine

This study utilises the University of Maine (UMaine) VolturnUS-S 15 MW reference semi-submersible floating offshore wind turbine [1]. The choice of this turbine is based on its status as a publicly available model and its alignment with the expected minimum size of future floating wind turbines. The turbine has also been subject to extensive research, providing a solid base for future research. The data provides a semi-submersible platform

with three radially spaced columns and one central column, on which the tower of the 15 MW wind turbine is mounted. Details of the turbine and the floating platform are listed in Table 3.2, with specific dimensions illustrated in Figure 3.2.

Parameter	Value	Units
Turbine rating	15	MW
Hub height	150	m
Freebord	15	m
Draft	20	m
Platform mass	17,839	t
Tower mass	1,263	t
Total system mass	20,093	t
Hull displacement	20,206	m^3

Table 3.2: Details of the semi-submersible platform and wind turbine [1]

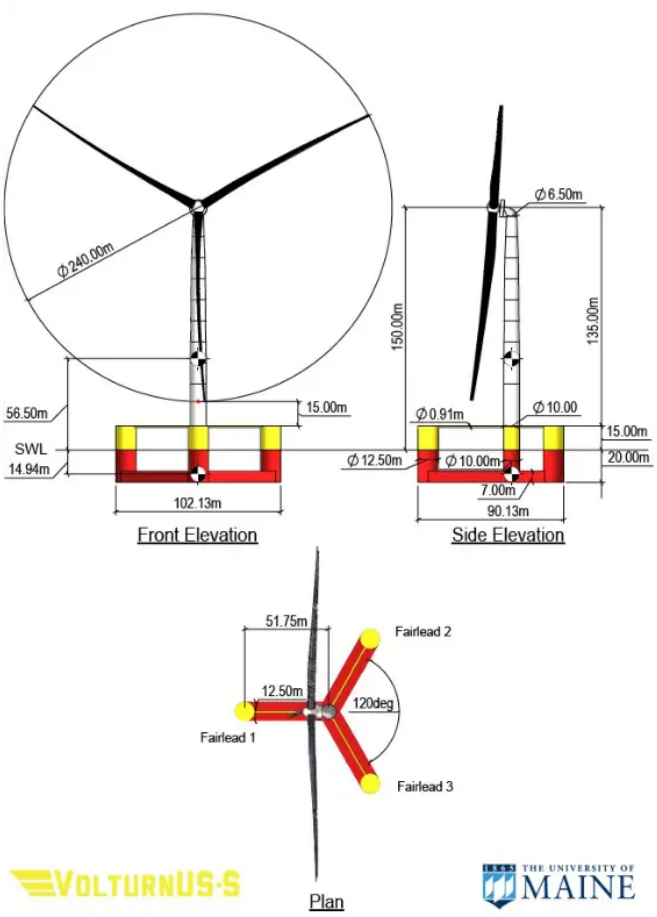

Figure 3.2: Dimensions of the VolturnUS-S platform and turbine [1]

Polyester rope

The lower section of the polyester rope includes a buoyant cover designed to prevent the line from making contact with the seabed. Details of the rope without the buoyant cover are provided in Table 3.3.

Parameter	Polyester Rope
Nominal diameter	210 mm
Axial stiffness	190,300 kN
MBL	14,710 kN
Weight	0.35 kN/m
Submerged weight	0.087 kN/m

Table 3.3: Properties of the polyester rope

Mooring chain
The characteristics of the mooring chain are listed in Table 3.4. The chain is a studless design with a nominal diameter of 175 mm. Figure 3.3 provides a perspective on the size of the links, highlighting their substantial size, weight, and the associated challenges in handling these chains.

Parameter	Value	Unit
Nominal diameter	175	mm
Axial stiffness	2.6×10^6	kN
MBL	1.8×10^4	kN
Weight	5.98	kN/m
Submerged weight	5.19	kN/m

Table 3.4: Mooring chain properties

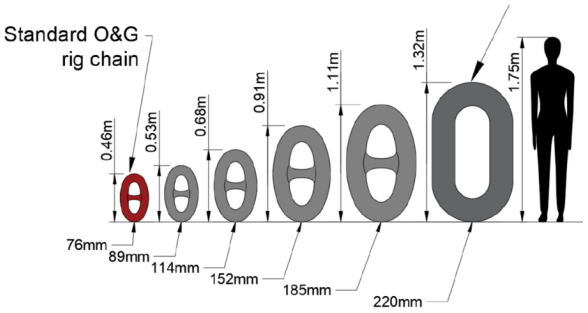

Figure 3.3: Chain size comparison

3.2. Installation

Different installation methods offer varying benefits and challenges, as outlined in Section 2.5. This study examines a three-line mooring system, where a dry chain link connection is preferred for the first two lines, while an off-vessel connection method is used for the third line. The reason for this distinction is that tensioning equipment, such as an inline or fairlead tensioner, is expensive. For large-scale deployments, the dry chain link method is expected to be financially advantageous. However, this method does not allow for tensioning of the mooring system, which is an important step to ensure the required PT is reached after the hook-up or pre-stretching. More detail is provided in Section 3.2.2. This study assumes that applying a pulling force to one of the three lines is sufficient to gain the necessary pre-stretch for the entire mooring system, and therefore two lines can be installed without tensioning equipment, while only the third line requires it.

This research assumes that for off-vessel connection methods in a three line mooring system, the use of permanent top chain is considered to be less critical compared to the dry chain link method. These connections are made in the water column, and temporary work chains or lines can be used to complete the connection. The need for permanent chain can even be eliminated by using temporary chains to tension the mooring system, resulting in a line consisting entirely of fibre rope, apart from the chain in the bottom segment of the mooring system. Section 3.2.2 discusses how pre-stretching could influence the required top chain length. However, this approach relies on the feasibility of pre-stretching all three lines of the mooring system by pulling a single line. This process and its underlying assumptions require further investigation, which is beyond the scope of this study. The detailed analysis in this research focuses on determining the required top chain length for the dry chain link method.

3.2.1. Installation sequence

This section describes the selected hook-up installation sequence applied in this research. The first two lines are referred to as fixed-length lines because their lengths cannot be adjusted after hook-up, unlike the third line, which incorporates a tensioning system. The first part focuses on the connection method of the first two lines, creating an H-link connection between the lower and upper segment of the mooring line on the deck of the Anchor Handling Tug Supply (AHTS) vessel. In this process, the upper segment of the top chain is attached to the floating platform, while the lower segment is pre-laid on the seabed.

Figure 3.4 illustrates the steps involved in connecting the FOWT to its mooring system. The floating turbine is towed to the site using tug boats (blue). The tow line of the tug boats could either be directly connected to the floating platform, or to the upper segment of the top chain. The lower segment of the mooring line is pre-laid well in advance of the hook-up operation. The AHTS vessel (black) connects to one of the upper segment top chains (3.4a) and positions itself above the first pre-laid fixed-length mooring line (3.4b). For the fixed-length lines, it is preferable to position the vessel as close as possible to the anchor to create slack in the pre-laid mooring line. After the connection is made, the procedure is repeated for the second and third lines (3.4c and 3.4d). During the hook-up, tugboats assist with station keeping to restrict the displacements of the floating turbine.

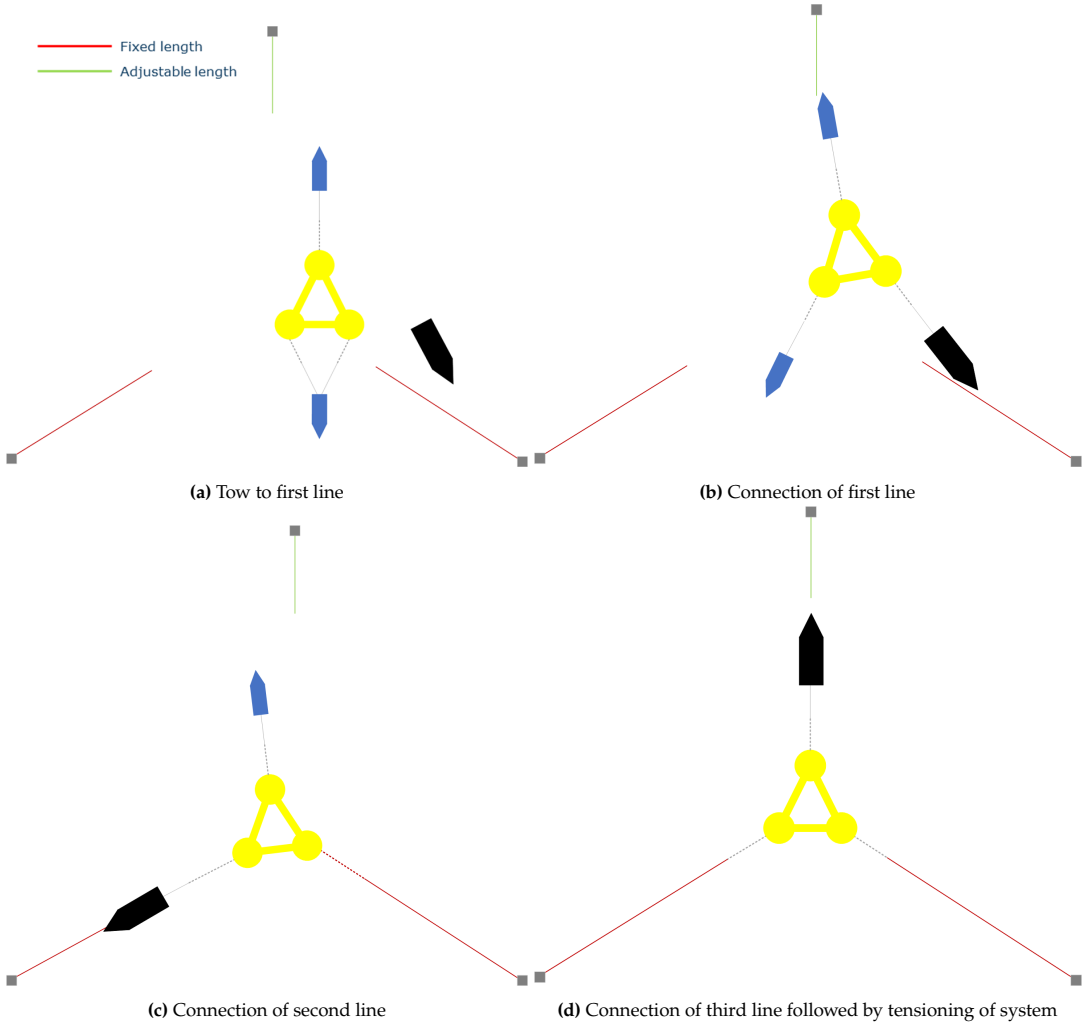

(a) Tow to first line

(b) Connection of first line

(c) Connection of second line

(d) Connection of third line followed by tensioning of system

Figure 3.4: Hook-up sequence

Figure 3.5 shows the installation steps of creating an H-link connection on the deck of the AHTS. The grey dotted line resembles chain, the red line polyester and the green line a work line or recovery wire. First, the upper segment of the chain is gathered onto the AHTS using the ROV and connected to a winch. The winch is paid out to maintain a slack line (3.5a and 3.5b). Then the ROV recovers the pre-laid mooring line and the line is laid on the deck and locked into shark jaws (3.5c and 3.5d). The AHTS reverses towards the floater by paying in on the winch until the upper segment of the chain can be locked into the shark jaws as well (3.5e). Once both chain ends are locked, the H-link connection is made.

At this stage, the upper segment chain length becomes critical, as it forms a fixed-length connection between the floating turbine and the AHTS. High tensions or an overly taut chain could cause significant issues or even lead to failure. It is essential for the chain to have sufficient length to maintain adequate sag while avoiding overly conservative estimates. For large-scale projects, even a few extra metres of chain per line could provide significant benefits in terms of cost savings. The same considerations apply to the operational limits of the hook-up procedure. Once the connection is made, the mooring line is attached to the winch and deployed (3.5f). The second line follows the same procedure. The third line is connected using either a sea-bed, in-line or fairlead

tensioner, which is described in more detail in the next Section.

It should be noted that these steps represent a subset of the full installation process for creating the H-link connection. Certain procedures, such as checking for twist in the line, are not included in this description.

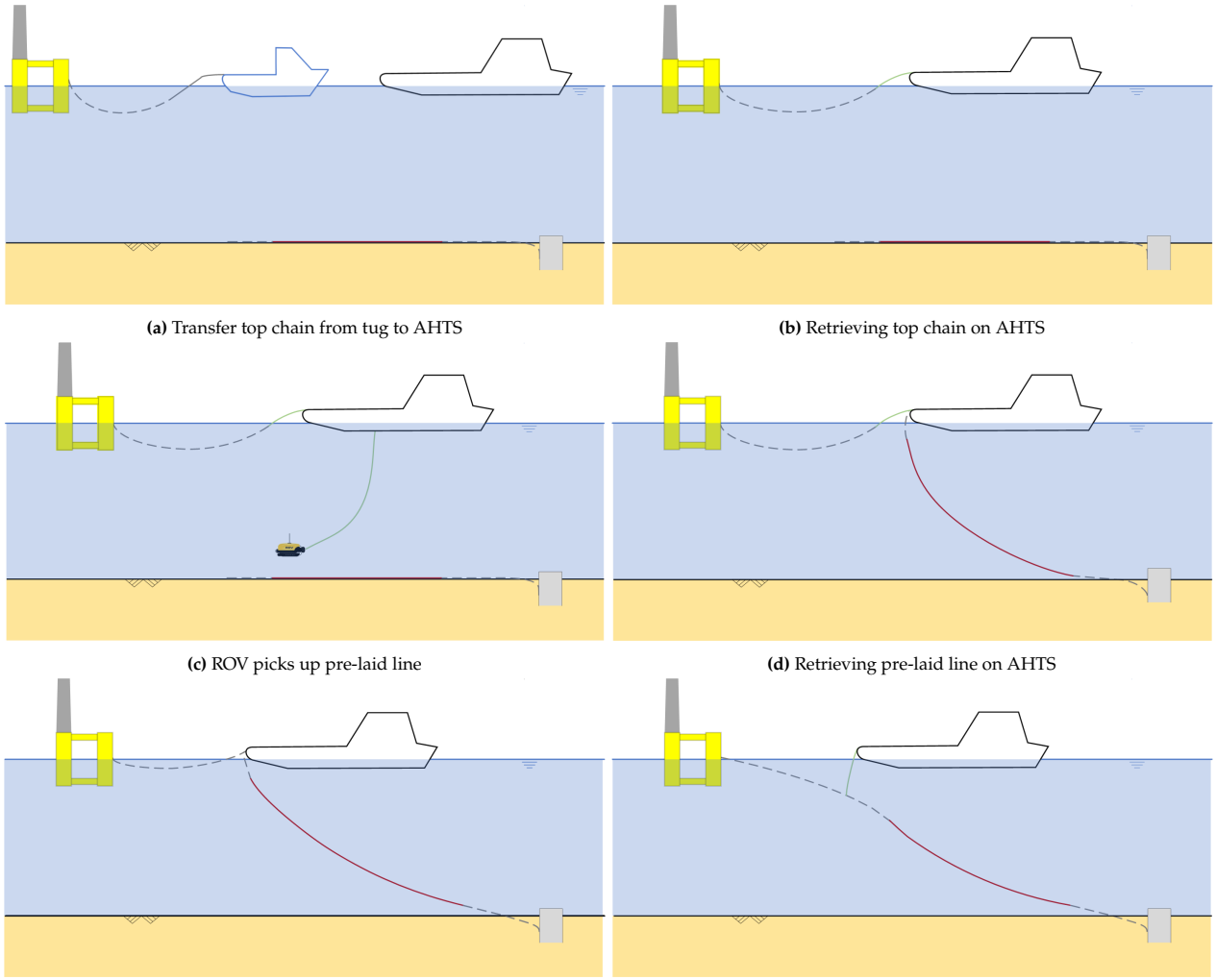

(a) Transfer top chain from tug to AHTS

(b) Retrieving top chain on AHTS

(c) ROV picks up pre-laid line

(d) Retrieving pre-laid line on AHTS

(e) H link connection is made

(f) Mooring line is deployed

Figure 3.5: Dry chain link connection sequence

For this installation method, the chain length required depends on both segments of the mooring line. For the bottom segment, the critical factors include avoiding contact between the fibre ropes and the stern of the vessel, as well as preventing contact between the line and the thrusters of the AHTS. For the upper segment, the requirements are primarily influenced by the distance between the AHTS and the FOWT and the vessel's ability to maintain a fixed distance during installation. Further details are provided in Section 4.3.2.

3.2.2. Tensioning and pre-stretch

The mooring system of a FOWT should achieve a specific PT once installation is completed. After the third and final mooring line is connected, a tensioner is used to establish the desired PT. As highlighted in the literature review in Section 2.3, managing the stretch removal of fibre ropes is a critical part of the installation process. The two main parameters during this operation are the maximum load in the line and the holding duration at this load. The remaining part of this section focuses on polyester.

The management of polyester rope length and elongation is a complex aspect, and a thorough understanding of its properties and behaviour is essential to successfully apply pre-stretching when installing a FOWT. Rope lengths must be defined at various tensions to account for different stages, including installation, start-of-life and end-of-life conditions. As polyester elongates over time, its quasi-static stiffness increases, which affects critical design parameters such as floater offsets. Key properties, including quasi-static stiffness, dynamic stiffness, and

strain behaviour, are determined based on lifetime mooring loads. The end-of-life strain is then used to calculate back what rope length should be applied that fits all stages of its life time.

When stretch removal is applied, both elastic and plastic elongation occur in the polyester rope, resulting in a permanent increase in length. In the context of the mooring system, this increased rope length reduces the system's PT. However, as previously discussed, this issue can be addressed by designing and defining the rope length for various stages of its lifetime. By accounting for pre-stretching during the design process, the required PT can be maintained without the need for significant re-tensioning. When aiming to reduce chain length, the stretch in the polyester rope could be accounted for in the top chain's design. By shortening the top chain to compensate for the expected stretch, the desired total mooring line length can be achieved after pre-stretching, resulting in a smaller chain-to-polyester ratio. If slight adjustments of the PT are still required, the tensioner of the third mooring line can be used. Re-tensioning can be achieved using a temporarily chain, removing the need for sufficient spare top chain. Figure 3.6 demonstrates an example of an inline tensioner in use. It shows how the connection between the lower and upper segments is established, as well as the use of a temporary chain, represented by the black line.

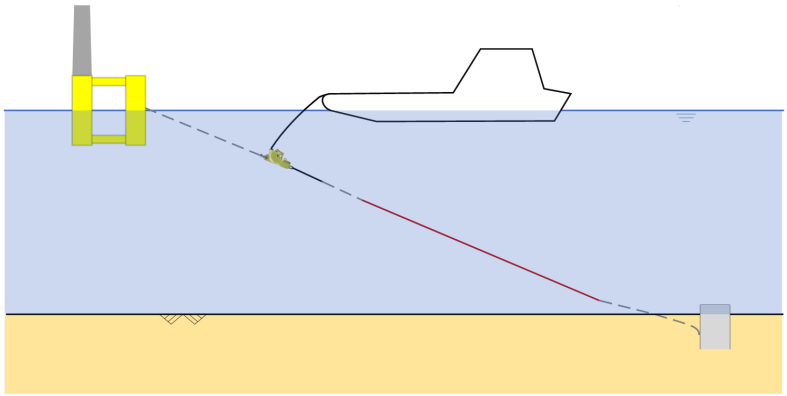

Figure 3.6: Use of an inline tensioner and temporarily chain

It is evident that pre-stretching plays a vital role in mooring design. Figure 3.7 illustrates the relationship between the tension applied during installation and the resulting rope elongation. This relationship is visualised using the Syrope model, where increase in tension leads to a shift to a new working curve for the polyester rope. The values presented in the figure are based on literature and internal testing conducted by Seaway7. The additional elongation values are determined based on the rope returning to the same PT. The allowable stretch and resulting elongation are influenced by factors such as the specific tension, project requirements, and material properties. The example using the Syrope model is provided solely to illustrate what this could mean for mooring design and top chain length.

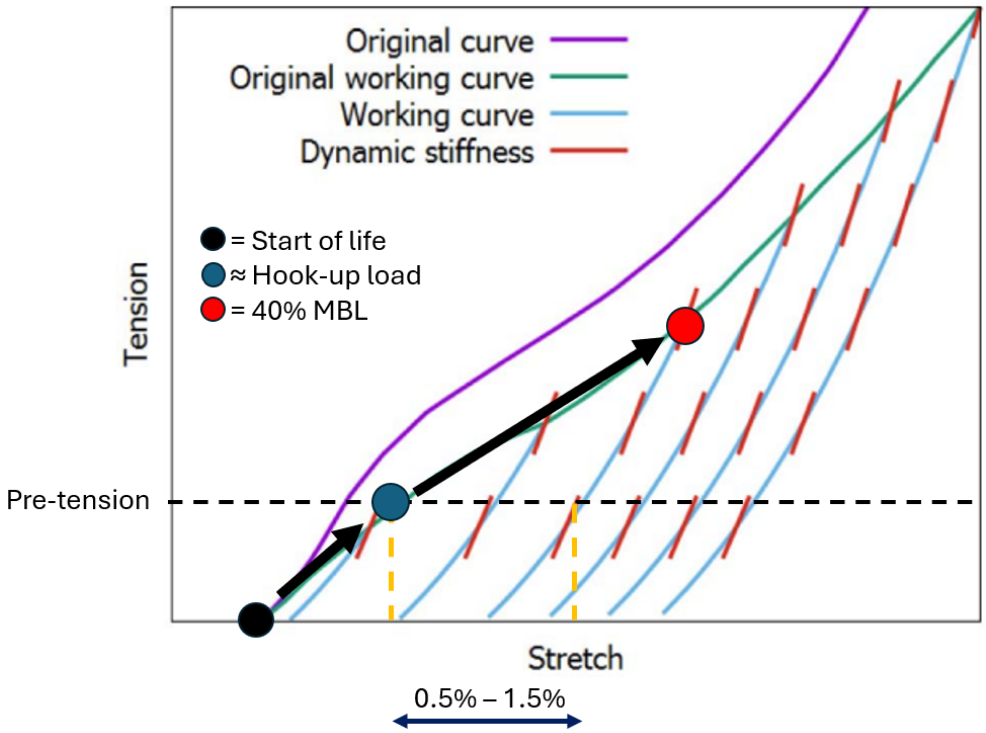

Figure 3.7: Elongation of polyester due to pre-stretching

The black arrows in the figure represent the shift on the original working curve, corresponding to the maximum tension that has been applied to the polyester rope. The resulting stretch at the desired PT level is determined by tracing the working curve downwards. The distance between the two dotted orange lines indicates the amount of permanent stretch induced in the polyester rope due to pre-loading up to 40% MBL, compared to the stretch after hook-up. The range of this elongation is given as 0.5% to 1.5%, serving just as an indication. The difference is highly dependent on the material properties, the duration of applied tensions and the hook-up and tensioning methods used. The 0.5% additional elongation is primarily based on the findings from the study shown in Figure 2.10 [43], where an initial loading of 26% MBL was applied. This loading is expected to be significantly higher than typical loads during hook-up, indicating that the PT in the system was substantial after the hook-up process. The upper limit of 1.5% is derived from tests performed in [23], corresponding to a low holding time in their tests.

The high initial load reported in [43] presents a beneficial situation if such a high load can be achieved during the hook-up process. In Figure 3.7, this would correspond to moving the blue point upward along the black arrow. Ideally, the blue point would reach the original working curve above the right dotted yellow line. From this position, if the rope is subsequently loaded and held at 40% of its MBL, the tension-stretch relationship would follow the working curve downward, starting at the red point and stabilising at the desired PT level. This would remove the need for re-tensioning the system after loading the line up to 40% MBL.

4
Method

This chapter outlines the methods and tools used in this research. Model inputs are described, followed by the modelling choices and assumptions made during the analysis. Additionally, the different sections of the top chain are identified and illustrated, each with its own criteria for evaluation.

4.1. Methodology

This section outlines the methodology used to analyse the dynamics during the hook-up operation of a FOWT. For the hook-up operation, specifically for the dry chain link connection method, the objective is to establish a relationship between the top chain length, the connection height of the chain to the FOWT, and the operational design limits. OrcaFlex is used as a tool to guide this analysis, providing a platform for developing a model that simulates the hook-up operation. As described in Sections 3.2.1 and 4.4.3, during the hook-up of the mooring lines, station keeping of the floating turbine is provided by two tug boats. The top chain must not contribute to the force equilibrium, as slack in the line is required to ensure safe working conditions on the installation vessel. This means that the tug boats must counteract the loads caused by wind and waves, as further detailed in Section 4.4.3.

Input variables include the length of the top chain, the vessel type, the tug assistance, environmental loads and the FOWT itself. Ideally, during real-life operations, the installation vessel would follow the displacements of the floating turbine. This can be achieved using its dynamic positioning (DP) system, incorporated with a system measuring the relative distance, to maintain a consistent distance from the floating platform. Further details on this approach are described in Section 4.4.2.

Two types of calculations, distinguished by how vessel and floater motions are handled, model the hook-up operation in OrcaFlex: Displacement RAOs and Load RAOs. The difference lies in how the motions and loads experienced by the floater and vessel are defined and applied. Displacement RAOs describe the first order harmonic motions of the vessel and floater in response to incoming waves, encompassing all six degrees of freedom (DOF) [51]. These motions are predefined as amplitudes and phases for a range of wave periods and directions. In this method, the vessel and floater's motions are superimposed on their primary positions, and no external station-keeping tools, such as mooring lines or tugboats, are required. This approach does not account for external forces or dynamic interactions, providing a controlled representation of vessel and floater motion.

Load RAOs, in contrast, define the first order wave forces and moments acting on the vessel and floater due to incoming waves. The motion of the floater and vessel are calculated based on these forces and moments. In this method, the vessel and floater interact through the top chain. Without station keeping measures, such as tugboats or a DP system, the vessel and floater would drift away under the influence of environmental forces.

Figure 4.1 illustrates the six DOF that apply to both the vessel and the floater. In summary, the Displacement RAO method prescribes harmonic motions for all six DOF around their initial position, while the Load RAO method calculates motions dynamically based on wave forces, allowing for more realistic interactions between the vessel, floater, and mooring components. Further details on the applications and advantages of these methods are discussed in 4.4.2.

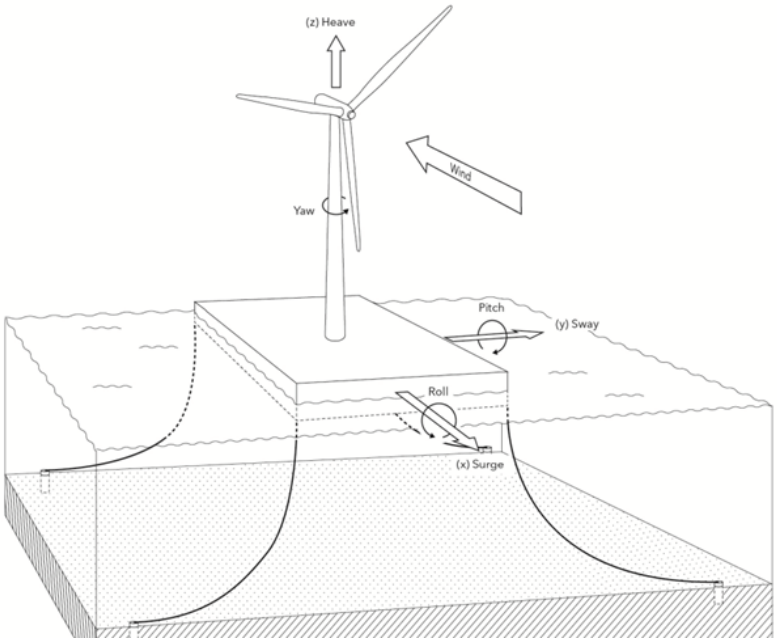

Figure 4.1: Degrees of freedom of a FOWT [18]

Simulations are performed in both the frequency and time domains. In the frequency domain, lines and other objects do not influence the expected behaviour of a vessel or FOWT. However, it provides the maximum expected responses for all six degrees of freedom, based on a specified storm duration. In the time domain, both the Displacement RAO and Load RAO methods are applied.

The Displacement RAO method forms the foundation for developing a functioning model, ensuring that its behaviour aligns with expectations. This method serves as the basis for further refinement and analysis. Frequency domain simulations determine the six degrees of freedom of both the installation vessel and FOWT for waves varying in direction, height, and period. These results identify workable sea states and guide the selection of cases for more detailed investigation.

Subsequently, the Load RAO method in the time domain is the primary approach used to analyse the dynamics of the vessel, floater, and top chain. It also verifies the correspondence between the behaviour predicted in the frequency domain and the observed dynamics in the time domain.

4.1.1. OrcaFlex

The analysis of the operation is performed using OrcaFlex, a specialised dynamics software designed for offshore marine applications. OrcaFlex is capable of solving six-degree-of-freedom rigid body motions for vessels and offshore platforms, as well as performing finite element modelling for line structures such as mooring lines and risers. It supports simulations in the time domain, using both explicit and implicit numerical methods to solve for non-linear system behaviour, as well as analysis in the frequency domain for linearised problems. The software incorporates both first- and second-order wave load transfer functions, allowing for detailed modelling of wave-structure interactions [47].

The hydrodynamic model of the VolturnUS semi-submersible platform was created using OrcaWave, a diffraction analysis tool that complements OrcaFlex. This model includes frequency-dependent added mass, radiation damping, wave response amplitude operators (RAOs), and second-order quadratic transfer functions (QTFs) [49, 66].

The mooring lines are modelled using OrcaFlex's finite element capabilities, capturing inertial, elastic, and hydrodynamic forces in multiple degrees of freedom. OrcaFlex's line-type wizard is used to define chain properties such as geometry, mass, and strength, in accordance with established standards. The line types for the mooring chain and polyester rope are derived from a reference project, which also utilised OrcaFlex's line-type wizard. DNV code checks are also included in the OrcaFlex software. It offers a wide range of objects next to rigid bodies and lines, such as winches, links, springs and turbines. Environmental factors, such as sea state, seabed characteristics, wind, waves, and currents, can also be incorporated into the simulation.

OrcaFlex provides built-in interfaces for Python and Excel, enabling both pre-processing and post-processing of simulation data. The Python interface allows for automated setup of simulations, data extraction, advanced analysis, and custom scripting. The Excel interface facilitates direct input of model parameters and export of results for further processing. These tools are used to enhance efficiency and flexibility throughout the analysis.

4.2. Acceptance criteria

The main acceptance criteria are based on the installation vessel's behaviour, the distance between the floater and installation vessel, the tension in the top chain and the angle of the lower segment of the mooring line to the thrusters of the installation vessel.

With significant wave heights in the range of 2 to 3.5 m, it is expected that the maximum roll, pitch and yaw rotations of the installation vessel will be based on workable limits. Green water, which refers to the overflow of waves onto the deck, is not accounted for in this research. However, according to [58], the significant wave height limit for green water for AHTS vessels is often between 4 and 6 metres. The maximum allowable values for roll, pitch and yaw values are listed in Table 4.1. These values have been reviewed with Seaway7 and align with findings from the literature [35].

Contact between the lower segment of the mooring line and the rudders, thrusters, or keel of the AHTS must be avoided, as it is deemed unacceptable. A limit has been established to prevent such contact, defined by the angle of the mooring line relative to vertical, as shown schematically in Figure 4.2. This angle is limited to approximately 30 degrees and differs slightly for each vessel. For this criterion, it is assumed that the AHTS vessel is aligned with the mooring line being hooked up. While this was less of a concern in the oil and gas industry, the shallower water depths typically associated with FOWTs could result in the 30-degree limit being exceeded, depending on the installation method.

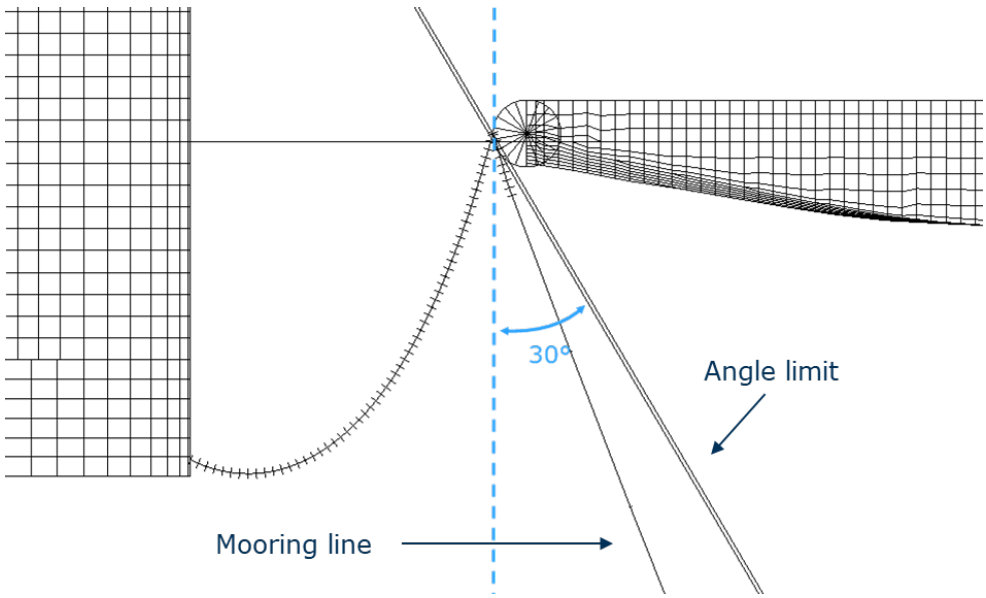

Figure 4.2: Mooring line angle to AHTS thruster and rudders limit

According to DNV-ST-N001, DP vessels must maintain a safe clearance from nearby offshore structures, other DP vessels, or any obstructions. This clearance, whether above or below the surface, must be no less than 10 metres at all times [19]. During the hook-up operation, the initial distance between the installation vessel and the floater should be larger than 10 metres to ensure a margin above this minimum requirement.

The tension in the top should ideally remain as low as possible throughout the installation. While no strict limit on chain tension is defined, the primary focus is on minimising the dynamic tension variations relative to the static state. The chain must remain slack; any instance where it becomes taut is deemed unsafe, and the operation would no longer meet safety criteria. The limits discussed in this section are summarised in Table 4.1.

Parameter	Critical value	Unit
Vessel roll	5	°
Vessel pitch	3	°
Vessel yaw	10	°
Angle, mooring line to vessel thruster	30	°
Vessel to floater distance	>10	m

Table 4.1: Acceptance criteria

4.3. Model input data

4.3.1. Environmental loads

Both wind and wave loads are incorporated in this study. As described in 2.4.1, FOWT applications are expected to be installed in regions with large sea states. It is therefore recommended that the hook-up operations of floating wind turbines are feasible in conditions with at least $H_s = 2$ m, and preferably higher. The significant wave height, wave period, and wave direction vary throughout this research, enabling an investigation into the relationship between top chain length and wave conditions. H_s ranges from 2 metres to 3.5 metres, T_p ranges from 4 to 16 seconds, and the wave direction is adjusted in 30-degree increments from 0 to 180 degrees. The headings are visualised in Figure 4.3. The combinations of wave height and period are based on data from an offshore area potentially suitable for a floating offshore wind farm. This area is located in the North Sea, off the Norwegian coast. Figure 4.4 illustrates the data of the wave height and period, with the colour scale representing their relative occurrence as a percentage of all data points.

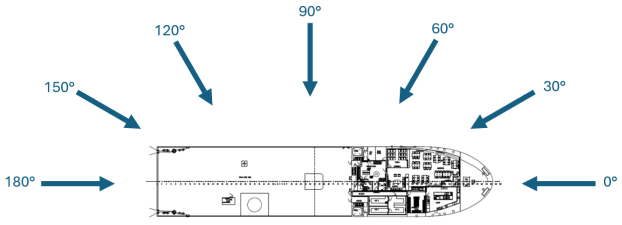

Figure 4.3: Wave headings relative to the installation vessel, top view of the vessel adapted from [53]

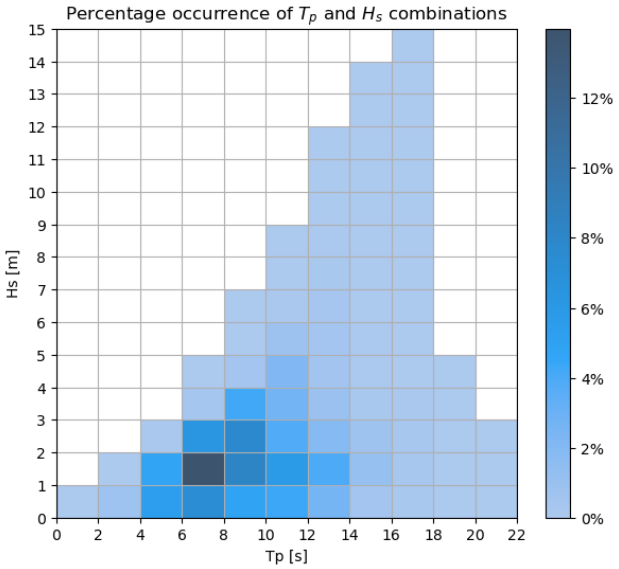

Figure 4.4: Percentage distribution of wave periods and heights from measurements taken in the North Sea, off the Norwegian coast

The waves are modelled using a JONSWAP spectrum. Based on H_s and T_p, the value of the peakedness parameter γ is calculated as prescribed by DNV. The calculation of gamma for North Sea conditions is given in Equation 4.1.

$$\gamma = \begin{cases} 5.0 & \text{if } \frac{T_p}{\sqrt{H_s}} \leq 3.6 \\ 1.0 & \text{if } \frac{T_p}{\sqrt{H_s}} \geq 5.0 \\ \exp\left(5.75 - 1.15 \cdot \frac{T_p}{\sqrt{H_s}}\right) & \text{otherwise} \end{cases} \tag{4.1}$$

For a specified wave direction, a spreading of cos^4 is included to create a distribution of wave energy and avoid concentrating all energy in one specific direction. To limit the number of variables, wind is assumed to have a constant speed of 10 m/s aligned with the wave direction. The relationship between wind speed, wave period,

and wave height depends on multiple factors and varies by location. Figure 4.5 illustrates this relationship as defined in DNV-ST-0111 [19], showing that a wind speed of 10 m/s corresponds to H_s values ranging from 2 m to 3.5 m. No current is applied in the model.

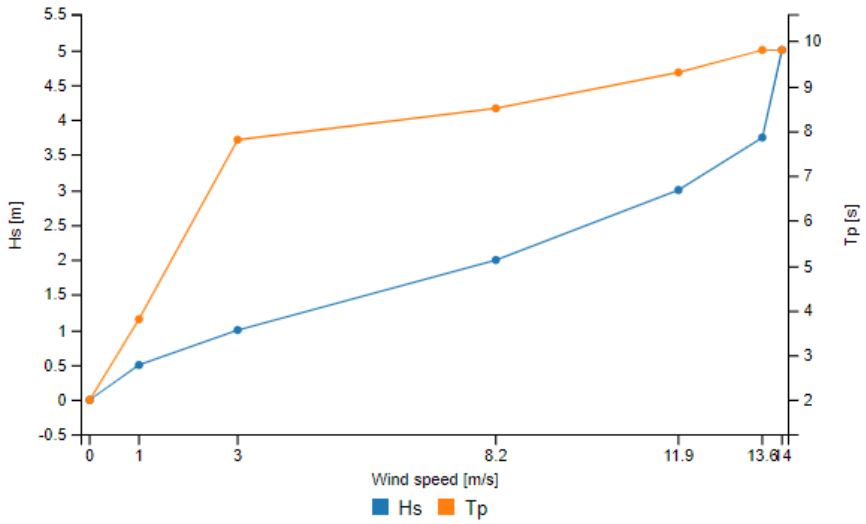

Figure 4.5: Wind-wave relation according to DNV-ST-0111 [19]

FOW example area

The significant wave heights from hourly measurements taken in the North Sea, as used for determining combinations of H_s and T_p, are presented in Figure 4.6 for three arbitrary years, with one data point per hour. These wave heights highlight the necessity of installing FOW farms in relatively high sea states. The case in Korea (Section 2.4.1) further supports the importance of developing the capability to operate and install under challenging sea conditions.

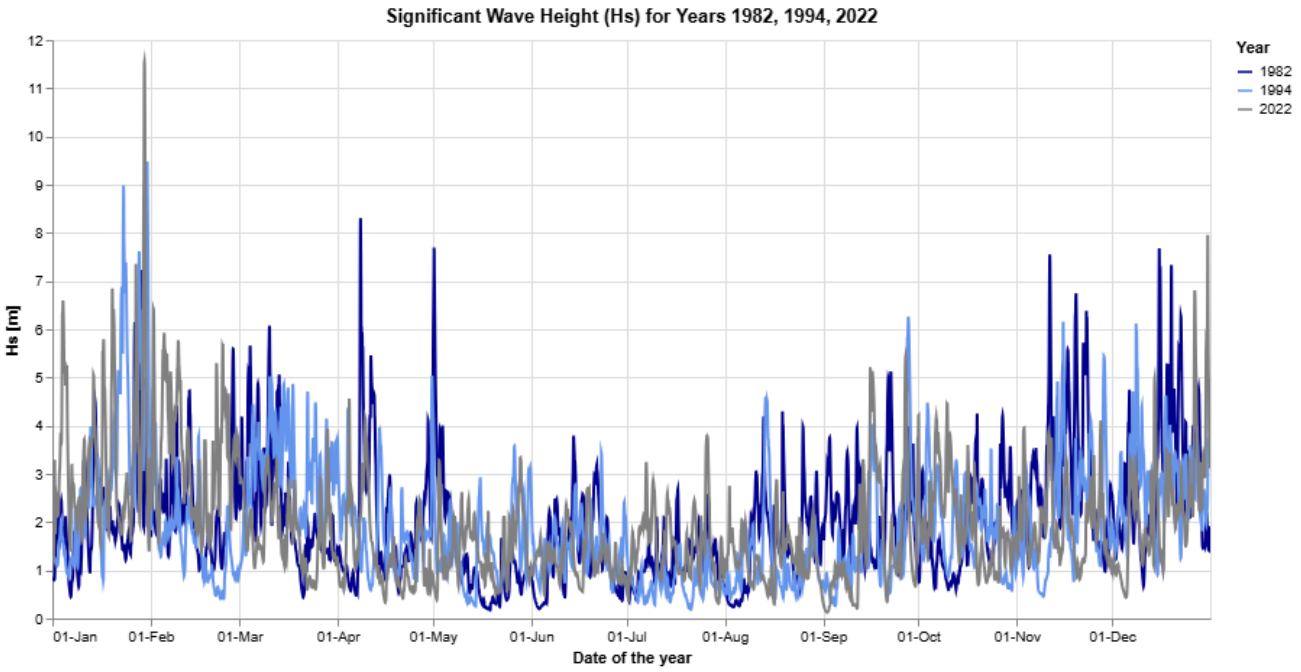

Figure 4.6: Significant wave height at a potential FOW farm area

4.3.2. Top chain length

The top chain is divided into three distinct segments, each with individual criteria for their required length. These segments are visualised in Figure 4.7, followed by an explanation of the method used to determine their length.

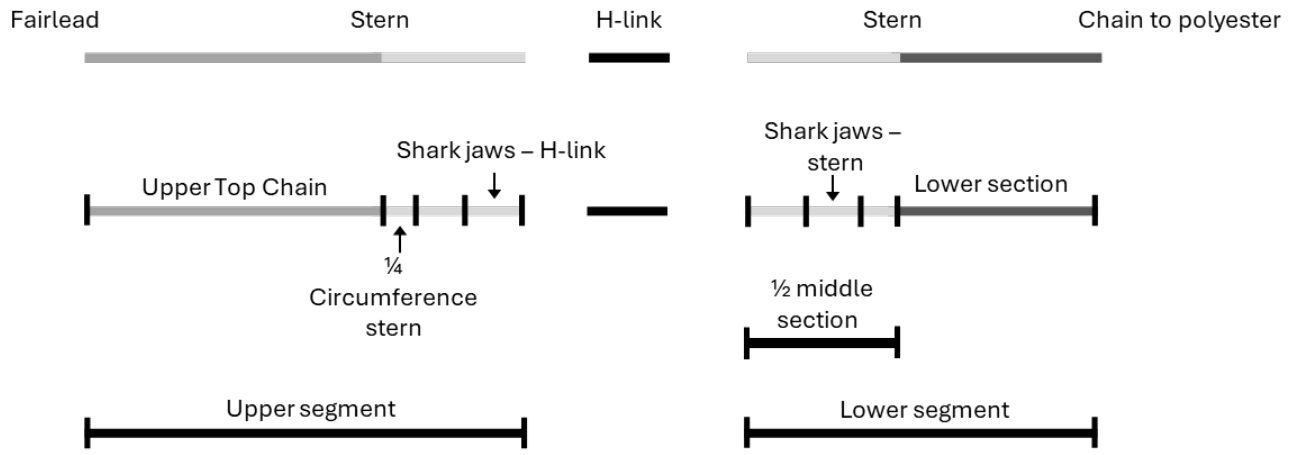

Figure 4.7: The total top chain divided into three distinct sections, each analysed individually

Upper top chain

The upper top chain (UTC) covers the part of the top chain between the connection point at the floater and the stern roller of the installation vessel. This section is also illustrated in Figures 4.2 and 4.13. The dynamic behaviour of this part is analysed through the model of the hook-up operation created in OrcaFlex. Analysis in both the time and frequency domains leads to the formulation of an approach to determine a range for the required UTC length. The approach is based on the maximum displacements of both end points of the UTC, expressed as their largest deviations in the x, y, and z directions from their static positions. These deviations account for both translational and rotational motions of the vessel and floater. The approach is visualised in the diagram in Figure 4.8.

The maximum displacements of the end points of the UTC in the x, y, and z directions are calculated in the frequency domain. Specifically, the Most Probable Maximum (MPM) values over a 3-hour storm duration for the x, y, and z positions of both the UTC endpoints, relative to their static positions, are used to determine the required UTC length. In the diagram, these variables are represented by the MPM of either X_{vessel}, Y_{vessel} and Z_{vessel} or X_{floater}, Y_{floater} and Z_{floater}, where 'vessel' and 'floater' denote the respective connections of the chain end. As the frequency domain primarily relies on the RAOs of both the vessel and the floater, along with the wave spectrum, it significantly reduces computational effort compared to time-domain simulations. This allows for a relatively quick way of determining the UTC length.

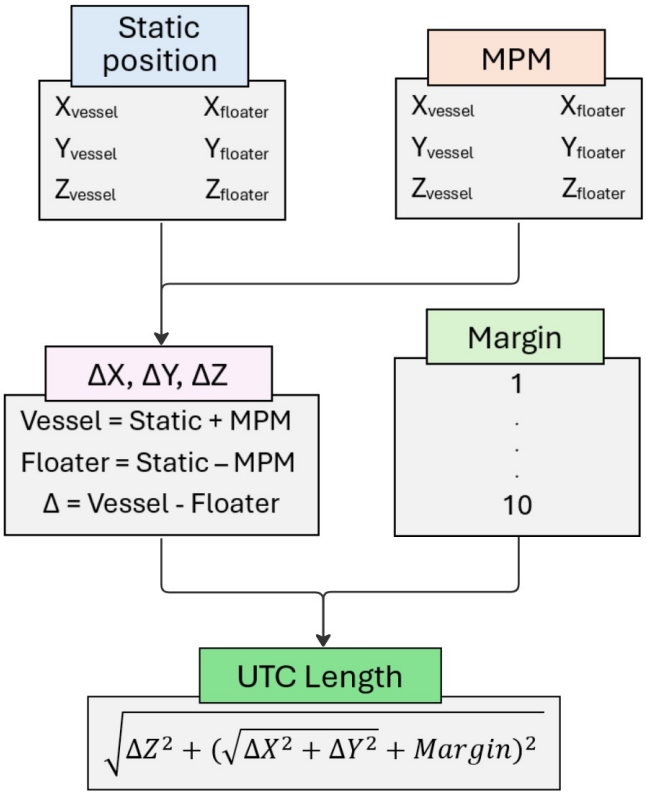

Figure 4.8: Calculation of upper top chain length through frequency domain results

The approach assumes the offset of both UTC end points occur in exactly opposite directions. Therefore, the MPM values of the vessel are added to their static position, while for the floater, these are subtracted. Subsequently, a margin is added to the 2D distance between the UTC endpoints. This margin accounts for typical DP system accuracy, operational uncertainties, and potential errors during installation. It is derived from the findings in the literature discussed in Section 2.4.1 and considers the typical water depths and sea states expected during the hook-up operation of floating wind turbines. The margin adds to the combined x and y deviations in completely opposite directions for both UTC ends. The installation vessel will aim to maintain a fixed distance to the floating turbine during the hook-up operation. The margin ranges from 1 to 10 metres, where a 1-metre margin accounts for the DP accuracy of the vessel relative to the floater, and a 10-metre margin assumes both the vessel and the floater drift an additional 5 metres each in opposite directions. For real-time operations, it is recommended that expected deviations in translation specific to the operation be considered and translated into an appropriate margin.

The UTC length is calculated as the 3D distance between the endpoints. Choosing an UTC length that precisely matches the distance between its endpoints would result in a taut chain, which is highly undesirable. While extreme opposite motions between the floater and the vessel are highly unlikely to occur, incorporating these values into the starting positions creates a configuration where the chain includes a sag. During time-domain analyses, it was observed that the floater and vessel rarely move completely out of phase during simulations, meaning their maximum potential displacement difference (assuming extreme opposite motions) tends to be significantly larger than the actual difference observed in the simulations.

The calculated chain lengths are applied in time-domain analyses to verify that the expected behaviour is achieved, with UTC tensions remaining close to their mean and static values. Various cases are distinguished to analyse the dynamic behaviour of the upper top chain under varying conditions. The following variables are adjusted: H_s, T_p, the connection height of the UTC to the floater, the starting distance between the vessel and the floater and the vessel type. An overview of these cases is listed in Table 4.2. For Case 6, the middle connection height does not actually correspond to the middle of the floating platform. Instead, it is positioned at the same height as the connection at the vessel, representing a scenario with no height difference between the UTC's endpoints. A combination of H_s = 2 m and $Waveheading$ = 60° is predominantly used, as it represents favourable conditions for the primary installation vessel employed in the dynamic simulations. Higher sea states often exceed workable limits, making them less representative of real-time operational scenarios. Further details about the vessel are provided in Section 4.3.4.

Although the required UTC length varies depending on T_p, the length corresponding to the largest T_p value is applied uniformly across all models within a single case. For most models, this results in a UTC length that is longer than required based on the proposed approach. This simplification avoids the additional effort of repositioning the tug boats to match each adjusted chain length, to ensure a consistent starting distance of 20 metres between the vessel and the floater. However, in real-world operations, the design and length of the top chain would likely be based on the worst-case scenario and applied uniformly across all FOWTs, meaning individual lengths corresponding to low H_s or T_p values would not be applied. This limitation applies to all cases except Case 7.2, where the UTC length is adjusted per T_p according to the approach. This allows to compare the results with Case 7.1, where the same UTC length was applied throughout all T_p values.

In Case 8, a margin of 10 metres is applied to both the UTC length and the 2D starting distance between the floater and the vessel. This simulates a scenario where the distance between the vessel and the floater increases by the margin, done to verify if the expected behaviour is still achieved under these conditions.

Case	Wave heading [°]	Hs [m]	Tp [s]	Starting distance [m]	Connection height	Δz [m]	Margin [m]
1	60°	2.0	4-16	20	Bottom	19.5	1
2	60°	2.0	4-16	20	Bottom	19.5	10
3	60°	2.0	4-16	15	Bottom	19.5	10
4	60°	2.0	4-16	15	Bottom	19.5	1
5	60°	2.0	4-16	30	Bottom	19.5	1
6	60°	2.0	4-16	20	Middle	0.0	1
7.1	60°	2.0	4-16	20	Top	13.5	1
7.2*	60°	2.0	4-16	20	Top	13.5	1
8**	60°	2.0	4-16	30	Bottom	19.5	10
9	0°	3.0	4-16	20	Bottom	19.5	1
10	30°	3.0	4-16	20	Bottom	19.5	1
11	60°	3.0	4-16	20	Bottom	19.5	1

Table 4.2: Summary of input variables for validation models (*UTC length is adjusted per peak wave period, **Margin is added to both UTC length and starting distance)

Middle section

This section covers the distance between the stern roller connection point of the UTC to the H-link, as well as the distance from the H-link back to the stern roller for the lower segment. Both the lower and upper segment make contact with the stern and the deck of the AHTS before being locked into the shark jaws. Beyond the shark jaws, sufficient chain is required to connect the H-link between the two segments. A top-view sketch of a section of the deck of an AHTS vessel is provided in Figure 4.9. The stern roller is located on the left side of the sketch, which in this case has a radius of 2 metres. The distance from the stern roller to the shark jaws is 4 metres, and an estimated additional 4 metres of chain is required beyond the shark jaws for both segments. These distances correspond to the deck layout of AHTS 1. The tow pins are used to guide the chain during operations, preventing excessive lateral movement.

For this vessel, the total amount of chain required on the deck and stern roller is calculated as two times 4 m, plus a quarter circumference of the stern roller. Thus, the total chain length on the deck per segment is calculated as follows:

$$\text{Length} = \text{quarter circumference of the stern roller} + \text{distance stern to shark jaws} + \text{length beyond shark jaws}$$

$$= \frac{\pi \times \text{diameter}}{4} + 4 + 4 = 11.15\,\text{m}$$

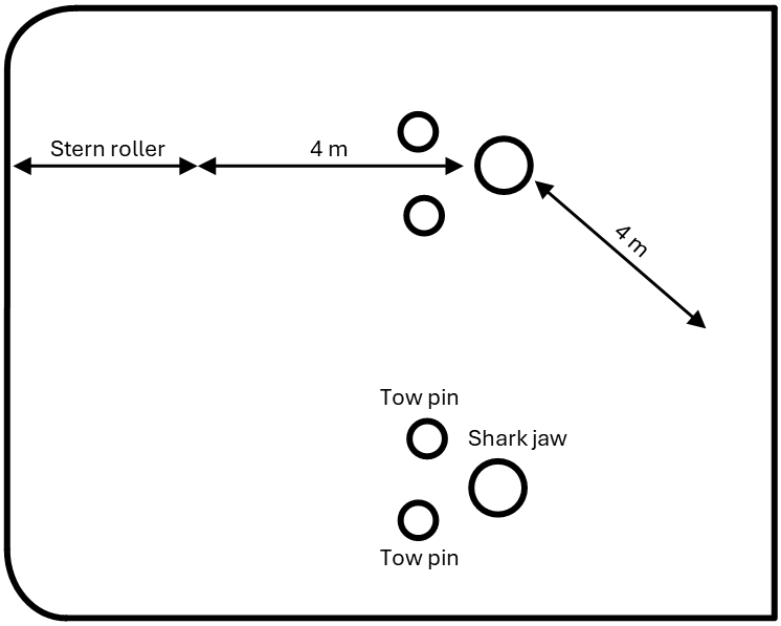

Figure 4.9: Chain length on the deck of an AHTS

Lower section
This section covers the part between the stern roller and the chain to polyester connection. The lower segment of the mooring line must avoid contact with the rudders or thrusters of the installation vessel. To ensure the 30-degree limit relative to the vertical is not exceeded, a few additional metres of chain are necessary. The additional chain weight helps maintain this angle and prevents fibre rope contact with the lower quarter circumference of the stern roller. For the first mooring line that is connected, this length is considered less critical compared to the second line, as for the first the installation vessel can position itself close to the anchor point, resulting in sufficient slack in the upper segment of the mooring line. However, for the second line, positioning is constrained by the length of the already connected line.

The total length of the top chain will thus include two times the length that makes contact with the vessel, an additional few metres for the lower section and a certain extra amount of length for the upper top chain.

4.3.3. Tow line

The characteristics of the tow line, made of Nylon, are presented in Table 4.3, with further details on the tow line provided in Section 4.4.3.

Parameter	Tow Line
Nominal diameter	100 mm
Axial stiffness	1,180 kN
MBL	1,640 kN
Weight	0.064 kN/m
Submerged weight	0.0065 kN/m

Table 4.3: Properties of the tow line

4.3.4. Installation vessel

Large AHTS vessels with high bollard pull capabilities and heavy winches will be required for the installation of floating offshore wind turbines. Bollard pull refers to the maximum pulling force a vessel can deliver for offshore holding at zero forward speed.

One vessel model is primarily used throughout this research due to its availability, referred to as AHTS 1. Additionally, two other AHTS vessels are included in the OrcaFlex model for comparison. These vessels are larger than AHTS 1 and are used to emphasise the need for large AHTS vessels for FOWT installations. Table 4.4 provides details of the three vessels, with mass representing the value used in the OrcaFlex models. Vessel sizes

increase progressively from AHTS 1 to AHTS 3. AHTS 1 represents the lower limit of vessel size suitable for FOWT installations, while AHTS 3 approaches the upper limit of current anchor handling vessels.

Winch capacities for large AHTS vessels typically range around 500 t. The winch plays a critical role both before and after locking the mooring line segments into the shark jaws, as it supports the lines during these stages. Additionally, this capacity represents the practical limit of pre-tension that can be applied by the vessel.

Parameter	AHTS 1	AHTS 2	AHTS 3	Units
Length	88	103	108	m
Breadth	18	16	24	m
Draught	5.5	6.7	8	m
Mass	5,371	9,018	8,800	t

Table 4.4: Dimensions of the AHTS vessels used in this study

A model of AHTS 1 is added to OrcaFlex using a hydrodynamic data file generated in ANSYS AQWA. The AQWA file contains frequency-dependent hydrodynamic properties, such as added mass, radiation damping, and wave load response amplitude operators (RAOs). By importing this file into OrcaFlex, the vessel's hydrodynamic behaviour can be accurately represented within the simulation, ensuring realistic interactions with environmental forces.

4.4. Model assumptions and setup

This section describes the modelling choices and inputs regarding the hook-up operation.

4.4.1. Assumptions

Tug boat modelling

In the model, the two assisting station-keeping tugboats are represented as fixed points in the coordinate system. This assumption neglects the dynamic behaviour of the tugboats, which can influence their station-keeping performance. Inaccuracies or errors in the station-keeping or DP system of the tugboats could result in increased FOWT offsets. These potential deviations should be accounted for through the margin described in Section 4.1.

AHTS orientation

Throughout most models where the wave heading is between 0° and 180°, the FOWT rotates slightly due to incoming waves and wind. In practice, it would be preferable for the AHTS to rotate along with the FOWT. However, aligning the AHTS with the FOWT is an iterative process as the static position of the FOWT must first be calculated, which in turn depends on the positioning of the AHTS. Furthermore, if the AHTS rotates to align with the FOWT, the relative wave heading for the AHTS changes. This adds complexity and increases the time required to determine the exact wave heading, and to create a setup that has similar headings as in the frequency domain models. Therefore, for simplicity, it is assumed in the models that the AHTS does not rotate along with the FOWT. As a result, the measured distance between the AHTS and the FOWT throughout the simulations represents the distance between the upper top chain endpoints, rather than the actual closest distance between the AHTS and the FOWT. The setup applied in most models is illustrated in Figure 4.10a, while the setup preferred in practice is shown in Figure 4.10b, with the oval indicating the direction of the UTC.

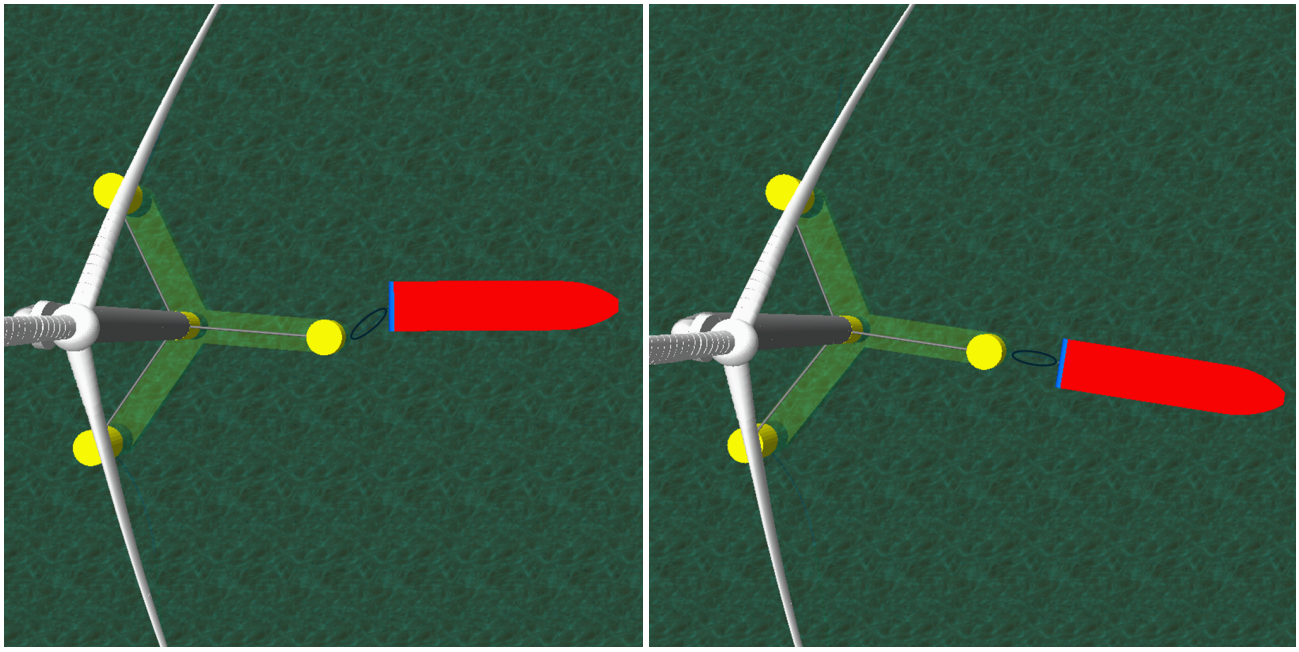

(a) Assumption applied in most models **(b)** AHTS aligned with FOWT

Figure 4.10: Comparison of AHTS not aligned with FOWT (a) and aligned with FOWT (b)

Line connection points to AHTS

Both the lower and upper segments of the mooring line are connected to the stern along the AHTS's centreline. In practice, these connections would be positioned slightly off the centreline. As a result of this assumption, additional vertical motions caused by the AHTS's roll are not accounted for. However, these effects are assumed to have minimal influence, as the offset from the centreline is relatively small. The maximum vertical motion that could occur due to roll, assuming a 2 metre offset of the chain from the centreline of the AHTS with a 5 degree roll according to the workable limits, is approximately 0.18 metres. This is calculated by multiplying the distance from the centreline by the tangent of the roll angle. In comparison, the maximum vertical displacement caused by a pitch of 3 degrees, for a vessel with a length of 88 metres, is around 3 metres. This displacement is further increased by heave, indicating that the vertical motion caused by roll is relatively small.

Fluid interaction effects

Given the close proximity of the AHTS to the FOWT, it is likely that fluid interaction effects occur between the two. These effects could be captured by performing a multibody analysis, where the meshes of the two floating objects are placed in close proximity, and their diffraction is calculated. In OrcaFlex, this calculation can be conducted in OrcaWave, and the resulting diffraction data can be imported into the model [50]. However, the time required for this analysis is considered not to be proportional to the main focus of this research and is therefore excluded.

4.4.2. Installation vessel and floater modelling

The recommended vessel type for the hook-up of the mooring lines of floating offshore wind turbines is an AHTS. As described in Section 4.3.4, AHTS 1 is primarily implemented through dynamic analyses. OrcaFlex provides an extensive range of options for modelling, including a large number of calculation methods designed for various offshore applications. Section 4.1 introduced two modelling approaches, Displacement RAOs and Load RAOs, which distinguish how vessel and floater motions are handled in OrcaFlex.

In the Displacement RAO method, the vessel and floater oscillate harmonically about a fixed position in response to wave excitation forces. The magnitude of these motions is determined by the wave height, wave period, and the corresponding RAOs of the vessel or floater. Predefined harmonic motions, derived from their RAOs, are superimposed on the vessel's and floater's primary positions. The RAO consists of two values per DOF, wave direction, and wave period: an amplitude, which relates the DOF's motion to the amplitude of the wave, and a phase, which defines the timing of the DOF's response relative to the wave [51]. These motions represent the prescribed responses of the vessel or floater to wave excitation, but they do not account for wave-induced forces or interactions with connected lines or objects, such as the upper top chain or tugboat assistance. This approach assumes an idealised system where the floater and vessel maintain a nearly constant relative distance, resembling the behaviour of a perfect DP system. However, it ignores operational inaccuracies, external forces, and dynamic

interactions, which make such station keeping unachievable in practice (see Section 2.4.1). In this research, the Displacement RAO method is employed as a preliminary approach to quickly identify operational limits and validate expectations before progressing to a more dynamic model.

In contrast, the Load RAO method calculates the motions of the vessel and floater dynamically, incorporating wave-frequency effects and interactions with connected objects such as mooring lines. To ensure both the floater and vessel maintain their position, external assistance is required. The floater is held in position by tug boats, as described in more detail in Section 4.4.3. The objective of the vessel is to follow the floater's displacements to maintain a fixed distance, achieved through its DP system. Additional details can be found in the next section, titled "Dynamic positioning". For both the floater and vessel, only first-order wave effects are considered. The DP system of the installation vessel is capable of counteracting wave drift (second-order effects), while tug boat assistance mitigates these effects for the floater. As a result, only wave-frequency effects are included, and low-frequency effects are excluded.

Results of this method in the time domain form the basis for analysing the system's dynamic behaviour, focusing specifically on the effective tension within the upper top chain. The six degrees of freedom of both the vessel and floater can be compared to the expected maxima derived from the frequency domain, allowing validation and cross-checking of results. Furthermore, this method incorporates the modelling of DP and tug boat assistance, ensuring a robust representation of the hook-up operation dynamics.

Figure 4.11 provides an overview of the whole system modelled in OrcaFlex. The blue part at the stern of the AHTS represents the stern roller. This is modelled as a shape to capture contact between the mooring line segments and the stern of the vessel. A closer view is shown in Figure 4.13, while the coordinate system used throughout the models is illustrated in Figure 4.12.

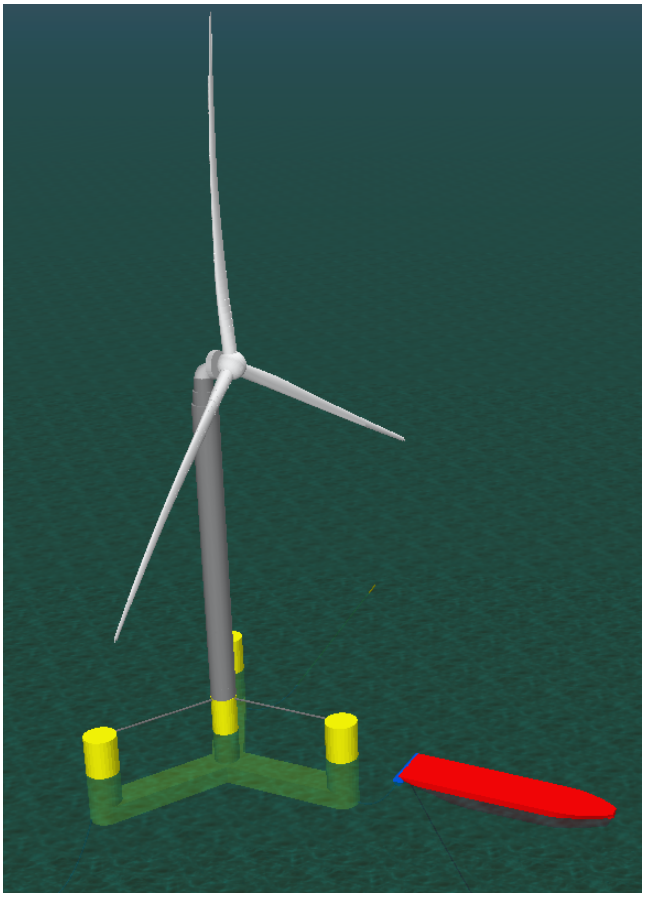

Figure 4.11: Overview of the floating wind turbine and installation vessel

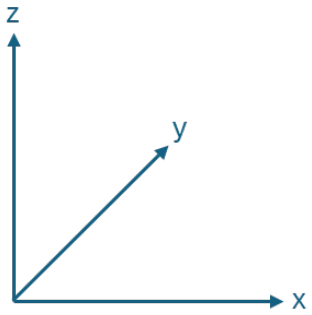

Figure 4.12: 3D coordinate system

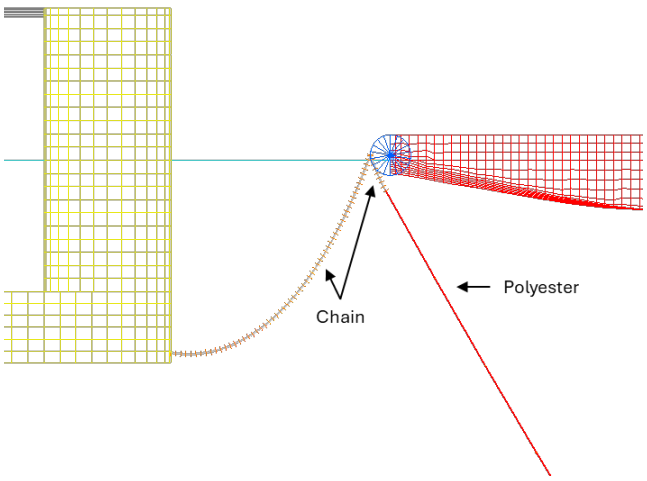

Figure 4.13: Mooring segments and connection to stern roller of the AHTS

Dynamic positioning
The DP system of the installation vessel should be used in combination with a system such as a Fanbeam, which is a laser or radar-based system that measures the relative distance to another floating object, in this case the floating wind turbine. In the model, a "soft mooring" system is implemented to constrain the surge and sway of the AHTS. Winch objects are used to provide the AHTS with some flexibility in terms of displacements, while aiming for maintaining a fixed distance to the floater. The winch object includes both a winch drive, representing the hydraulics that drive the drum, and a winch wire [52]. The desired behaviour is achieved by configuring winches with a very large length and relatively moderate stiffness. The exact values for the winch parameters are determined through extensive iterations, adjusting combinations of length, stiffness, and the number of winches. These iterations are evaluated using the surge and sway displacements of the AHTS in a time-domain analysis. The winches apply a mean tension rather than abrupt pulling forces, resulting in a smooth response of the vessel.

4.4.3. Tug boat modelling

Tug boats are essential for station-keeping of the floater during the installation process. Their primary role is to minimise and constrain the motions of the floater while preventing excessively high tensions in the towing lines. The length of the chains connected to the floater results in a large weight that provides significant natural damping to the system, which aids in controlling the dynamic behaviour of the floater. These chains are connected to the tug boats via tow lines, creating a mechanical system that balances stiffness and flexibility. The end point of the tow lines is a fixed point in the model, meaning motions of the tug boats are neglected.

The material, length, and configuration of the tow lines are carefully selected to achieve a relatively stiff model that reduces the offset of the floater while keeping line tensions within acceptable limits, defined as tensions below 20% of their MBL. The tow line material is Nylon, chosen for its ability to provide the desired combination of strength and elasticity. Nylon's properties allow the tow line to respond gradually to the floater's motions, avoiding sudden reaction forces that could destabilise the system or increase tensions to critical levels. Instead, the tow lines allow the floater to return to its position smoothly, maintaining stability and ensuring safe operations.

The tug boats apply a mean pulling force to the floating turbine, and their restoring forces must create an equilibrium with the environmental loads, including waves and wind. To achieve this balance, the configuration of the tug boats must be adjusted for various wave directions, ensuring consistent performance under changing environmental conditions. This process, combined with determining the tow line properties such as material, length, and stiffness, is carried out through iterative simulations and adjustments, guided by the objectives of minimising the floater's offset and maintaining line tensions below 20% of their MBL.

During the process it became evident that the behaviour of the floater is highly sensitive to the positioning and length of the tow lines. Small adjustments in these parameters significantly influence the floater's motions. If the floater is pulled too strongly away from the installation vessel by the tug boats, unsafe conditions for the upper top chain connecting the floater to the vessel could arise, with excessive tension posing structural risks. Conversely, insufficient restraint could allow the floater to drift too close to the installation vessel or deviate from its intended position, compromising the safety and efficiency of the operation. The pulling force applied by the tug boats primarily depends on the amount of chain tensioned, as the chain's belly rises or sags between the floater and the tug boat, depending on the distance between its end points. Figure 4.14 illustrates this behaviour: as the tug boat moves closer to the floater, the sag increases, resulting in a lower pulling force exerted by the tug boat on the floater.

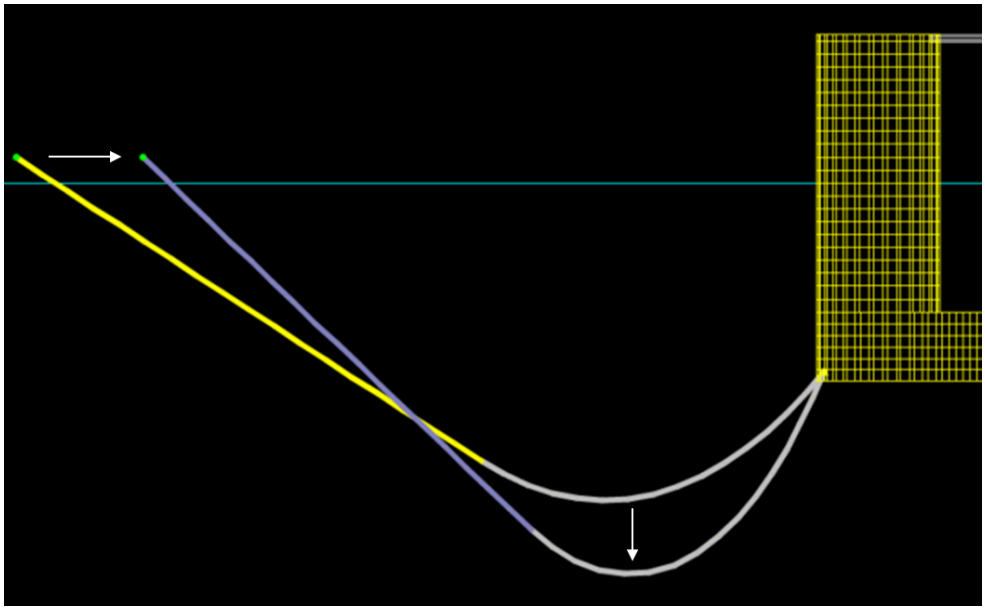

Figure 4.14: Model set-up of a tug boat

Alternative methods for modelling the tug boats are also tested, including the use of winches and links or springs. However, the self-weight of the chain proved to provide the best balance, offering natural damping and gradual responses to the floater's motions.

5
Numerical simulations

The numerical simulations conducted using OrcaFlex are performed in both the time and frequency domains. This chapter explains the distinctions between these two approaches and compares their results, focusing on the largest deviations in the x, y, and z directions of the UTC end points relative to their static positions. Additionally, a sensitivity analysis is carried out for the time domain simulations to assess the impact of time step and simulation duration on the outcomes.

5.1. Frequency domain analysis

The frequency domain approach provides a fast and computationally efficient method to assess the 6DOF of both the vessel and floater. The roll, pitch, and yaw responses of the AHTS are calculated in the frequency domain to determine whether these rotational motions remain within the workable limits described in Section 4.2. These results serve as a foundation for further analysis in the time domain. Additionally, calculations in the frequency domain focus on determining the Most Probable Maximum (MPM) of the deviations in the x, y, and z directions of the UTC at both its ends, compared to their static position. These values are used to determine the required UTC length corresponding to the considered sea states. As the UTC does not affect the 6DOF of both the installation vessel and the FOWT in the frequency domain, it is left out and the 3D deviations are calculated at the connection points of the UTC at both the installation vessel and FOWT.

Analysis in the frequency domain evaluates the steady-state responses of the system to harmonic wave loads by assuming linear system behaviour, where the motion response is directly proportional to the input load. While this assumption simplifies the computations and enables broad parameter investigations, it limits the ability to account for nonlinear effects, such as those caused by extreme wave interactions or complex mooring dynamics. This makes it necessary to complement frequency-domain analysis with time-domain simulations [45]. Both time and frequency domain simulations solve an Equation of Motion (EoM). In the time domain, this equation is expressed as:

$$M\ddot{x} + C\dot{x} + Kx = F(t), \tag{5.1}$$

where M is the inertia load, C is the damping load, K is the stiffness load, $F(t)$ is the external load, x represents the displacement vector in six degrees of freedom: $(x, y, z, \phi, \theta, \psi)$ and t is the simulation time. To transition to the frequency domain, the displacement $x(t)$ is represented as $X(\omega)e^{i\omega t}$, and its time derivatives are replaced by their frequency-dependent equivalents [11]:

$$x(t) \rightarrow X(\omega)e^{i\omega t}, \quad \dot{x}(t) \rightarrow i\omega X(\omega)e^{i\omega t}, \quad \ddot{x}(t) \rightarrow -\omega^2 X(\omega)e^{i\omega t}, \tag{5.2}$$

resulting in the frequency-domain equation of motion:

$$\big(-\omega^2 M + i\omega C + K\big)X(\omega) = F(\omega), \tag{5.3}$$

where $X(\omega)$ is the frequency-dependent displacement response, $F(\omega)$ is the Fourier transform of the external forcing function $F(t)$, ω is the angular frequency and i is the imaginary unit.

This formulation allows for the efficient computation of the response amplitude and phase for any frequency ω. By integrating the system's Response Amplitude Operators (RAOs) with the wave energy spectrum, the expected maximum response for each degree of freedom can be determined. The MPM is calculated by combining the

RAOs with the wave spectrum for specific combinations of significant wave height H_s, peak wave period T_p, and wave direction. It provides the maximum likely response under steady-state conditions for a 3-hour storm duration.

For a wide range of H_s and T_p combinations, and a wave heading of 30 degrees, the MPM values of roll, pitch and yaw for AHTS 1 are illustrated in figure 5.1. The red-coloured cells indicate that the maximum accepted values have been exceeded. This illustration highlights the need for large AHTS vessels for the installation of floating wind turbines, as the AHTS 1 shows workable conditions on deck only up to sea states of $H_s = 2$ m. It also supports why a significant wave height of 2 metres is primarily applied in the load cases listed in Table 4.2.

Hs \ Tp		4	5	6	7	8	9	10	11	12	13	14	15	16
Roll	2.0	0.9	1.2	1.4	1.6	1.7	2.0	2.4	3.0	3.6	4.3	5.0	5.4	5.7
Pitch		0.5	1.2	2.3	2.6	2.7	2.8	2.7	2.5	2.4	2.3	2.1	2.0	1.9
Yaw		0.5	0.8	1.0	1.1	1.2	1.3	1.3	1.3	1.3	1.3	1.3	1.3	1.3
Roll	2.5	1.1	1.5	1.8	2.0	2.2	2.5	3.0	3.7	4.5	5.4	6.2	6.8	7.2
Pitch		0.6	1.5	3.0	3.4	3.4	3.4	3.3	3.2	3.0	2.8	2.7	2.5	2.4
Yaw		0.7	1.0	1.3	1.5	1.5	1.6	1.6	1.6	1.6	1.6	1.6	1.6	1.6
Roll	3.0	1.3	1.8	2.2	2.4	2.6	3.0	3.6	4.4	5.5	6.5	7.4	8.1	8.6
Pitch		0.7	1.8	3.6	4.3	4.2	4.1	4.0	3.8	3.6	3.4	3.2	3.0	2.9
Yaw		0.8	1.1	1.6	1.8	1.9	1.9	1.9	1.9	1.9	1.9	1.9	1.9	1.9
Roll	3.5	1.5	2.1	2.5	2.9	3.1	3.5	4.2	5.2	6.4	7.6	8.7	9.5	10.0
Pitch		0.8	2.1	4.2	5.2	5.0	4.8	4.7	4.5	4.2	4.0	3.8	3.5	3.3
Yaw		0.9	1.3	1.9	2.2	2.2	2.2	2.2	2.2	2.2	2.2	2.2	2.2	2.2

Table 5.1: Frequency results of AHTS 1 with a wave heading of 30 degrees

5.2. Time domain analysis

The time domain analysis builds upon the results obtained in the frequency domain and further investigates the system's behaviour, with a particular focus on the effective tension in the upper top chain. For comparison with the frequency domain results, an UTC configuration corresponding to Case 1 is implemented in the time domain, with a connection to the FOWT at the bottom.

An explicit integration scheme is applied in OrcaFlex, which utilises a semi-implicit Euler method [46]. It solves the EoM for acceleration at the beginning of each time step, followed by integration to determine the positions and orientations of all nodes at the end of each time step. The time step Δt must be carefully selected, as large time steps can result in instability or inaccuracies, while small time steps can be computationally demanding. For a given Δt, the values are calculated at the end of each time step by:

$$\dot{x}_{t+\Delta t} = \dot{x}_t + \Delta t\, \ddot{x}_t \tag{5.4}$$

$$x_{t+\Delta t} = x_t + \Delta t\, \dot{x}_{t+\Delta t} \tag{5.5}$$

It is a robust solving method, but typically requires a short time step. Sensitivity of Δt is provided in the next section. In OrcaFlex, line objects are the most computationally demanding components of the simulation. To reduce computational time, lines are divided into multiple segments with varying element lengths between adjacent nodes. Critical parts of the system, where higher accuracy is required, are modelled with a greater number of nodes compared to less critical regions.

5.2.1. Time step and duration

A dynamic analysis in the time domain typically consists of at least two stages in OrcaFlex: a build-up stage followed by the main simulation stage. The build-up stage provides a smooth transition from the static position to dynamic motions by gradually introducing wave, vessel, and floater movements. In this research, a build-up stage of 60 seconds is applied, followed by 1 hour (3600 seconds) of simulation time, as visualised in 5.1.

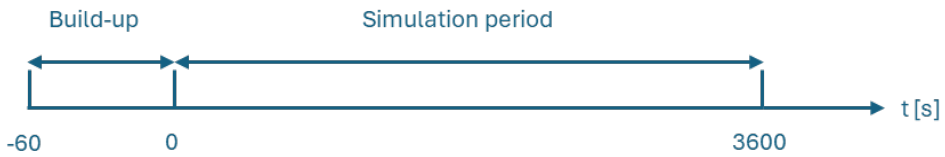

Figure 5.1: Simulation stages of time domain analysis

According to DNV standards, simulation times should be at least 1 hour and preferably 3 hours. A duration of 1 hour is found to be sufficient to represent a sea state reference period of 3 hours. Shorter simulations are also tested but were, in some cases, found to be insufficient in duration, as excessive motions or tensions that would have occurred later were not captured. The spectral density of the effective tension in the UTC at the vessel connection point is shown in Figure 5.2, comparing the results of 1-hour and 3-hour simulation times. The results are derived from Case 2 with a T_p of 10 seconds. The results indicate that the two simulation durations produce comparable outcomes.

A time step sensitivity study is conducted for Δt values of 0.1, 0.05 and 0.01 seconds. A time step of 0.1 seconds was found to be too large, as the results became unstable. In some cases, simulations with this time step require significantly longer runtimes because more iterations per step are needed to converge to a solution. In other cases, the instability is so severe that the simulation fails.

Comparing the effective tension in the UTC at the vessel end for time steps of 0.01 and 0.05 reveals minimal differences, as shown in Figure 5.3. The difference between time steps of $\Delta t = 0.01$ and $\Delta t = 0.05$ is presented as $\Delta t = 0.01 - \Delta t = 0.05$. In Figure 5.4, both results are shown and it is evident that the difference between the two is negligible. The maximum difference, around 0.25 kN observed in Figure 5.3, is minimal when compared to the mean tension of around 180 kN.

Based on the findings described above, a simulation duration of 3600 seconds with a time step of 0.05 seconds is chosen for its ability to provide accurate results while being significantly more efficient compared to a time step of 0.01 in terms of computational time.

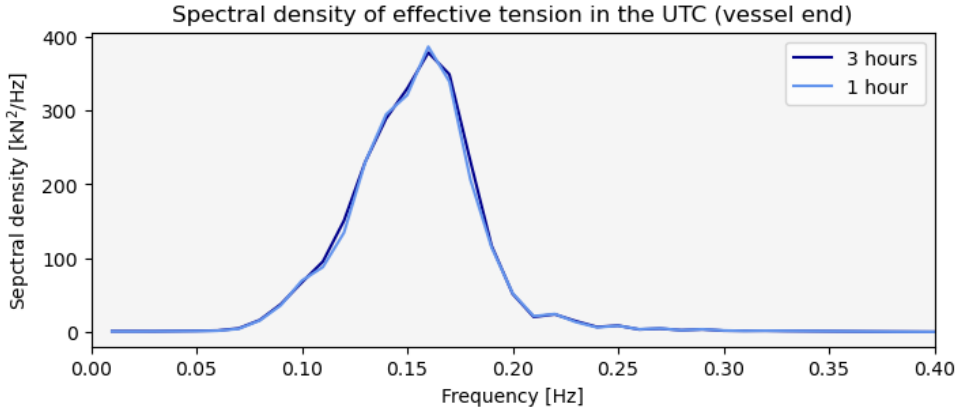

Figure 5.2: Simulation time comparison

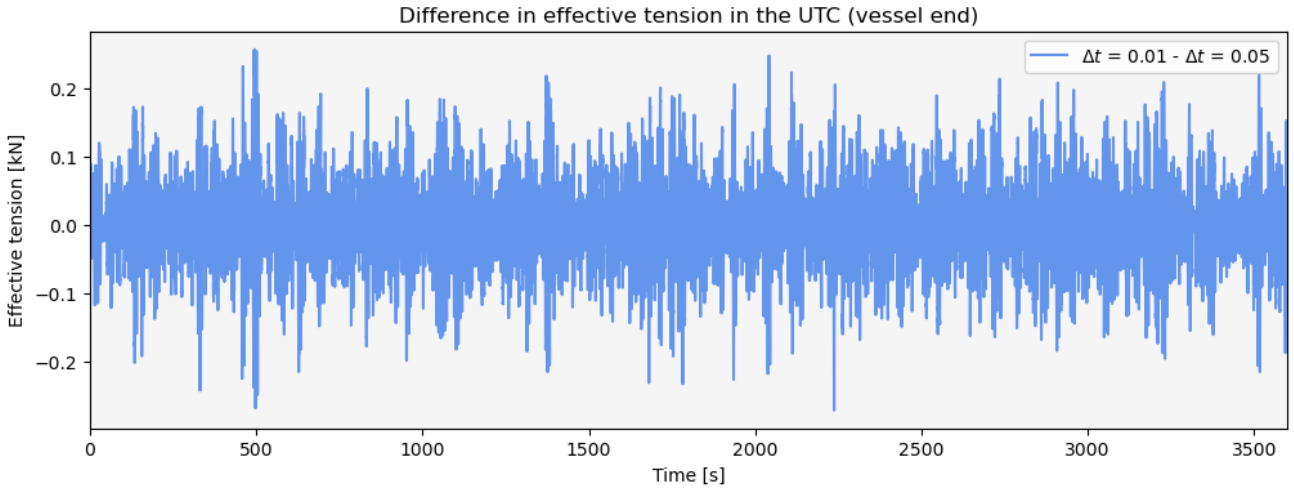

Figure 5.3: Difference in effective tension in the UTC at the vessel end for time steps of $\Delta t = 0.01$ s and $\Delta t = 0.05$ s

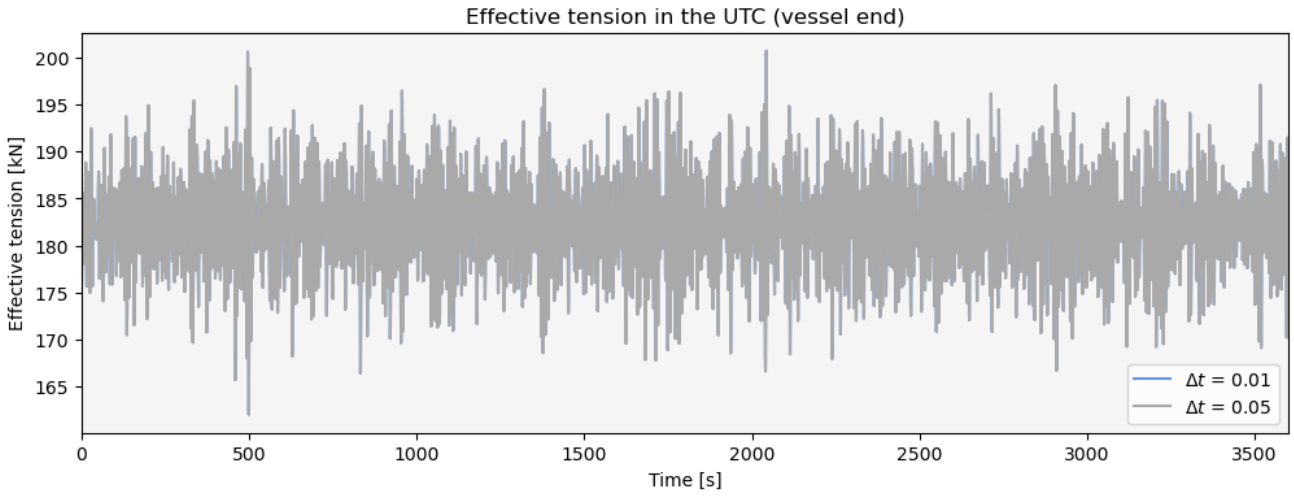

Figure 5.4: Comparison of effective tension in the UTC at the vessel end for time steps of $\Delta t = 0.01$ s and $\Delta t = 0.05$ s

5.3. Comparison of time and frequency domain analyses

Validation of results in both the time and frequency domains ensures the accuracy and reliability of both methods, with primary focus on comparing the largest deviations in the x, y, and z directions of the UTC end points relative to their static positions. Calculations in the frequency domain identify workable sea states based on AHTS roll, pitch, and yaw. Time domain simulations are only conducted for sea states where operations are possible. For these sea states it is verified that the system's behaviour in the frequency domain aligns with the behaviour observed in the time domain. MPM values for a 3-hour storm are compared to the maximum values observed over a 3600-second simulation period.

The results show that for the vessel connection point, the frequency domain generally predicts larger maxima than observed in the time domain, with differences increasing with T_p. In contrast, for the floater connection point, the frequency domain slightly underestimates the maxima. Figures 5.5 and 5.6 illustrate these differences through spectral density plots for both the vessel and the floater in the frequency and time domain. The wave conditions are similar to those used in the time step and duration sensitivity analysis. $Dynamic\ x$, y and z represent the deviations in the x, y, and z directions of both ends of the upper top chain relative to the static position. Specifically, at the stern roller for the vessel and the fairlead for the floater. Tables 5.2 and 5.3 illustrate the differences in x, y, and z deviations relative to the static position of the UTC connection points for a range of H_s and T_p combinations, where positive values (purple) indicate overestimation by the frequency domain, and negative values (blue) indicate underestimation. The same behaviour was observed for larger H_s values.

The differences in response likely arise because the frequency domain does not account for nonlinear effects, which can introduce transient dynamics or hydrodynamic damping effects. In the frequency domain, the system is assumed to respond linearly and consistently at the excitation frequencies based on the RAOs. Additionally, the effects of the UTC and other lines on the response of both the floater and vessel are not included in the frequency domain analysis. Furthermore, the results in the time domain are sensitive to the configuration of the soft mooring applied to the installation vessel. As the stiffness of the soft mooring increases, the horizontal displacements of the vessel are more restricted. Alterations in this setup lead to differences in behaviour between the time and frequency domain.

For the floater, the underestimation is partly attributed to the exclusion of wind loads in the frequency domain analysis. Comparisons with time domain analyses that also exclude wind loads showed much greater similarity in the results.

Based on these findings, frequency domain analysis can be effectively used for initial screening of sea states and identifying workable conditions, as for determining the length of the UTC. However, time domain simulations are essential for capturing nonlinear dynamics and wind-induced loads, particularly for floating wind turbines. Chain tensions are only analysed in the time domain, with the results presented in the next chapter. Future work could focus on incorporating wind effects into frequency domain analyses or developing correction factors for specific cases.

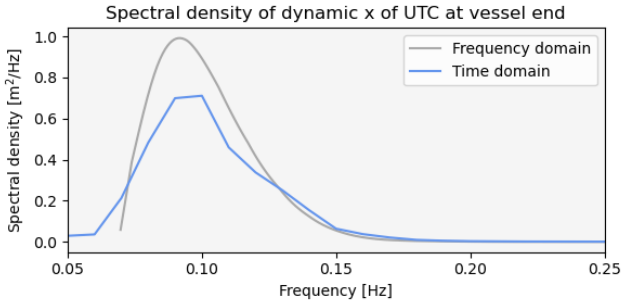

(a) Dynamic x

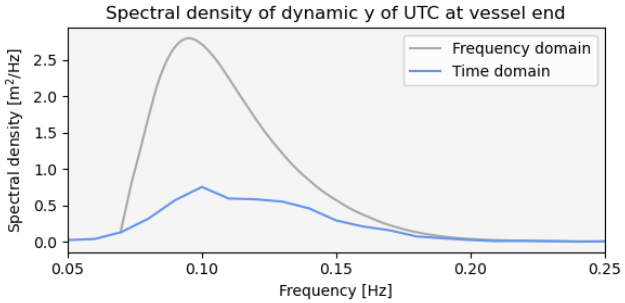

(b) Dynamic y

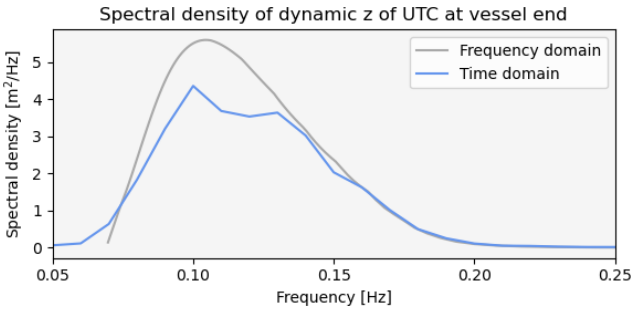

(c) Dynamic z

Figure 5.5: Time and frequency domain comparison of dynamic motions of the UTC connection point at the vessel: (a) x-direction, (b) y-direction, and (c) z-direction.

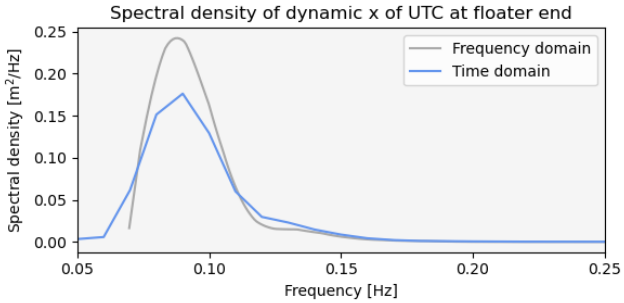

(a) Dynamic x

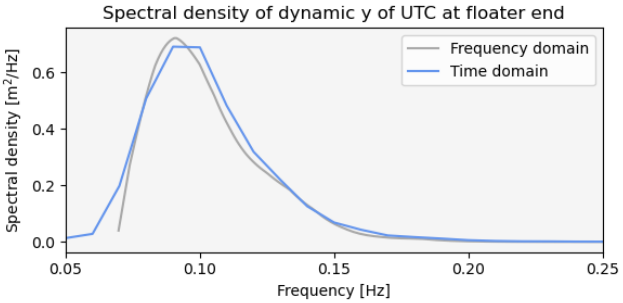

(b) Dynamic z

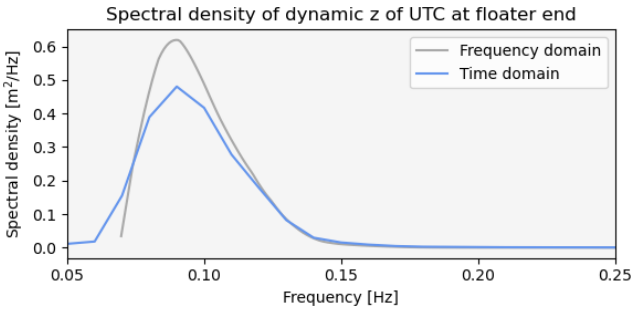

(c) Dynamic z

Figure 5.6: Time and frequency domain comparison of dynamic motions of the UTC connection point at the floater: (a) x-direction, (b) y-direction, and (c) z-direction.

	Hs \ Tp	4	5	6	7	8	9	10	11	12	13	14	15	16
Delta x	2.0	0.0	0.0	0.0	0.0	0.1	0.1	0.2	0.2	0.2	0.2	0.1	0.1	0.2
Delta y		0.1	0.2	0.2	0.3	0.3	0.5	0.5	0.6	0.7	0.7	0.7	0.8	0.9
Delta z		0.1	0.2	0.4	-0.1	0.4	0.3	0.3	0.3	0.3	0.2	0.2	0.2	0.3

Table 5.2: Differences in x, y, and z deviations relative to the static position of the UTC connection point at the vessel end, obtained by subtracting time domain results from frequency domain results for a wave heading of 60 degrees.

	Hs \ Tp	4	5	6	7	8	9	10	11	12	13	14	15	16
Delta x	2.0	-0.1	-0.2	-0.1	-0.1	-0.1	-0.1	-0.1	-0.1	-0.1	-0.2	-0.1	-0.2	-0.2
Delta y		-0.2	-0.2	-0.2	-0.1	-0.1	-0.1	-0.1	-0.1	-0.1	-0.2	-0.3	-0.4	-0.2
Delta z		0.0	0.0	0.0	0.0	0.1	0.1	0.1	0.0	0.0	0.0	-0.1	0.1	0.0

Table 5.3: Differences in x, y, and z deviations relative to the static position of the UTC connection point at the floater end, obtained by subtracting time domain results from frequency domain results for a wave heading of 60 degrees.

6 Results

This chapter presents the results of the analysis on the variables influencing the required upper top chain length. Section 6.1 examines the impact of sea state variables, while Section 6.2 discusses the dynamic loads in the UTC and the effects of its length and connection height to the floater on its dynamic behaviour. Section 6.4 addresses the required length of the entire top chain, and Section 6.5 provides a validation and verification of the dynamic simulations and modelling assumptions.

6.1. Influence of sea state variables on the UTC length

This section presents the results of the UTC length across various combinations of significant wave height (H_S), peak wave period (T_p) and wave heading, with the range of each parameter discussed in Section 4.3.1. The individual influence of these variables on the required UTC length is analysed, while the impact of varying UTC lengths on its dynamic behaviour is discussed in Section 6.2.3. Results detailing the UTC length for all considered sea state combinations, alongside the corresponding lower and upper margins, are provided in Appendix B.

6.1.1. Wave height and period

In Figure 6.1, the UTC length is presented for four significant wave heights and a wave heading of 0 degrees. The lengths with margins of 1 and 10 metres are shown, along with the range shaded between them. Additionally, the maximum distance observed in the time domain simulation is included in the graph for $H_s = 2$ m, providing a comparison between the calculated UTC length and the observed distance between the endpoints of the UTC. Two key observations can be made: first, the UTC length increases slightly with increasing H_s; second, it increases more significantly with T_p, showing a clear difference between $T_p = 4$ s and $T_p = 16$ s.

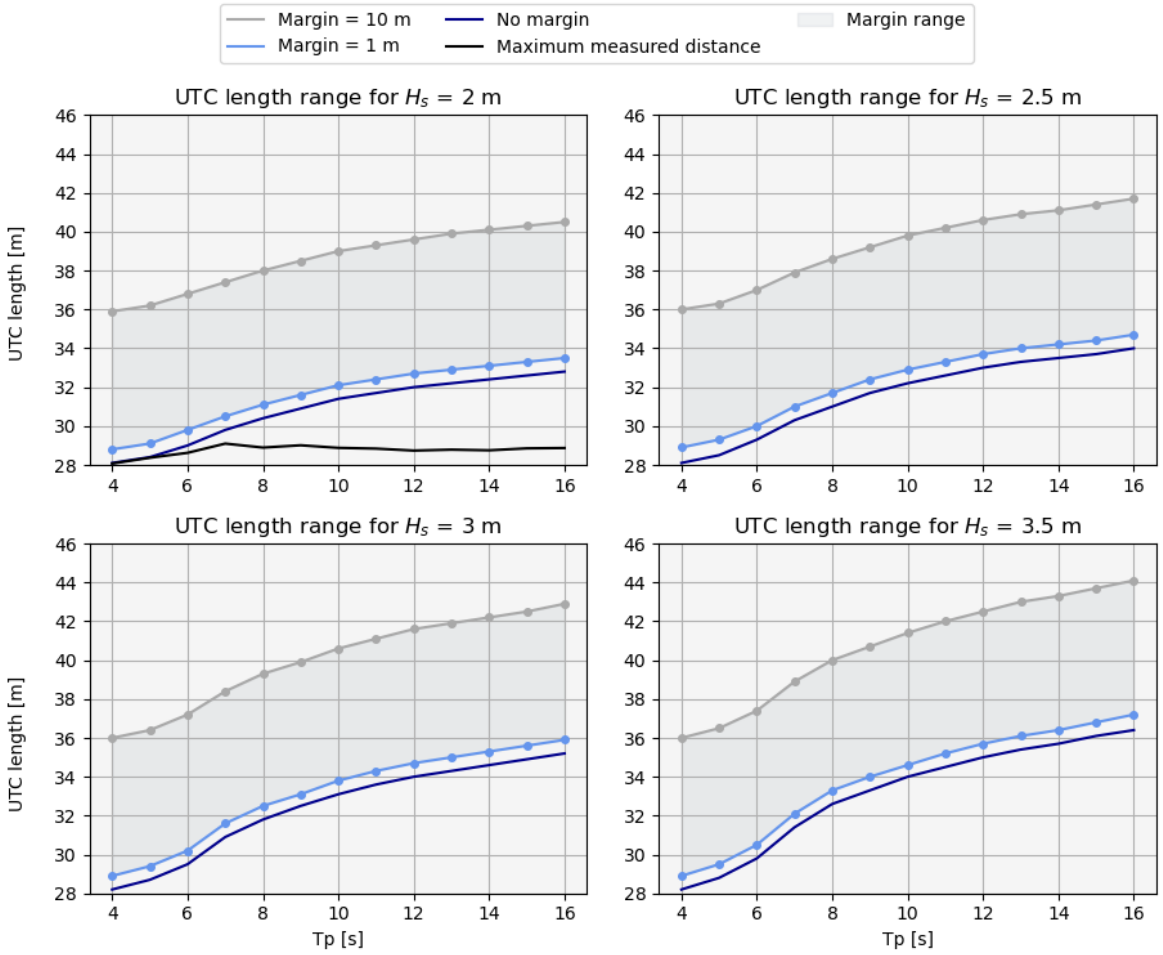

Figure 6.1: Range of UTC lengths with wave heading = 0°

The increase in UTC length with T_p can be attributed to the nature of longer-period waves, which correspond to longer wavelengths. These waves exert less frequent but more substantial forces on a floating object, resulting in larger MPM values for surge, sway and heave in the frequency domain and, consequently, a longer chain length. This behaviour is also reflected in the RAOs of surge, sway and heave of the vessel, displayed in Figures C.6, C.9 and C.8 in Appendix C for a wave heading of 60 degrees, where the responses become significant for wave periods greater than 5 seconds. The more rapid increase in UTC length just after a T_p of 6 seconds in Figure 6.1 also corresponds to the surge, heave and pitch RAOs of the vessel for a wave heading of 0 degrees, presented in Figures C.5, C.7 and C.1.

Besides for the translational RAOs, the vertical and horizontal motions of the UTC ends are also influenced by the pitch and yaw rotations of the floater and vessel, and by roll in the case of the floater. While the surge, sway, and heave responses are generally low for short wave periods and increase significantly around a specific wave period, the roll, pitch, and yaw responses are primarily governed by the alignment of the wave period with the object's natural period. The translational 3DOF responses of the vessel increase notably between wave periods of 6 and 8 seconds, as shown in the RAOs in Figures C.6, C.9 and C.8. For the rotational 3DOF, resonance may occur when the wave period matches the natural period, leading to amplified motions.

The frequency domain results confirm this behaviour. Figure 6.2 illustrates the MPM of the deviations in x, y, and z directions, relative to the static position, of the UTC connection point at both the vessel and the floater for a wave heading of 60 degrees, with similar trends observed for other wave headings. For the installation vessel, the x and y deviations increase with T_p, while in the z direction, the response is largest around the natural frequency of pitch of the vessel, further amplified by the heave response, with the RAOs presented in Figures C.2 and C.8.

In contrast, the FOWT motions increase consistently in all directions as T_p rises. This is expected, as most of the natural periods of the floating platform correspond to very long wave periods, with the platform being designed to provide stability for the turbine for wave periods that typically occur. Some of the RAOs of the floating platform are also presented in Appendix C.

	Hs \ Tp	4	5	6	7	8	9	10	11	12	13	14	15	16
Delta x	2.0	0.1	0.1	0.3	0.4	0.5	0.7	0.8	0.9	1.0	1.1	1.1	1.2	1.3
Delta y		0.4	0.6	0.9	1.1	1.2	1.4	1.5	1.6	1.7	1.8	1.9	2.0	2.1
Delta z		0.4	1.1	1.8	2.0	2.2	2.3	2.3	2.3	2.2	2.2	2.2	2.1	2.1

(a) MPM of x, y, and z deviations relative to the static position of the UTC connection point at the vessel

	Hs \ Tp	4	5	6	7	8	9	10	11	12	13	14	15	16
Delta x	2.0	0.0	0.0	0.1	0.1	0.2	0.3	0.3	0.4	0.5	0.5	0.6	0.6	0.6
Delta y		0.1	0.2	0.3	0.4	0.5	0.6	0.7	0.7	0.8	0.9	0.9	1.0	1.0
Delta z		0.0	0.0	0.1	0.2	0.4	0.5	0.6	0.7	0.7	0.8	0.8	0.9	1.0

(b) MPM of x, y, and z deviations relative to the static position of the UTC connection point at the floater

Figure 6.2: MPM of x, y, and z deviations relative to the static position of the UTC connection point at the vessel (a) and floater (b) (wave heading = 60°)

6.1.2. Wave heading

Figure 6.3 presents the UTC length for various wave headings with an H_s of 3 metres and a margin of 1 metre. At shorter wave periods, wave headings closer to 0 degrees appear to be slightly more favourable, though the differences are minimal. For larger wave periods, however, wave headings closer to 90 degrees result in shorter UTC lengths. The same behaviour was found for different values of H_s.

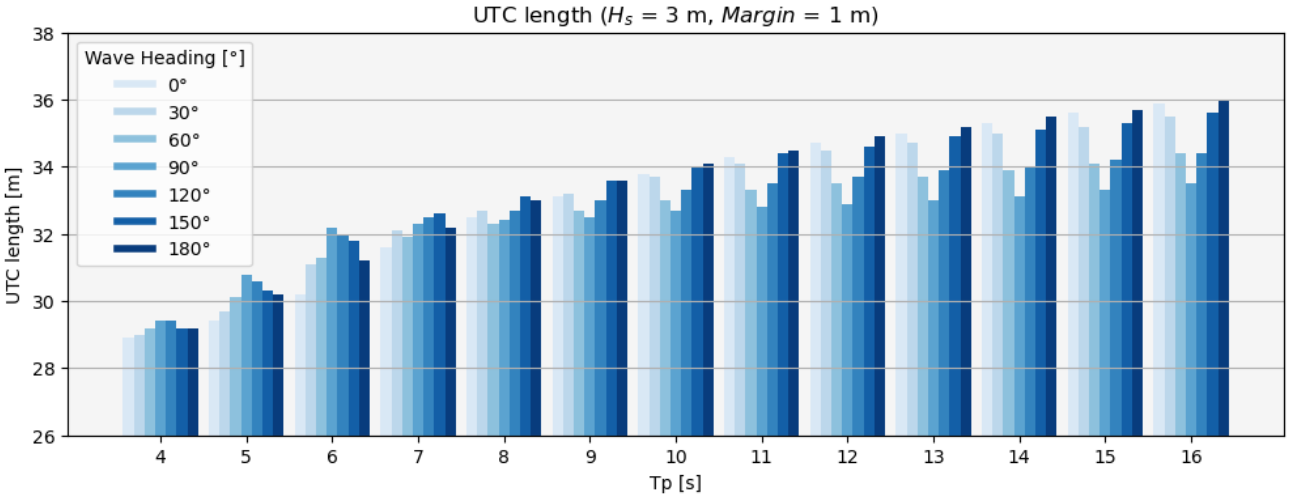

Figure 6.3: UTC length for various wave headings

6.2. Dynamic behaviour and load cases

The influence of various variables on the required UTC length and its dynamic behaviour is assessed through dynamic simulations. These variables include the connection height of the UTC to the floater, varying sea states, and the resulting ratio of UTC length to the distance between its endpoints. Simulations are conducted for the load cases provided in Table 4.2 in Section 4.3.2, with results for Case 1 and Case 7.2 presented in this chapter. The results for the other cases are provided in Appendix A. All load cases are simulated over a duration of 3600 seconds.

6.2.1. Static and dynamic tension in the UTC

The static shape of the UTC for Case 1 is visualised in Figure 6.4. The distance between the UTC end points is 27.93 metres, while its length, including a margin of 1 metre, is 32.4 metres. As described in Section 4.3.2, the UTC length corresponding to the largest T_p value is applied uniformly across all models within a single case. As discussed previously and shown in Figure 6.1, the largest UTC length corresponds to a T_p of 16 seconds. Consequently, for models with T_p < 16 s, the UTC lengths are longer than required based on the proposed approach.

The same limitation accounts for all other cases except Case 7.2, where the UTC length is adjusted per T_p according to the approach. This allows to compare the results with Case 7.1 where the same UTC length was applied throughout all T_p values.

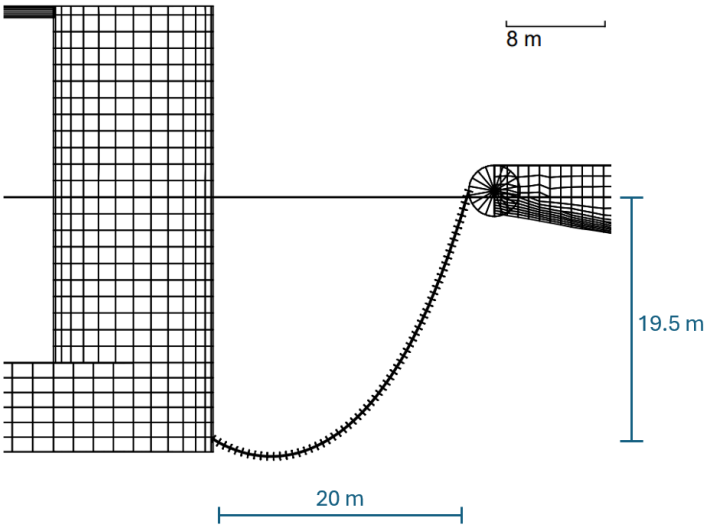

Figure 6.4: Static position of the UTC between the FOWT and AHTS, for a bottom connection height and a margin of 1 metre

The results of the effective tension in the UTC over time are presented as box plots for all cases. The tension values correspond to the point along the UTC with the highest tension. These box plots create a visualisation of the spread of measured tension over time. The line in the middle represents the median, which is closely similar to the mean and the static tension. The box extends from the first quartile (Q1) to the third quartile (Q3) and is called the interquartile range (IQR). The whiskers represent both Q1 - 1.5 * IQR and Q3 + 1.5 * IQR, where 1.5 corresponds to Tukey's original definition of box plots [25]. This configuration is consistently applied to all box plots presented throughout the report. For clarity, only the maximum tension is shown while all other points extending beyond the whiskers are left out.

The results of the effective tension of the UTC for Case 1 are presented in Figure 6.5. The mean tension is observed to be equal to the static tension, and the findings show that the effective tension in the chain exhibits minimal deviation from the mean throughout the simulations. This indicates that dynamic effects do not introduce significant additional stresses in the chain, and that increases and decreases in tension relative to the static state are balanced. For all peak wave periods, the dynamic factor, defined as additional loads due to dynamic effects compared to the static state, remains below 10%. This suggests that the dynamic loads are unlikely to pose any significant issues for the hook-up operation, provided that snap loads are effectively prevented. To illustrate the potential magnitude of snap loads, tensions exceeded 10,000 kN in simulations where they occurred.

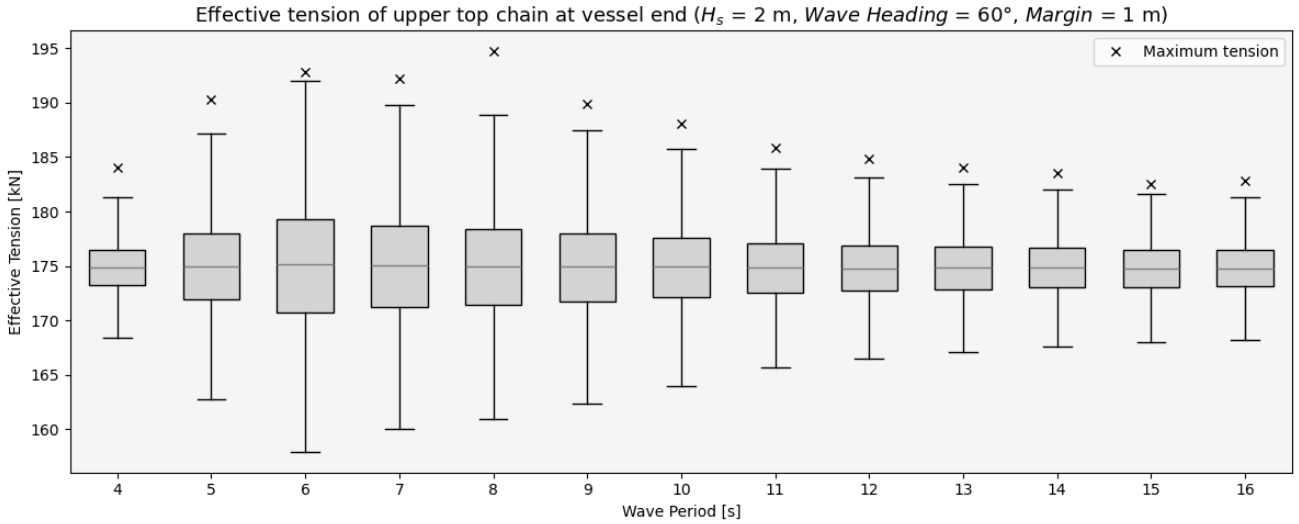

Figure 6.5: Effective tension at the vessel end of the UTC for Case 1, with a starting distance of 20 metres and a connection to the floater at the bottom

6.2.2. Dynamic tension with respect to static tension

The difference between the dynamic and static tension arises from the inertia of the UTC. The UTC resists changes in motion due to its inertia, requiring a force to change the direction of the motion at the end point of the UTC. The magnitude of the dynamic tension force is related to the acceleration of the UTC, with higher accelerations leading to increased tensions.

When the UTC moves upwards, its acceleration is in the opposite direction to gravity g, meaning the force required to move the chain upwards counteracts the gravitational force. Force is determined by $F = m \cdot a$, with F representing force, m the mass of the chain and a its acceleration. As the upward acceleration opposes the gravitational acceleration downwards, the two corresponding forces counteract each other, resulting in a lower net force and thus reduced tension at the UTC end.

Conversely, as the chain moves downwards, its acceleration aligns with gravity, resulting in a greater total acceleration and, consequently, higher tension [44]. This behaviour is evident in Figure 6.6, which shows the variation in tension, z position and vertical acceleration of the UTC end point at the vessel for a certain time period and a peak wave period of 6 seconds. The data in this figure is standardised by subtracting the mean and dividing by the standard deviation, allowing for clearer comparison of trends. The figure shows that as the end point of the UTC moves upwards, the acceleration decreases, as does the tension, and vice versa, illustrating the inverse relationship between upward motion and tension. Additionally, it demonstrates that the peak tension becomes larger with greater amplitudes of acceleration.

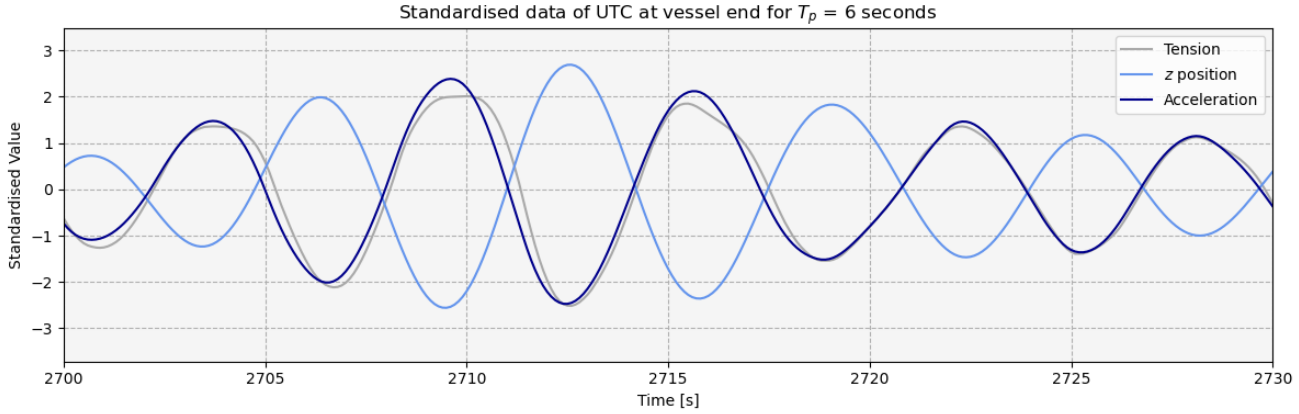

Figure 6.6: Effective tension, acceleration and z position of the UTC at vessel end for Case 1 and T_p = 6 s.

The increased tension in Figure 6.5 around a wave period of 6 seconds can be attributed to the pitch RAO, presented in Figure C.2, of the installation vessel. Around T_p = 6 s, the wave frequency aligns with the natural pitch frequency, resulting in larger pitch angles and thereby greater vertical displacements z of the UTC endpoint. Figure 6.6 demonstrates that for a given wave period, and therefore frequency, the amplitude of the acceleration increases with greater vertical displacements. Shorter wave periods lead to a higher frequency of oscillation, which increases the rate of change in the pitch angle, and consequently increases the angular velocity ω. Together, these effects lead to an increase in acceleration, as described by $a = \omega^2 \cdot z$ [44].

For longer wave periods, the vertical displacement at the UTC end point at the vessel may still be large, but it occurs at a lower frequency, resulting in smaller accelerations and therefore smaller deviations in tension from the mean. For shorter wave periods than T_p = 6 s, although the wave frequency is higher, the pitch response is smaller, which reduces the resulting vertical displacements and associated accelerations. This reduction in acceleration results in lower dynamic tensions compared to a T_p of 6 seconds.

The results of the vertical acceleration, for Case 1, of the UTC at the vessel's endpoint are presented in Figure 6.7. These plots exhibit the same pattern as the tension in the UTC (Figure 6.5), illustrating that the tension is directly related to the acceleration.

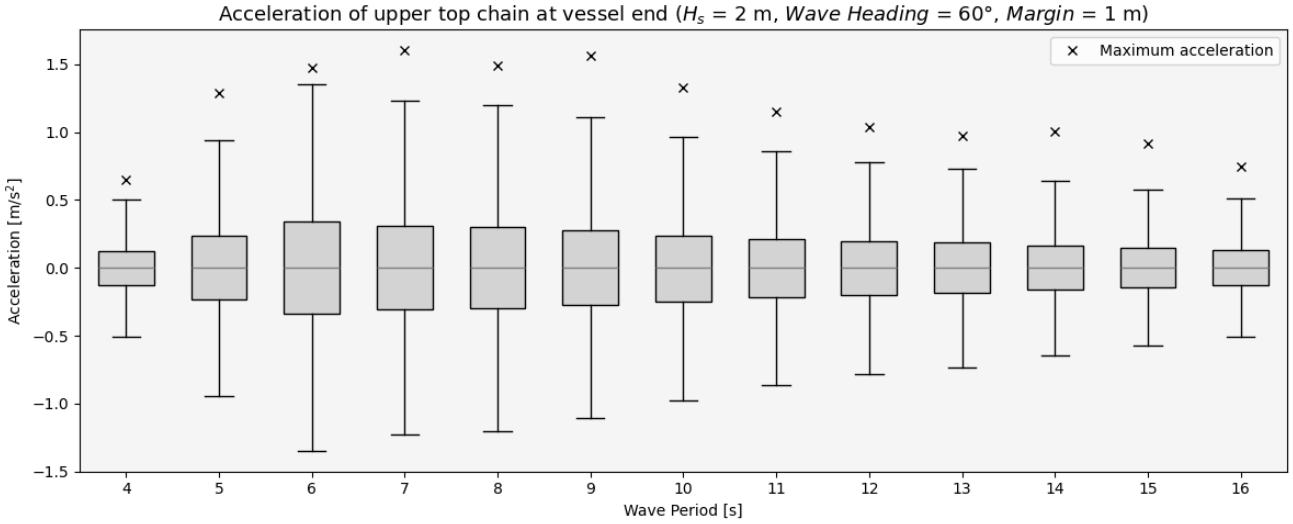

Figure 6.7: Acceleration at the vessel end of the UTC for Case 1

The findings of increased vertical motions of the chain at the vessel's endpoint, resulting in higher tension differences, are consistent with the research by [29], as discussed in Section 2.4.1.

6.2.3. Influence of UTC length

The length of the UTC itself does not significantly impact its behaviour, provided it contains a sag. A sag in the chain is critical; without it, the chain behaves more like a taut chain, leading to an increased tension and a higher likelihood of the chain becoming fully tensioned during the hook-up process.

In Case 7.2, with a connection height at the top, the UTC length is adjusted for each wave period. For a T_p of 4 seconds, the UTC does not contain a sag, while for T_p values of 5 to 7 seconds the sag is minimal. The results of the effective tension, presented in Figure 6.8, indicate that shorter UTC lengths corresponding to lower T_p values result in increased static tension, represented by higher median values. The greater deviation in maximum tension for T_p = 4 s is attributed to an additional factor, which is explained in the next section.

The higher static tension for lower T_p values arises because minimal sag in the UTC results in a more taut chain, thereby increasing tension. As the sag increases the tension decreases. However, for longer chains, the tension at the endpoints of the UTC increases again due to the additional self-weight of the chain. This is evident when comparing Case 1 and Case 2, which differ only in UTC length. The mean tension at the end point of the UTC is higher in Case 2, reflecting the effect of the increased chain length. The results of the effective tension in the UTC for Case 2 are presented in Figure A.2 in Appendix A.

Returning to the results of Case 7.2, the UTC contains sufficient sag for larger wave periods, resulting in nearly identical static and dynamic tensions between differing wave periods. This indicates that the UTC length itself

has no significant impact as long as a sag is present. The comparison between Case 1 and Case 2 further confirms that the effect of UTC length is minimal.

While the required UTC length is primarily governed by the sea state parameters, the length itself does not significantly affect the dynamic behaviour of the UTC, provided a sag is maintained. This relationship is evident in the results of Cases 9, 10, and 11, and particularly in the comparison between Case 1 and Case 11, where a higher H_s necessitates a longer UTC, leading to an increased mean tension at the chain's end due to the additional self-weight of the chain. Additionally, comparing Cases 9, 10, and 11 demonstrates the effect of wave heading on the maximum UTC tension. Although the UTC length slightly decreases, and thus the static tension at the vessel end, with wave headings closer to 90 degrees, the acceleration increases, leading to higher deviations in tension from the mean. However, these deviations remain insignificant. Comparing Figures C.1 and C.2 also shows an increased peak in the pitch RAO of AHTS 1 for a wave heading of 60 degrees, compared to 0 degrees, with increased pitch responses resulting in greater accelerations for a given wave period.

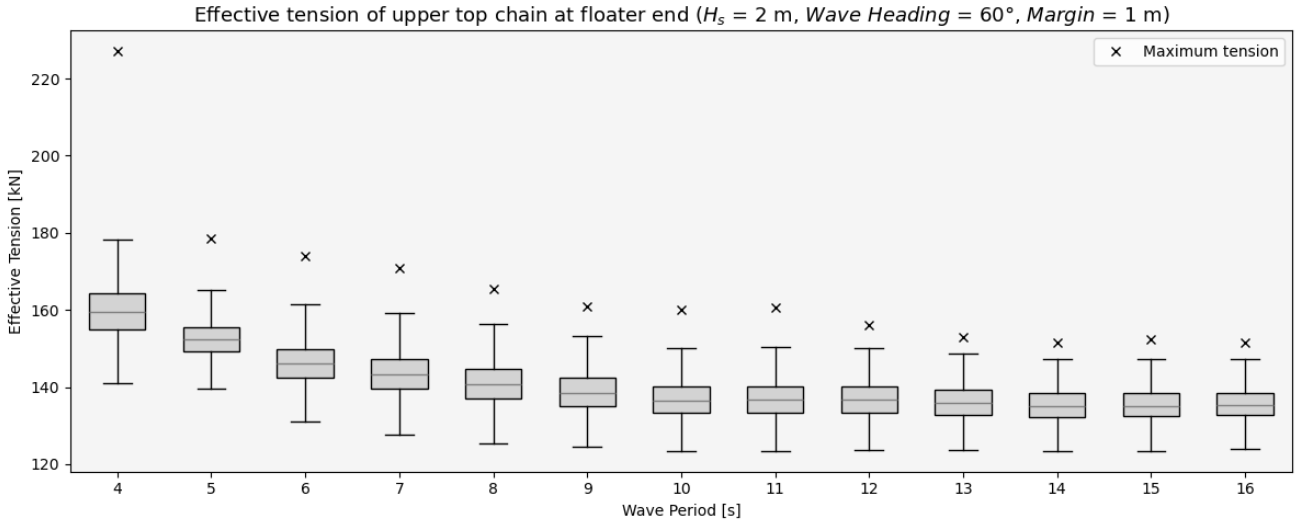

Figure 6.8: Effective tension of upper top chain for Case 7.2 with the connection height at the top of to floater, with varying chain length per T_p

The findings from Case 7.2 highlight that the approach of determining the UTC length results in short chain lengths for low wave periods. This is due to that the MPM values of the displacements at both ends of the UTC are very small for low T_p values. As a result, the chain length becomes too short to maintain sag which is not acceptable. It is therefore recommended to apply a larger margin than 1 metre to create an UTC with sufficient sag. The current approach would benefit from an analysis to determine up to which T_p value a larger margin should be applied and to quantify this margin. For larger T_p values, a smaller margin might suffice.

Besides, the DP system of the vessel does not react to rapid deviations in the x and y directions caused by short wave periods, potentially leading to abrupt changes in the distance between the UTC's endpoints, even though their magnitude is generally smaller compared to longer waves. In contrast, longer wave periods result in larger but more gradual displacements of both the floater and the vessel, which tend to affect both in a similar manner, causing them to move in the same general direction. These smoother movements make it easier for the DP system to maintain a fixed distance to the floater. It is therefore recommended to derive a variable margin throughout T_p, accounting for the differing effects of short and long waves.

6.3. Connection height

The connection height of the UTC to the floater does not significantly influence the dynamic behaviour of the UTC, provided it remains adequately submerged. In Case 7.2, the chain length corresponding to T_p = 4 s is entirely above the water surface in the static state and is only rarely submerged over time. The results presented in Figure 6.8 indicate a greater deviation in maximum tension for T_p = 4 s compared to other wave periods. Further analysis suggests that this behaviour arises due to a combination of two factors. While the specific criteria for the combination of these factors are not analysed in depth, the evaluation of various configurations of UTC connection height and wave period demonstrates that the additional dynamics arise only for wave periods up to 4 seconds when the chain is insufficiently submerged.

The maximum effective tension over time in the UTC is evaluated for five configurations listed in Table 6.1. Since a significant wave height of 2 metres combined with a peak wave period of 4 seconds (as in Case 7.2) is relatively uncommon, based on North Sea data shown in Figure 4.4 in Section 4.3.1, additional analyses are conducted for $H_s = 1$ m and $H_s = 1.5$ m with $T_p = 4$ s, while maintaining the UTC length from Case 7.2. The influence of submersion on the UTC behaviour is analysed by lowering the UTC configuration of Case 7.2 by 0.5 and 1.5 metres for $T_p = 4$ s. Further configurations examine the behaviour of an UTC positioned above the sea surface with longer wave periods. In all configurations except Configuration 5, the UTC length is consistent with Case 7.2 for $T_p = 4$ s. Configuration 5 resembles Case 7.2 with $T_p = 5$ s, where the UTC is moved upwards to be completely above the sea surface. In Configuration 6, while the UTC length and positioning remain consistent with Case 7.2 and $T_p = 4$ s, the peak wave period is adjusted to 5 s.

Configuration	Explanation
Configuration 1	UTC length of Case 7.2 and $T_p = 4$ s, for $H_s = 1$ m
Configuration 2	UTC length of Case 7.2 and $T_p = 4$ s, for $H_s = 1.5$ m
Configuration 3	UTC length of Case 7.2 and $T_p = 4$ s, where the entire UTC is lowered by 0.5 metres
Configuration 4	UTC length of Case 7.2 and $T_p = 4$ s, where the entire UTC is lowered by 1.5 metres
Configuration 5	UTC length of Case 7.2 and $T_p = 5$ s, where the entire UTC is moved upwards to be completely above the sea surface
Configuration 6	UTC length of Case 7.2 and $T_p = 4$ s, with waves having a T_p of 5 seconds

Table 6.1: Configurations that vary in wave period and submersion of the UTC

The effective tension in the UTC for the six configurations is presented as box plots in Figure 6.9. The results show that for a wave height of $H_s = 1$ m, the dynamic tension decreases significantly compared to the original case with $H_s = 2$ m. However, for $H_s = 1.5$ metres, larger deviations in tension are observed as well. The results also demonstrate that increased deviations in tension are mitigated when the chain is submerged. This is evident from the results of Configuration 4, where the UTC is lowered by 1.5 metres, as well as Case 7.1 with a T_p of 4 seconds, where the UTC is partially submerged as well. For a connection height at the middle and bottom, the UTC also showed no significant deviation in tension when a margin of 1 or less was applied to the UTC length.

For wave periods exceeding 4 seconds, no increased deviations in tension are observed, even when the UTC is fully positioned above the sea surface, as shown by the results of Configuration 5. Additional tests for longer wave periods confirm this behaviour, although their results are not included here. Configuration 6 further illustrates that the increased dynamic tensions observed in Case 7.2 for $T_p = 4$ seconds are mitigated when the wave period increases to 5 seconds. This implies that only rapid fluctuations in displacements at the end of the UTC cause additional dynamics. In configurations with increased dynamic effects, wave propagation within the chain becomes more pronounced, leading to larger fluctuations in tension. For connection heights at the middle and bottom to the floater, this behaviour does not occur, as the chain remains largely submerged in the water.

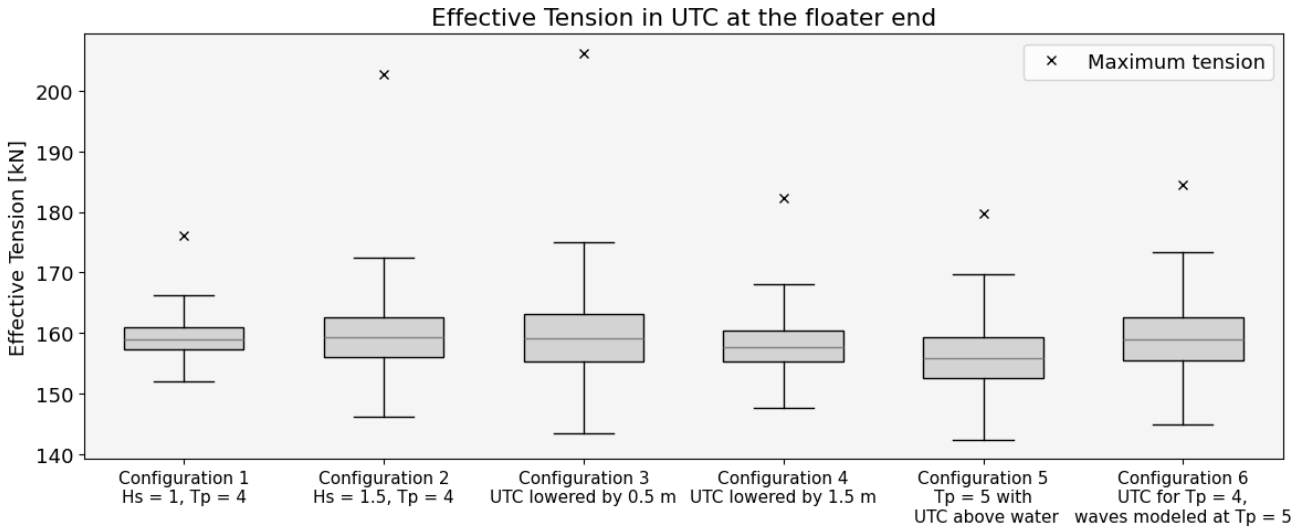

Figure 6.9: Results of the six configurations that vary in wave period and submersion of the UTC

Beyond this, the connection height influences only the mean or static tension along the UTC, with no significant effect on the maximum tension. This is evident in the results for the middle and top connection heights in Figures A.6 and A.7 in Appendix A, where a clear reduction in mean tension is observed compared to the bottom connection height. This can be attributed to the fact that the endpoint supports less chain weight due to the reduced height difference between the endpoints, which alters the chain's shape.

A range graph of the effective tension over time, including the minimum, mean, and maximum tension, is provided in Appendix A for the three different connection heights, where $H_s = 2\,\text{m}$, wave heading = 60°, $T_p = 16\,\text{s}$, and a margin of 1 metre is applied (Figures A.13, A.14 and A.15). The shape of the tension variation closely aligns with the actual shape of the UTC, allowing a comparison of the UTC shape for the three different connection heights. The mean tension in the UTC, which is nearly identical to the static state, remains consistent across different sea states. These figures provide a clear illustration of the tension variation over time along the UTC length. The higher tension at the vessel end is caused by the chain making contact with the stern roller of the vessel, which is modelled in OrcaFlex as a contact shape with a specified stiffness. This contact adds tension to the line in OrcaFlex, and in this case, to the UTC.

6.3.1. Influence on UTC length

Figure 6.10 compares the UTC lengths for three different connection heights For the reference wind turbine and its semi-submersible floater used in this study, these connection points represent the full range of height to the platform, with a margin of 1 metre maintained between the connection point and the actual top or bottom of the platform. The results suggest that the UTC length primarily depends on the vertical distance between its endpoints when considering connection height. For the connection heights at the middle and the top, the behaviour with increasing H_s is similar to that of the connection at the bottom, as visualised in Figure 6.1.

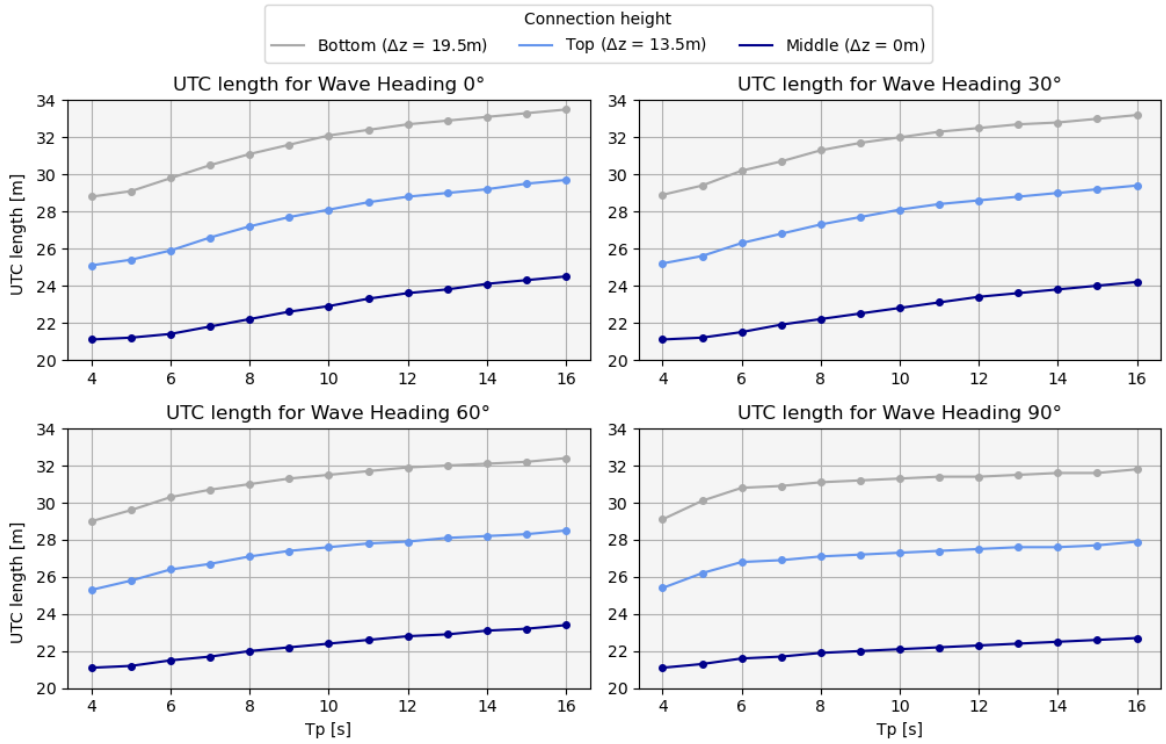

Figure 6.10: UTC length comparison between connection heights

6.3.2. Considerations for connection height

When considering other factors, a connection height at the bottom also appears to be a favourable option. As discussed in Section 2.2.1, current mooring applications generally use a minimum water depth of 100 metres as a limit for fibre rope deployment to mitigate risks associated with UV exposure, marine growth and sheaving or collisions with other objects. Connecting the top chain to the bottom of the floating platform, in this case at 19 metres below water level, already places the fibre rope well below the sea surface.

A connection at the middle results in the shortest chain length but introduces significant challenges. This connection lies within the splash zone, where it is more vulnerable to corrosion [59]. For a top connection, part of

the top chain remains in the splash zone, whereas a bottom connection avoids this issue entirely. Furthermore, if ROV operations are required for maintenance or inspections, they are more feasible when the chain is situated outside the splash zone. If the top chain must be decoupled from the floating platform, a connection in the splash zone would present substantial difficulties. A bottom connection would enable the vessel to position itself closer to the FOWT. With a higher connection, the vessel faces a greater risk of collision with the mooring line, while a connection beneath the vessel's draft effectively removes this risk, ensuring safer operations.

The impact of the connection height on platform stability is not analysed in this research, but it is recommended that it be considered when designing both the platform and mooring system.

6.4. Total top chain length

This section translates the lengths determined for the UTC into a range of values corresponding to workable sea states, which can be considered when connecting two mooring lines with 120-degree spacing by creating an H-link on the deck of the installation vessel. The required length for the lower section of the top chain is addressed, followed by a range for the total required length of the top chain.

6.4.1. Workable sea states and corresponding UTC lengths

Comparisons for different vessels highlight that operational sea states are primarily dependent on the vessel's motion responses. Larger vessels are shown to be critical for achieving stable operations in sea states with increasing H_s and T_p. Figure 6.11 illustrates the workable sea states for the three vessel types considered in this research, showing that the range of operable sea states for AHTS 1, the smallest vessel, is much more limited compared to AHTS 3, the largest vessel. These sea states are determined based on the vessels' MPM values for roll, pitch, and yaw. Although wave heading may slightly influence the UTC length, the workable limits appear to be far more significant, as wave headings have a crucial impact on the vessel's motion responses and, consequently, its operational limits within a given sea state. Wave headings greater than 90° are not displayed to maintain clarity. The workable sea states at headings of 120°, 150°, and 180° were found to be similar to, but slightly less favourable than, those at 60°, 30° and 0° respectively.

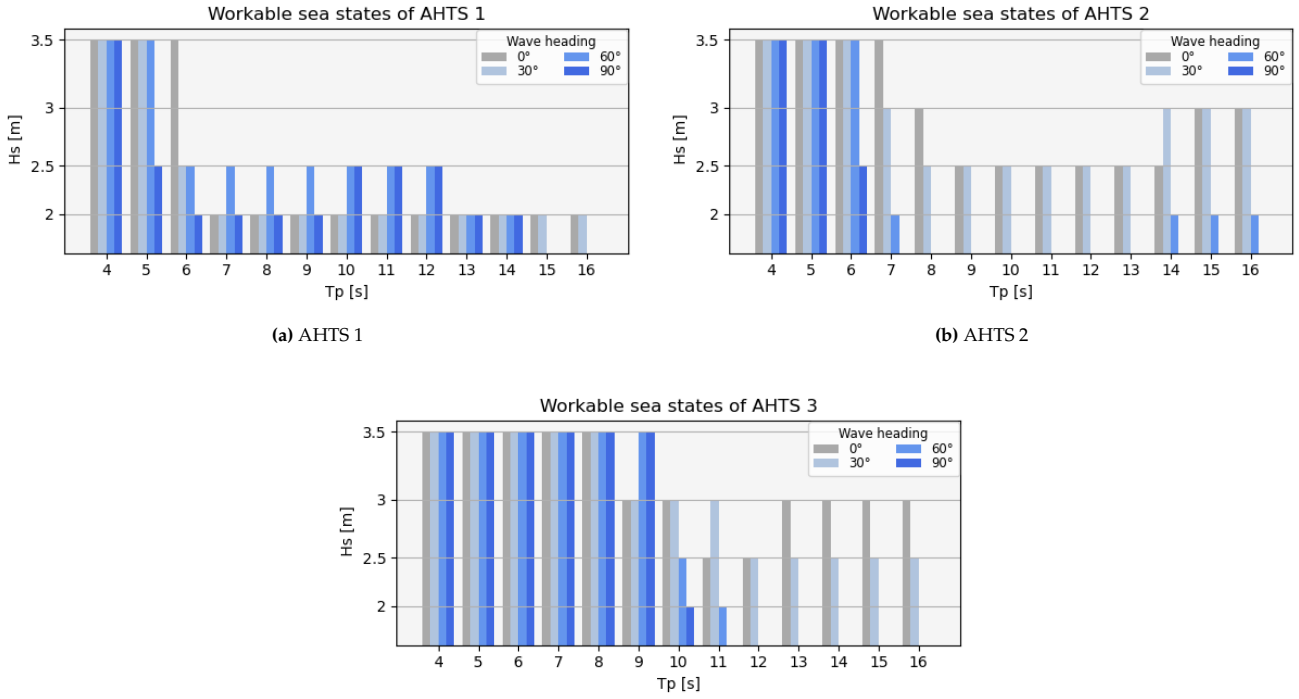

(a) AHTS 1

(b) AHTS 2

(c) AHTS 3

Figure 6.11: Comparison of workable sea states for three distinct vessels: (a) AHTS 1, (b) AHTS 2, and (c) AHTS 3.

The relationship between the workable sea states and the corresponding upper top chain lengths is shown in Figure 6.12 for both AHTS 1 and AHTS 3. A margin of 5 metres is applied to the UTC length, representing the midpoint of the range from 1 to 10 metres. The figure clearly shows the minimum UTC length required for specific sea state conditions, covering only the section between the stern roller and the FOWT. Wave headings

greater than 90° are again excluded for clarity.

As Figure 6.11 clearly shows, a large AHTS is essential as the installation vessel for FOWTs operating in significant wave heights greater than 2 metres. AHTS 1 is not a suitable vessel for installation under these conditions. For larger peak wave periods, wave headings closer to 0° are more favourable for workable conditions. However, the difference in UTC length across varying wave headings remains relatively small.

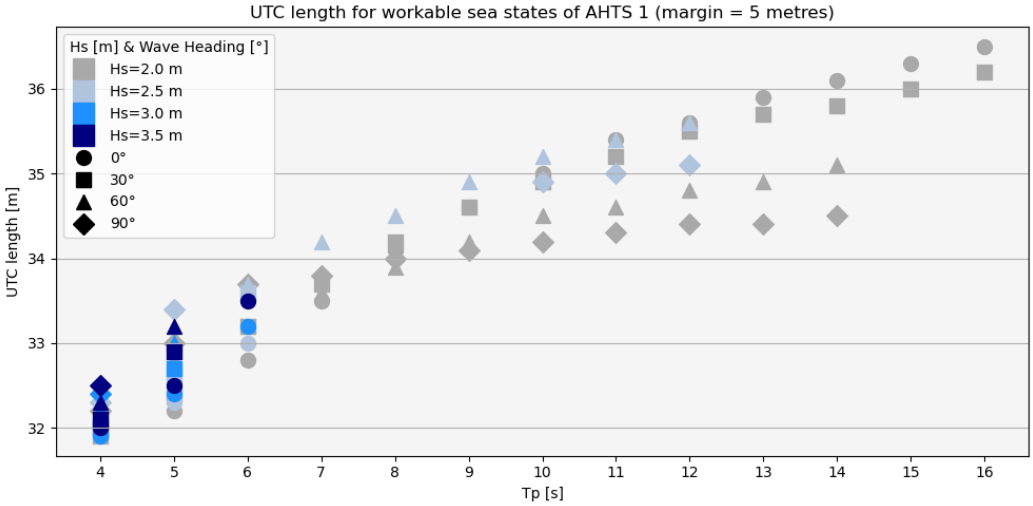

(a) AHTS 1

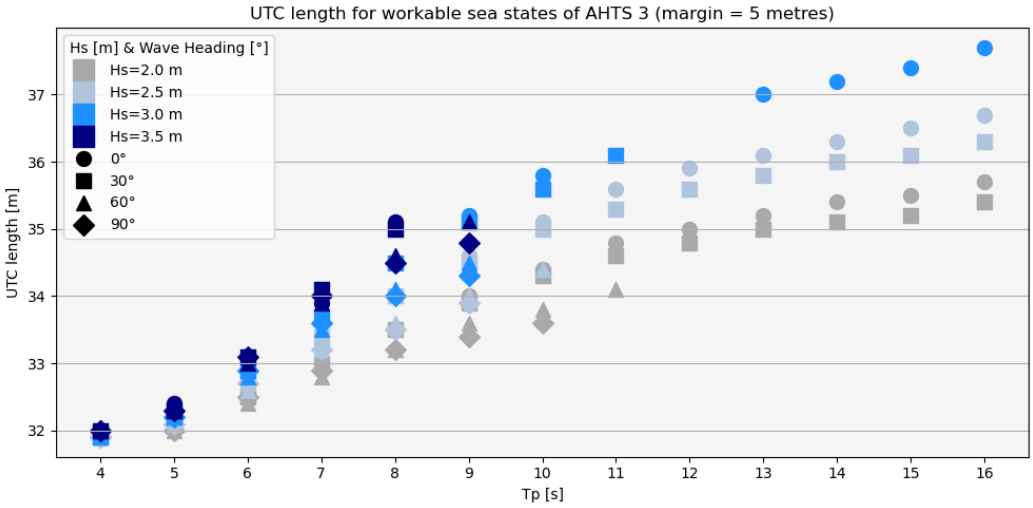

(b) AHTS 3

Figure 6.12: Upper top chain length per workable sea state for: (a) AHTS 1, (b) AHTS 3.

During the hook-up operation of a FOWT, the wave heading experienced by the installation vessel will change throughout the process if the wave direction remains constant during the installation of a single turbine. The connection of the first line offers ample flexibility. The AHTS is free to position itself as the pre-laid mooring line can more or less freely rotate around its anchor point. This flexibility allows the AHTS to adjust its heading and alignment without constraints imposed by the mooring system. Figure D.1 illustrates an example where the AHTS positions itself far from the target position of the FOWT after installation to achieve a wave heading closer to 0°. This choice is supported by Figure 6.11, which indicates that wave headings within ±30° are preferable for larger AHTS vessels, which are necessary for the operation.

However, the second mooring line introduces considerable restrictions. The already connected line imposes a limit on the floater's movement and positioning, as the distance between the floater and the anchor point of the first line is constrained by the length of the mooring line. Additionally, the AHTS must align itself with the pre-laid line during the second connection. While there is some margin in the alignment, this restriction further limits the range of possible wave headings relative to the AHTS. Figure D.2 illustrates the limited positioning

options for the AHTS, with the blue circle representing the stretched length of the already connected mooring line.

The third mooring line is not considered in this analysis, as an off-vessel connection method is used for its installation. The range of wave headings for the second mooring line connection, relative to the first, results in a range of wave heading combinations during the dry chain-link connection operations. It is recommended that, for a range of wave directions, the possible wave heading combinations are evaluated during the hook-up of the first and second mooring lines. The flexibility offered by the first line should be utilised effectively to ensure that preferred wave headings are achievable during the second connection. Additionally, the order in which the lines are connected significantly impacts the range of feasible wave headings. It was found that if the order of all three mooring lines is flexible, the wave heading for the second line can always be maintained within 30° to 60° of the first line. This range aligns with the operational preferences for large AHTS vessels, as shown in Figure 6.12b. In real-time conditions, the wave heading may, of course, vary throughout the installation. However, certain dominant wave headings are likely to occur frequently, while others may rarely or never be encountered.

6.4.2. Lower section of the top chain

The lower section of the top chain should have adequate length to prevent contact between the lower segment of the mooring line and the rudders or thrusters of the installation vessel. This criterion closely aligns with the analysis above. For the first installed mooring line, this issue is not expected to arise, as the AHTS can position itself close to the anchor to create ample slack in the line. However, for the second line, positioning is constrained by the length of the already connected line.

The 2D views in Figure 6.13 provide a side view corresponding to the top-down layout shown in Figure D.2. In this scenario, the AHTS is unable to move significantly closer to the anchor of the second line if it is assumed that the first line may only be stretched until its full length. It is recommended to assess how far the AHTS can move away from the anchor of the first line. This assessment depends on the maximum allowable tension in the line and the pulling force that the AHTS, together with the assisting tugboats, can exert. The BP of these vessels will determine their ability to apply the required force.

The amount of chain required in the lower segment to avoid exceeding the 30° angle depends on how close the AHTS can position itself to the anchor. Additionally, the dimensions and weight of the mooring materials used, as well as the ratio between the mooring line length and the anchor radius, play a significant role. Another influencing factor is the orientation of the AHTS relative to the pre-laid mooring line, which is influenced by its desired heading with respect to the wave direction. For the scenario illustrated in Figure D.2, a comparison is made between using 10 and 15 metres of chain starting from the stern roller, excluding the chain length in contact with the vessel (Figures 6.13a and 6.13b). The green line indicates the 30° limit. The little section between the grey line (chain) and red line (polyester) represents a connector that connects the two materials. This connector has a significant weight which contributes to maintaining sufficient clearance to the thrusters.

The results indicate that a chain length of at least 10 metres is required to maintain sufficient clearance between the mooring line and the thrusters of the AHTS. However, a length of 15 metres significantly enhances this clearance, offering greater operational flexibility. The figures presented reflect clearance in a static state. During operation, the vessel's pitch or translational motions could bring the mooring line closer to the AHTS thrusters and rudders. It is evident that longer chains in the lower segment extend the distance from the anchor at which installation remains feasible. The 30-degree angle limit is of course applicable up to a certain depth below the vessel, at which point the mooring line is sufficiently far from the rudders and thrusters. This depth depends on the vessel type and its layout.

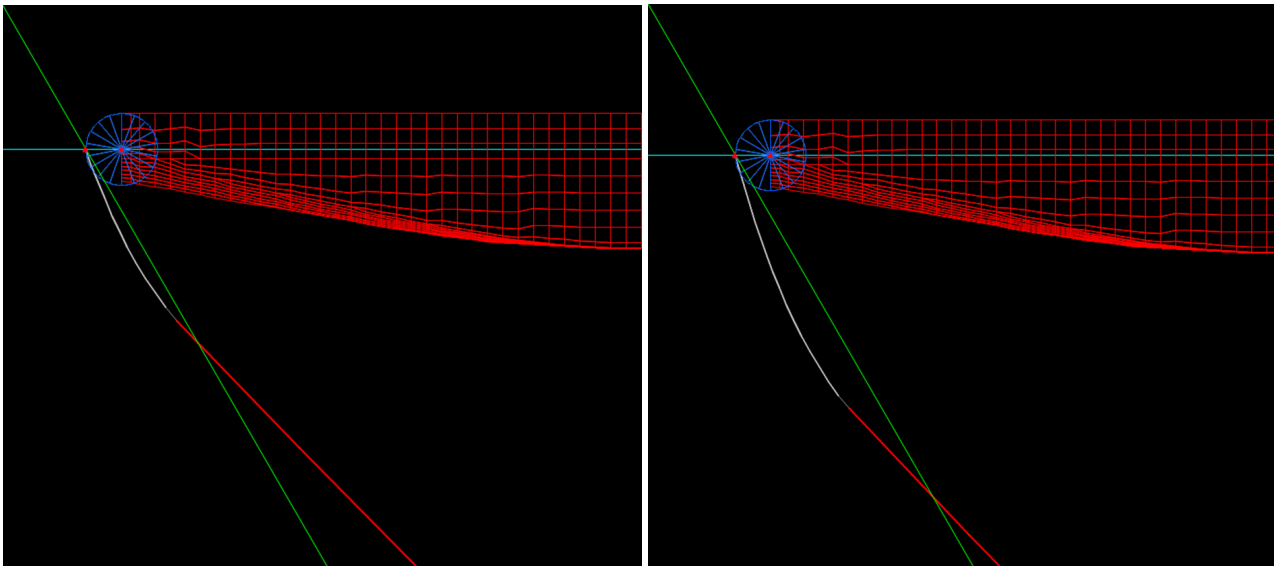

(a) 10 metres of chain **(b)** 15 metres of chain

Figure 6.13: Comparison of mooring line to AHTS thruster angle, with the green line indicating the 30° limit

Total top chain length

The total top chain length, combining the three segments, consists of the portion on the deck and stern roller of the AHTS, the upper top chain between the stern and the floater, and the lower section which prevents contact with the thrusters. The deck segment is determined by the vessel layout, particularly the radius of the stern roller and the distance from the stern roller to the shark jaws. Using AHTS 1 as an example, the total top chain length can be derived from Figure 6.12a, combined with two times 11.15 metres on the deck and at least 10 metres for the lower segment. Based on the range shown in Figure 6.12a, where a margin of 5 metres is applied, the total top chain length varies between 64 and 69 metres. The total top chain, with the individual section lengths, is illustrated as an example in Figure 6.14; for other combinations of margin, sea states, vessel design, and mooring configuration, the total length would differ. The length of the H-link closely matches the length of a single chain link with a nominal diameter of 175 mm.

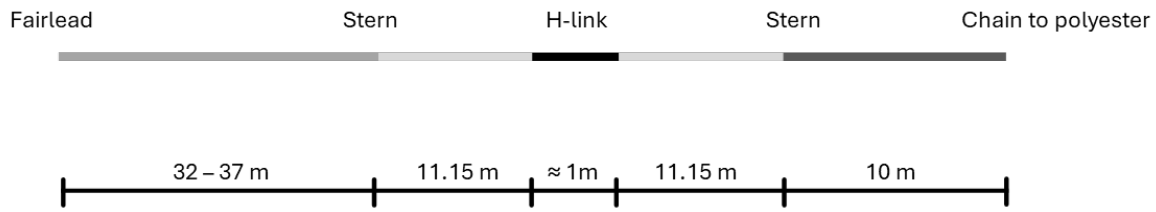

Figure 6.14: Example of total top chain length divided into individual sections

6.5. Validation and verification

This section discusses the validation and verification processes applied in this research. Verification focuses on ensuring that the model and methods are implemented correctly and are appropriate for the intended analysis. Validation, on the other hand, involves comparing the model's results to expected physical behaviour to assess its accuracy [63]. For the hook-up installation model developed in OrcaFlex, full-scale validation is not possible due to the absence of comparable studies. To address this, a simplified model is created to study the behaviour of the UTC under predefined excitations at both ends, as described in Section 6.5.1.

Orcina, the developer of OrcaFlex, has conducted extensive validation studies to establish the software's credibility. These include comparisons with real-world data, such as measurements from model tests and full-scale operations, and benchmarks against other established programs. This ensures that OrcaFlex can reliably simulate complex offshore systems [48]. Another approach used for validation in this research is face validity [55], which involves consulting knowledgeable individuals to assess whether the model and its behaviour are reasonable. The model creation and setup has been discussed with OrcaFlex experts at Seaway7, and the model has been shared with Orcina who provided feedback on the model inputs.

Graphically visualising the model's behaviour is also a form of validation, referred to as animation validation [55]. OrcaFlex provides a visual representation of the model over the simulation time, allowing users to observe the behaviour of different components. This method is used to check whether the observed behaviour of various parts in the model is realistic and aligns with expected physical responses. Sensitivity for time steps and simulation durations is covered in Section 5.2.1.

6.5.1. Chain behaviour

A model in OrcaFlex is developed to focus specifically on the behaviour of the upper top chain under predefined excitations. In this model, winch objects are placed at both ends of the chain to simulate controlled motions, where the winches alternately pay in and pay out the chain. The purpose of this model is to demonstrate that high tensions within the chain are only reached when the distance between its endpoints approaches the total chain length, leaving little to no sag.

Insights from the time-domain simulations of the full-scale model indicated that the vertical translation periods at both endpoints closely align with the peak wave period. Three distinct periods are applied to the winch excitations in the simplified model to determine the influence of oscillation frequency on the chain's tension. The model assumes that the two ends move completely out of phase, representing the extreme case, to provide a clear understanding of the tension dynamics for different endpoint distances and chain length ratios. Only vertical translations are considered.

Five different cases are considered, each with three different wave periods: $T_p = 4$ s, $T_p = 8$ s and $T_p = 12$ s, as listed in Table 6.2. The cases feature decreasing UTC lengths, with both the initial distance and maximum distance presented. $Dynamic\ z$ represents the total increase in vertical distance generated by the winches, with Δz representing the initial height difference between the chain's endpoints. The results for the effective tension in the UTC are depicted as box plots in Figure 6.15. These results indicate that tension increases significantly more once the distance between the endpoints matches or exceeds the chain's length, whereas the increase in tension is more gradual just before this threshold. This behaviour is favourable because the tension in the UTC only becomes significant when the chain approaches its fully stretched state.

Case	Δz [m]	Dynamic z [m]	UTC length [m]	Initial distance [m]	Maximum distance [m]	Maximum tension (Tp=12) [kN]
Case1	19.5	0.5	30	27.93	28.28	174
Case2	19.5	0.5	29	27.93	28.28	200
Case3	19.5	0.5	28.3	27.93	28.28	287
Case4	19.5	0.5	27.94	27.93	28.28	473
Case5	19.5	1.1	27.94	27.93	28.71	848

Table 6.2: Input cases of model capturing UTC behaviour

Lower T_p values result in greater dynamic effects on the chain, as indicated by the wider boxes and higher maximum values. However, this effect partly arises from the abrupt pulling forces applied by the winches. With shorter time periods between upward and downward motions, the residual effect of the pulling force remains when the next force is applied. In contrast, for longer periods, the chain has time to relax which reduces this effect.

Moreover, $Dynamic\ z$ remains constant throughout the varying wave periods, whereas it would normally vary. Especially for $T_p = 4$ s, the vertical displacements are larger than would actually occur. Tests that included varying $Dynamic\ z$ values, which matched the actual vertical displacements for the corresponding wave period measured in the full-scale model, showed reduced differences in dynamic tension between small and large wave periods, making their effects more similar. However, these results are not shown here. As the magnitude of $Dynamic\ z$ influences the required UTC length, $Dynamic\ z$ is kept constant to maintain a consistent UTC length, ensuring similar static tensions across the varying wave periods.

For smaller T_p values, the tension is also over estimated as in real time and in the full-scale model, the transition between upward and downward motion is more smooth. This results in a gradual variation in the acceleration of the UTC, which in turn leads to a more gradual variation in the UTC tension. In the winch model, this transition is sharp and abrupt, resulting in higher tension peaks accompanied by additional oscillations.

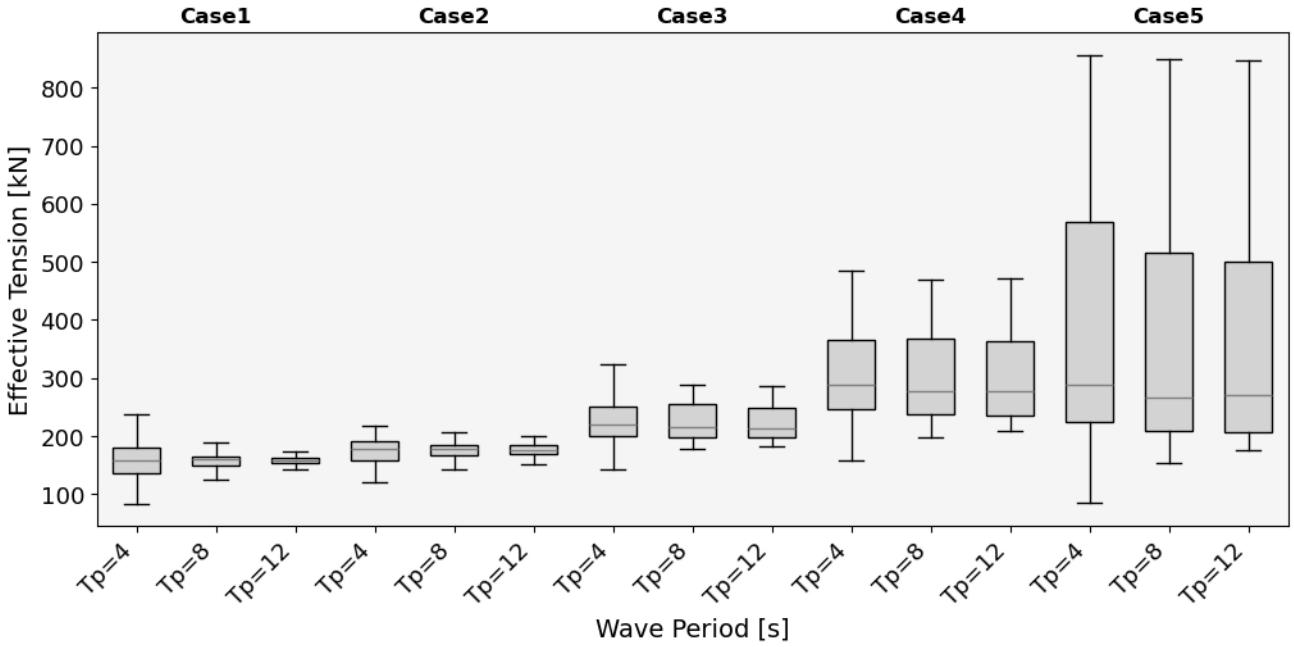

Figure 6.15: Maximum effective tension in the UTC for the model containing only the chain

The model results of effective tension in the UTC are compared directly to the full-scale model for three different T_p values, with H_S = 2 m and a wave heading of 0°. In the full-scale model, the maximum vertical distance between the UTC endpoints is measured. The corresponding z positions are applied to both ends of the UTC in the chain-only model by adding these positions to the pay-in and pay-out values of the winches. The results of the effective tension in the UTC are presented in Figure 6.16. In the chain-only model, only extreme displacements are considered, which explains the greater spread observed compared to the full-scale model. To accurately compare the behaviour, a broader range of predefined excitations should be incorporated into the model.

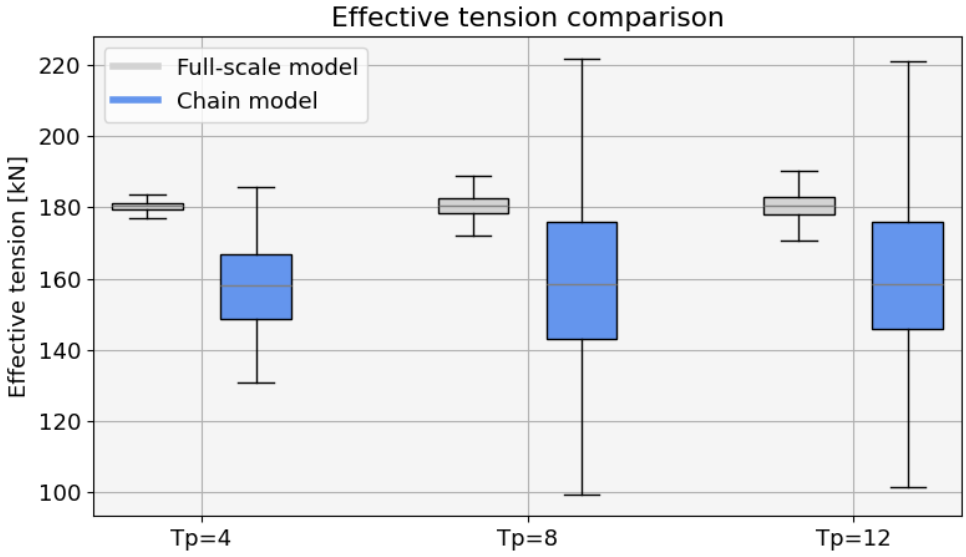

Figure 6.16: Full-scale and chain only model comparison

6.5.2. Tow line tensions

The dimensions of the tow lines are determined iteratively until the desired properties and response are achieved. Two criteria are that the tension must remain below 20% of the MBL, while the lines provide a smooth, reactive restoring force against the environmental loads. The range of normalised tensions over time is illustrated as box plots in Figures E.1 and E.2. The normalised tension is defined as as the tension in the line divided by its MBL.

The length of the upper top chain influences the pulling force of the tow lines, as the extra weight of the chain must be accommodated. This effect can either increase or decrease the tow tension, depending on the specific setup. For a wave heading of 0°, the tow tensions are equal, but for other wave headings their pulling forces are less evenly balanced. The results indicate that maximum tensions remain well within the defined limit, and the spread in tension is small. Figures E.1 and E.2 present data derived from Case 2.

6.5.3. Vessel heading

As described in Section 4.4.1, most models assume that the installation vessel does not remain aligned with the FOWT during the simulation. As a result, the measured distance reflects the distance between the UTC ends rather than the actual distance between the floater and vessel. To validate that this assumption does not lead to significantly different results, a model is created in which the installation vessel rotates along with the floater. Both the tension within the UTC and the distance between its endpoints are compared, as shown in Figure 6.17. The results indicate that the difference in tension is minimal. While the 2D distance shows slight variations, these are attributed to the high sensitivity of the setup and the positioning of the tugboats.

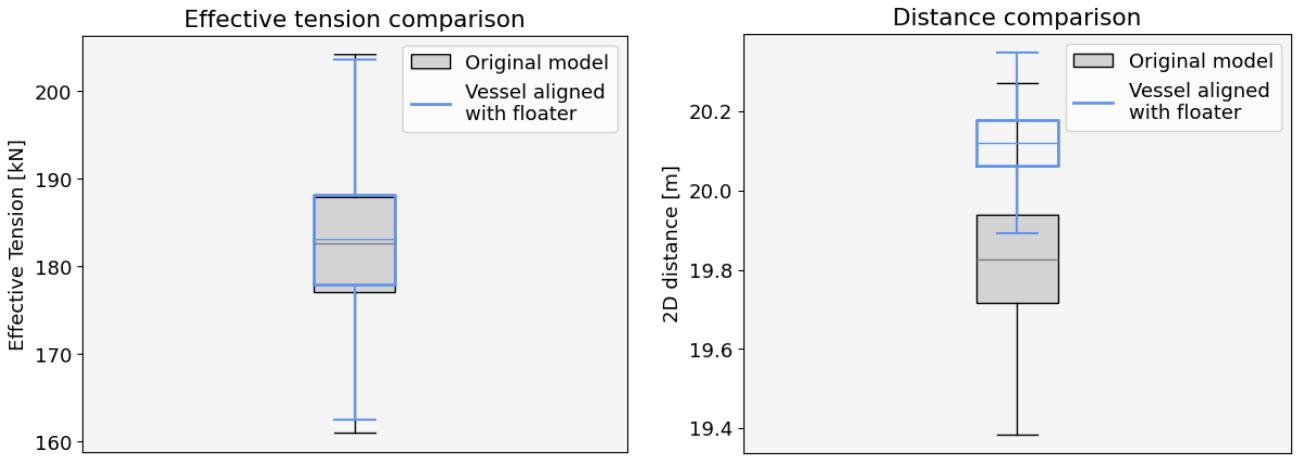

(a) UTC tension comparison

(b) 2D distance comparison

Figure 6.17: Comparison of UTC tension (a) and 2D distance between end points (b) of original model and model with vessel aligned with floater

7
Conclusion

This research aimed to determine the required top chain length for hook-up operations of semi-submersible Floating Offshore Wind Turbines (FOWTs). A simulation model has been created to analyse the dynamic behaviour of the top chain during the hook-up installation, with a specific focus on a dry chain link connection method on the deck of the installation vessel. For stretch management, applying the bow-string method to one line is assumed to be feasible and sufficient to achieve the required pre-stretch for the three-line mooring system. Under this assumption, the dry chain link method is considered critical in terms of the required top chain length for hook-up operations of a three-line mooring system. However, a detailed analysis is required to verify the feasibility of this assumption. In the following sections, the sub-questions are addressed, followed by a conclusion regarding the main research question.

How does the depth below the sea surface influence the need for top chain?
Fibre ropes are particularly vulnerable to factors such as UV radiation, collisions or sheaving with other objects, such as vessels or the fairlead, increased water or air temperatures, and the penetration of marine growth. Current practice dictates that fibre ropes are typically applied only in water depths of 100 metres or more to mitigate these risks. Protection covers and filters against UV radiation and marine growth are already in use and have proven successful in practice. Ongoing advancements in these protective measures are being actively tested, with several tests already showing promising results. These developments could enable the use of fibre ropes in mooring systems at shallower depths, potentially reducing the reliance on chain.

Does fibre stretch management during the installation of a FOWT affect the required top chain length?
Managing the stretch removal of fibre ropes is a critical aspect of the installation process. A thorough understanding of the tension versus stretch behaviour of fibre ropes is required to design the system effectively. Pre-stretching polyester ropes to 40% MBL introduces permanent stretch, which is, according to tests, sufficient to maintain adequate mooring performance over the FOWT's lifetime, even after exposure to extreme storms. When properly designed, the rope length is determined at multiple tensions corresponding to different stages of its lifetime. Mainly two different outcomes are distinguished. When designed and operated accordingly, the mooring system stabilises at the desired pre-tension after applying pre-stretch. Alternatively, if the pre-tension drops below the desired level, a temporary chain can be used to re-tension the system. Consequently, under the assumption described at the beginning of this chapter, fibre stretch management is not considered a critical factor requiring a specific amount of top chain. In fact, when designed accordingly, the top chain length of the adjustable-length mooring line may even be shorter compared to fixed-length lines by accounting for the expected elongation of the fibre ropes.

How does the connection height of the top chain influence its required length?
The primary relation between the connection height and the length of the top chain is driven by the height difference between the chain's endpoints. An increased height difference results in a greater distance between the endpoints, necessitating a longer top chain length. However, the results indicate that a combination of short wave periods up to 4 seconds and a top chain with minimal sag that is insufficiently submerged can lead to increased dynamic effects, raising the risk of snap loads. That said, the combination of wave heights exceeding 1.5 metres and a period of 4 seconds is uncommon, and when the top chain length is designed for larger wave periods, the corresponding length, according to the approach, is sufficient to mitigate these dynamic effects. Beyond this, the connection height does not significantly affect the top chain's behaviour, with dynamic tensions showing small deviations from the static tension during the hook-up operation.

When looking at the water below the sea surface, a lower connection height is advantageous as it positions the top chain in significantly deeper water. Depending on the depth limit of the fibre rope, connections to the top of the floater would require a longer top chain as a larger height difference must be bridged before fibre rope

deployment becomes acceptable. Additionally, removing the top chain from the splash zone by making the connection below the sea surface offers benefits in terms of corrosion.

How do variations in sea states and weather conditions affect the required length of the top chain?
The results showed that significant wave height has a slight impact on the required top chain length, with higher wave heights leading to marginally longer chains. The increase in top chain length was more pronounced with increasing peak wave periods. Wave heading also influences the required length: for short wave periods, headings closer to 0° correspond to the shortest chain lengths, whereas for wave periods of around 8 seconds and longer, headings closer to 90° result in shorter chain lengths.

However, the results also revealed that the top chain length itself is less critical than the workable limits imposed by the installation vessel. These limits define the workable sea states, and for such conditions, the corresponding minimum required top chain lengths are determined. The workable sea states are highly vessel-dependent, and it is evident that large AHTS vessels are essential for installing FOWTs in sea states with significant wave heights exceeding 2 metres, when employing a dry chain link connection method.

What is the minimum length of the top chain required for hook-up operations of a semi-submersible floating offshore wind turbine?
The top chain has been divided into three distinct sections, each with specific criteria. The criteria for the lower section are primarily aimed at preventing contact between the lower segment of the mooring line and the rudders or thrusters of the installation vessel. The increased weight of the chain, compared to polyester, aids in maintaining sufficient clearance between the lower segment of the mooring line and the thrusters. At least 10 metres of chain are required for this lower section.

When establishing a chain link connection on the deck of the installation vessel, both the lower and upper segments of the mooring line are recovered onto the deck. To prevent damage, contact between the polyester rope and the vessel must be avoided. The middle section of the top chain accommodates the total length on the deck during hook-up. For AHTS 1, approximately 22.3 metres of chain (two segments of 11.15 metres) are required for this section.

The length of the upper top chain is analysed through dynamic simulation models representing the hook-up operation. Frequency domain analyses of the 3D displacements at both ends of the chain were used to determine the required length between the FOWT fairlead and the stern roller of the installation vessel. By accounting for the distance between extreme opposing motions, along with a margin ranging from 1 to 10 metres, the upper top chain achieves sufficient sag to prevent excessive loads during the hook-up operation. As long as a sag is present and the upper top chain is not exposed to a combination of wave periods up to 4 seconds and little submersion, deviations in dynamic tensions in the chain remain close to the mean and static tension. While variations in connection height and sea states influence the required length of the upper top chain, the chain length itself has minimal impact on its dynamic behaviour.

For a connection height at the bottom of the FOWT, with AHTS 1 as the installation vessel, the required length of the upper top chain ranges from 29 to 44 metres. This range incorporates both the lower and upper margin, H_s values of 2 to 3.5 metres (in 0.5 metre increments), T_p values from 4 to 16 seconds and wave headings ranging from 0° to 180° (in 30° increments). The total top chain length required for hook-up operations, combining all three sections, ranges from 61 to 76 metres. However, the size of the installation vessel plays a critical role in determining which combinations of sea states and corresponding top chain lengths are feasible. The considerations discussed, including hook-up method and mooring design, involve a trade-off between optimising performance and simplicity, while aiming to make FOWTs financially attractive for large-scale deployment.

8

Discussion & recommendations

The implementation of fibre ropes and a dry chain link connection method are anticipated to be among the most cost-effective options for the floating wind industry. While the primary focus of this research is on determining the required top chain length for a dry chain link hook-up method, it is important that other related factors are also taken into account. The conclusions regarding the relationship between fibre stretch management and the required top chain length are based on a three-line mooring system, with the assumption that sufficient pre-stretch can be achieved by pulling just one line of the mooring system. Changes in mooring configurations could affect these conclusions, and further analysis is required to validate this assumption.

Shallow water depths remain an under explored location for the deployment of fibre mooring ropes. Ongoing advancements in protection against the penetration of marine growth, such as protective covers and filters, have shown promising results. Without effective protection, fibre ropes would need to be positioned significantly below the sea surface, with common practice being depths of 100 metres, to mitigate risks such as losing performance or experiencing failure. Connecting the mooring line to the bottom of the floater naturally removes the upper segment from the splash zone. For the reference turbine in this study, the draft already places the connection point 19 metres below sea level.

For hook-up operations, the connection height has no significant impact on the dynamic behaviour of the top chain. Lowering the connection height, however, increases the required top chain length compared to aligning it with the installation vessel's stern roller, as a greater distance must be bridged between the chain's endpoints. For AHTS 1, the top chain length for a connection at the bottom ranges from 61 to 76 metres, as described earlier. In contrast, for a connection height equal to the stern roller of the installation vessel, the required length ranges from 53 to 68 metres. This indicates a saving of 8 metres in top chain length when the chain is connected at the middle of the platform. However, the height difference of 19.5 metres between these connection points means that the middle connection does not reach as far below the sea surface. Both connection heights and their corresponding lower limit top chain lengths are implemented into the reference application, with the total mooring line length kept constant by adjusting the polyester length. For the bottom connection, the polyester section begins at a 40-metre depth, whereas for the middle connection, it starts at a 17-metre water depth.

This reduced depth could necessitate a longer top chain length in certain conditions, depending on the effectiveness of the protective filters and covers used and the specific installation location. Therefore, a shorter top chain length required for robust hook-up operations does not necessarily imply that the total top chain length will be shorter overall. A high connection point would, under these criteria, be inefficient. Additionally, in terms of corrosion, it is preferable to remove the top chain entirely from the splash zone. A bottom connection also offers benefits for potential operations throughout the lifetime of the FOWT.

Frequency domain results, specifically the Most Probable Maximum (MPM) values of the deviations in x, y and z direction of the top chain endpoints relative to their static positions, were used to determine the required top chain length during installation. Additionally, the MPM values for the rotational DOF of the installation vessel helped identify the workable sea states. A limitation of this approach is that it captures only linear effects, excluding both wind loads and the influence of connecting objects such as the top chain itself. Future studies are recommended to incorporate non-linear effects and wind loads when determining the required top chain length during installation. Nonetheless, without accounting for these factors, the resulting top chain retains sufficient sag and exhibits small deviations in dynamic tensions relative to the static tension.

This holds true, except for top chain lengths corresponding to short wave periods, where the approach for determining the UTC length results in little to no sag in the top chain when a margin of 1 is applied. For short wave periods, the MPM results of the 3D motions of the installation vessel at the UTC connection point are relatively small, leading to shorter required chain lengths. It can be argued that the rapid responses of both the

floating turbine and the installation vessel to short wave periods cause abrupt changes in the distance between the chain's endpoints. In contrast, longer wave periods result in larger but more gradual displacements of both the floater and the vessel. These smoother movements are more likely to simplify the DP system's task of maintaining a fixed distance to the floater, whereas the system does not react to the high-frequency motions associated with shorter wave periods. Moreover, the displacements of the floater and vessel are typically aligned in the same direction during longer wave periods, further facilitating the DP system's ability to maintain this distance. The current approach could therefore benefit from a margin that is variable per T_p, with larger margins applied to shorter T_p values and potentially smaller margins for longer T_p values. It is also recommended to incorporate an actual DP system into the model. On the other hand, the length of the top chain would likely be based on the worst-case scenario and applied uniformly across all FOWTs in a floating wind farm. This means individual lengths corresponding to low H_s or T_p would not be applied.

Another important criterion arose from the hook-up process. The analysis revealed that increased dynamic effects in the top chain during hook-up operations result from a combination of insufficient submersion and minimal sag, particularly under short wave periods ($T_p \leq 4\,\text{s}$). Insufficient submersion eliminates the damping effect of water, causing the top chain to oscillate more intensely in response to wave-induced motions. These rapid fluctuations in tension increase the risk of snap loads. Adjustments to increase submersion depth showed that even partial submersion of the sagged section significantly reduces dynamic behaviour. This highlights that adequate submersion and sag are essential in configurations with higher connection heights exposed to short wave periods during operations. However, the top chain length would still be determined by the case requiring the highest length, which corresponds to longer wave periods. Additionally, as discussed earlier regarding shallow water depths, a connection at the middle or lower part of the platform is preferred. These connection heights would also eliminate the risk of the chain being insufficiently submerged.

During the installation process, longer chain lengths in the lower segment of the mooring line allow the installation vessel to position itself at a greater distance from the anchor point of the second installed mooring line while maintaining sufficient clearance between the lower segment and the vessel's rudders and thrusters. The vessel's positioning is constrained by the length of the already connected mooring line. It is recommended to assess the maximum stretch length of this line during the phase when the second line is being connected. This analysis should account for the pulling force required from both the installation vessel and assisting tugboats. While longer chains offer greater flexibility in vessel positioning, the use of clump weights could also be considered to ensure sufficient clearance. Evaluating the trade-offs between cost and effectiveness will be necessary to determine the optimal solution.

Some limitations are related to environmental conditions. The wind was assumed to be constant and aligned with the wave direction, while currents were not included in the analysis. Additionally, potential fluid interaction effects between the floating turbine and installation vessel were ignored, which may influence the dynamic behaviour of the system under real-world conditions. In the simulation model, the top chain was only modelled starting 240 degrees clockwise on the stern roller, neglecting the section up to the shark jaws.

Furthermore, the accuracy of the DP system, integrated with systems such as Fanbeam, should be carefully evaluated, along with other potential errors, to define an appropriate margin to be added to the top chain length. Lastly, this research assumes that a 40% pre-stretch is feasible for FOWTs using the bow-string method, although this may be water depth-dependent. Not achieving the desired pre-stretch could alter the conclusions regarding the top chain length requirements in relation to the tension versus stretch behaviour of fibre ropes.

It is therefore recommended to conduct an in-depth analysis of the feasibility of pre-stretching a three-line mooring system of a semi-submersible FOWT by pulling one line. Based on these findings, a conclusion can be drawn regarding whether, for a three-line mooring system, two lines can be installed using the dry chain link method and how much top chain is required for the third line. Additionally, it is recommended to assess whether the connection height of the top chain influences platform stability and to verify that variations in top chain length have minimal impact on the mooring performance of the FOWT.

References

[1] C. Allen et al. *Definition of the UMaine VolturnUS-S Reference Platform Developed for the IEA Wind 15-Megawatt Offshore Reference Wind Turbine*. Tech. rep. National Renewable Energy Laboratory, 2020.

[2] American Bureau of Shipping. *Guidance Notes on the Application of Fiber Rope for Offshore Mooring*. Technical Report. American Bureau of Shipping, June 2021. URL: https://ww2.eagle.org/content/dam/eagle/rules-and-guides/archives/offshore/90_fiberrope/fiber_rope_gn_e-feb14.pdf.

[3] O. Andrade and A. Duggal. "SS: Fiber Moorings, Recent Experiences and Research: Analysis, Design and Installation of Polyester Rope Mooring Systems in Deep Water". In: vol. All Days. OTC Offshore Technology Conference. May 2010, OTC-20833–MS. DOI: 10.4043/20833-MS.

[4] I. Aryawan et al. "Innovative Fatigue Design Improvement for Mooring Systems - Floating Offshore Wind Turbine Application". In: vol. Day 3 Wed, May 08, 2024. OTC Offshore Technology Conference. May 2024, D031S002R001. DOI: 10.4043/35169-MS.

[5] N. Atallah. "Learnings from Offshore Oil and Gas: Key Translational Success Factors in Mooring Hookup and Tensioning Methods for Floating Wind". In: vol. Day 2 Tue, May 07, 2024. OTC Offshore Technology Conference. May 2024, D021S004R004. DOI: 10.4043/35163-MS.

[6] M. T. Bach-Gansmo et al. "Parametric Study of a Taut Compliant Mooring System for a FOWT Compared to a Catenary Mooring". In: *Journal of Marine Science and Engineering* 8.6 (2020). ISSN: 2077-1312. DOI: 10.3390/jmse8060431.

[7] M. B. Bastos and A. L. N. Silva. "Evaluating Offshore Rope Fibers: Impact on Mooring Systems Integrity and Performance". In: vol. Day 2 Tue, May 05, 2020. OTC Offshore Technology Conference. May 2020, D021S028R007. DOI: 10.4043/30830-MS.

[8] B. Cerfontaine, S. Gourvenec, and D. White. "Specificities of floating offshore wind turbines for risk and safety evaluation of anchoring systems". In: Sept. 2024, pp. 154–166. ISBN: 9781003431749. DOI: 10.1201/9781003431749-10.

[9] C.-A. Chen et al. "Design of Mooring System for a 15MW Semi-Submersible, TaidaFloat, in Taiwan Strait". In: vol. Volume 5: Ocean Engineering. International Conference on Offshore Mechanics and Arctic Engineering. June 2023, V005T06A071. DOI: 10.1115/OMAE2023-104394.

[10] R. Chitteth Ramachandran et al. "Floating wind turbines: marine operations challenges and opportunities". In: *Wind Energy Science* 7.2 (2022), pp. 903–924. DOI: 10.5194/wes-7-903-2022.

[11] A. K. Chopra. *Dynamics of Structures: Theory and Applications to Earthquake Engineering*. 4th. Harlow, England: Pearson, 2014. ISBN: 978-0132858038.

[12] A. Clayson. "Developments in Subsea Tensioning of Mooring Lines". In: vol. Day 1 Wed, February 14, 2018. SNAME Offshore Symposium. Feb. 2018, D013S004R003. eprint: https://onepetro.org/SNAMETOS/proceedings-pdf/TOS18/1-TOS18/D013S004R003/1161845/sname-tos-2018-015.pdf.

[13] A. Crowle. "Floating offshore turbines - installation methods". In: International Journal of Research GRANTHAALAYAH. Mar. 2024. DOI: https://doi.org/10.29121/granthaalayah.v12.i2.2024.5459.

[14] A. Crowle and P. Thies. "Challenges during installation of floating wind turbines". In: 5th International Conference on Offshore Renewable Energy. Aug. 2021. URL: http://hdl.handle.net/10871/126969.

[15] C. Del Vecchio et al. "Advances Towards Replacing Top Chain with Fiber Rope for Offshore Moorings: A DeepStar Study". In: vol. Day 1 Mon, May 06, 2024. OTC Offshore Technology Conference. May 2024, D011S013R001. DOI: 10.4043/35339-MS.

[16] J. Deter et al. "Boat anchoring pressure on coastal seabed: Quantification and bias estimation using AIS data". In: *Marine Pollution Bulletin* 123.1 (2017), pp. 175–181. ISSN: 0025-326X. DOI: https://doi.org/10.1016/j.marpolbul.2017.08.065.

[17] DNV. *Design, testing and analysis of offshore fibre ropes*. Tech. rep. DNV-RP-E305. DNV GL, 2019. URL: https://standards.dnv.com/explorer/document/18FB841A75F54526AD67A1747E6BCCEE/3.

[18] DNV. *Dynamic Positioning Systems - Operation Guidance*. Recommended Practice DNV-RP-E306. DNV, July 2021. URL: https://standards.dnv.com/explorer/document/72990A2C4023405DA43C92C46D02950C/6.

[19] DNV. *Marine operations and marine warranty*. Standard DNV-ST-N001. Høvik, Norway: Det Norske Veritas, 2021.

[20] Energy Sector Management Assistance Program. *Offshore Wind Technical Potential Analysis and Maps*. 2025. URL: https://www.esmap.org/esmap_offshorewind_techpotential_analysis_maps (visited on 01/03/2025).

[21] E. Falkenberg, V. Åhjem, and L. Yang. "Best Practice for Analysis of Polyester Rope Mooring Systems". In: vol. Day 3 Wed, May 03, 2017. OTC Offshore Technology Conference. May 2017, D031S034R006. DOI: 10.4043/27761-MS.

[22] G. Ferri et al. "Platform and mooring system optimization of a 10 MW semisubmersible offshore wind turbine". In: *Renewable Energy* 182 (2022), pp. 1152–1170. ISSN: 0960-1481. DOI: https://doi.org/10.1016/j.renene.2021.10.060.

[23] Ø. Gabrielsen et al. "Polyester Mooring Lines–Change-In-Length and Stiffness Properties in Operation". In: vol. All Days. International Ocean and Polar Engineering Conference. June 2023, ISOPE-I-23–153. eprint: https://onepetro.org/ISOPEIOPEC/proceedings-pdf/ISOPE23/All-ISOPE23/ISOPE-I-23-153/3165041/isope-i-23-153.pdf.

[24] H. Ghafari and M. Dardel. "Parametric study of catenary mooring system on the dynamic response of the semi-submersible platform". In: *Ocean Engineering* 153 (2018), pp. 319–332. ISSN: 0029-8018. DOI: https://doi.org/10.1016/j.oceaneng.2018.01.093.

[25] GraphPad Software. *Five ways to plot whiskers in box and whisker plots*. 2024. URL: https://www.graphpad.com/support/faq/five-ways-to-plot-whiskers-in-box-and-whisker-plots/ (visited on 12/22/2024).

[26] W. Guachamin Acero et al. "Methodology for assessment of the operational limits and operability of marine operations". In: *Ocean Engineering* 125 (2016), pp. 308–327. ISSN: 0029-8018. DOI: https://doi.org/10.1016/j.oceaneng.2016.08.015.

[27] guidetofloatingoffshorewind. *Guidetofloatingoffshorewind*. URL: https://guidetofloatingoffshorewind.com/guide/b-balance-of-plant/b-3-mooring-system/ (visited on 05/13/2024).

[28] S. Hong et al. "Floating offshore wind farm installation, challenges and opportunities: A comprehensive survey". In: *Ocean Engineering* 304 (2024), p. 117793. ISSN: 0029-8018. DOI: https://doi.org/10.1016/j.oceaneng.2024.117793.

[29] W.-t. Hsu et al. "Snap Loads on Mooring Lines of a Floating Offshore Wind Turbine Structure". In: vol. Volume 9A: Ocean Renewable Energy. International Conference on Offshore Mechanics and Arctic Engineering. June 2014, V09AT09A036. DOI: 10.1115/OMAE2014-23587.

[30] W.-H. Huang and R.-Y. Yang. "Water Depth Variation Influence on the Mooring Line Design for FOWT within Shallow Water Region". In: *Journal of Marine Science and Engineering* 9.4 (2021). ISSN: 2077-1312. URL: https://www.mdpi.com/2077-1312/9/4/409.

[31] F. Huo et al. "Study on characteristics of mooring system of a new floating offshore wind turbine in shallow water by experiment". In: *Frontiers in Energy Research* 10 (2023). ISSN: 2296-598X. DOI: 10.3389/fenrg.2022.1007996.

[32] Kongsberg Maritime. *Hydroacoustic Aided Inertial Navigation: A New Reference for DP of Vessels*. Technical Report. Accessed on 31-10-2024. Kongsberg Maritime. URL: https://www.kongsberg.com/globalassets/kongsberg-discovery/commerce/navigation--positioning/hain/hain_-a-new-reference-for-dp-of-vessels.pdf.

[33] Y. Lian et al. "Effects of Mooring Line with Different Materials on the Dynamic Response of Offshore Floating Wind Turbine". In: *Journal of Marine Science and Engineering* 11.12 (2023). ISSN: 2077-1312. DOI: 10.3390/jmse11122302.

[34] T.-H. Lin and R.-Y. Yang. "Stability Analysis and Environmental Influence Evaluation on a Hybrid Mooring System for a Floating Offshore Wind Turbine". In: *Journal of Marine Science and Engineering* 11.12 (2023). ISSN: 2077-1312. URL: https://www.mdpi.com/2077-1312/11/12/2236.

[35] Ø. H. Lund and T. S. Sjøberg. "Evaluation and Comparison of Operability and Operational Limits of Service Vessel Designs in Exposed Aquaculture". MA thesis. Norwegian University of Science and Technology, 2018. URL: https://ntnuopen.ntnu.no/ntnu-xmlui/handle/11250/2567227.

[36] K.-T. Ma et al. "Chapter 8 - Anchor selection". In: *Mooring System Engineering for Offshore Structures*. Ed. by K.-T. Ma et al. Gulf Professional Publishing, 2019, pp. 155–174. ISBN: 978-0-12-818551-3. DOI: https://doi.org/10.1016/B978-0-12-818551-3.00008-9. URL: https://www.sciencedirect.com/science/article/pii/B9780128185513000089.

[37] K.-t. Ma et al. "A Historical Review on Integrity Issues of Permanent Mooring Systems". In: vol. All Days. OTC Offshore Technology Conference. May 2013, OTC-24025–MS. DOI: 10.4043/24025-MS.

[38] K.-t. Ma et al. "Mooring Designs for Floating Offshore Wind Turbines Leveraging Experience From the Oil and Gas Industry". In: vol. Volume 1: Offshore Technology. International Conference on Offshore Mechanics and Arctic Engineering. June 2021, V001T01A031. DOI: 10.1115/OMAE2021-60739.

[39] K. Maritime. *Vessel Tensioner (VT)*. URL: https://www.kongsberg.com/maritime/products/deck-machinery-and-cranes/deck-machinery/floating-production-storage--offloading-unit-fpso/vessel-tensioner/ (visited on 06/04/2024).

[40] I. Marshall and A. Todd. "The thermal degradation of polyethylene terephthalate". In: *Transactions of the Faraday Society* 49 (1953), pp. 67–78.

[41] Mermaid Consultants. *FPSO MOORING HOOK UP PROCEDURE*. Mermaid Consultants. 2024. URL: https://www.mermaid-consultants.com/fpso-fso-hook-up-procedure.html.

[42] J. D. Miller, M. A. O'Driscoll, and M. Farrow. "Extending Anchor Handling Vessel Capabilities and the Technical Innovations that Make it Possible". In: vol. All Days. OTC Offshore Technology Conference. May 2015, OTC-26044–MS. DOI: 10.4043/26044-MS.

[43] H. Moideen et al. "Design Considerations for Polyester Construction Stretch Removal and its Impact on Mooring System Design". In: vol. Day 3 Wed, August 18, 2021. OTC Offshore Technology Conference. Aug. 2021, D031S034R003. DOI: 10.4043/31171-MS.

[44] OpenStax. *University Physics I: Mechanics, Sound, Oscillations, and Waves*. Accessed: 2025-01-06. OpenStax, 2020. URL: https://phys.libretexts.org/Bookshelves/University_Physics/University_Physics_%28OpenStax%29/Book%3A_University_Physics_I_-_Mechanics_Sound_Oscillations_and_Waves_%28OpenStax%29/05%3A_Newton%27s_Laws_of_Motion.

[45] Orcina Ltd. *Dynamic Analysis: Frequency Domain Solution*. Orcina Ltd. 2024. URL: https://www.orcina.com/webhelp/OrcaFlex/Content/html/Dynamicanalysis,Frequencydomainsolution.htm (visited on 11/18/2024).

[46] Orcina Ltd. *Dynamic analysis: Time domain solution*. Orcina Ltd. 2024. URL: https://www.orcina.com/webhelp/OrcaFlex/Content/html/Dynamicanalysis,Timedomainsolution.htm (visited on 11/19/2024).

[47] Orcina Ltd. *General Data: Analysis*. Orcina. 2024. URL: https://www.orcina.com/webhelp/OrcaFlex/Content/html/Generaldata,Analysis.htm (visited on 11/15/2024).

[48] Orcina Ltd. *OrcaFlex validation*. Orcina Ltd. 2024. URL: https://www.orcina.com/resources/validation/ (visited on 11/27/2024).

[49] Orcina Ltd. *Use of diffraction analysis data*. Orcina. 2024. URL: https://www.orcina.com/webhelp/OrcaFlex/Content/html/Useofdiffractionanalysisdata.htm (visited on 11/15/2024).

[50] Orcina Ltd. *Vessel types: Multibody data*. Orcina Ltd. 2024. URL: https://www.orcina.com/webhelp/OrcaFlex/Content/html/Vesseltypes,Multibodydata.htm.

[51] Orcina Ltd. *Vessel types: RAOs*. Orcina Ltd. 2024. URL: https://www.orcina.com/webhelp/OrcaFlex/Content/html/Vesseltypes,RAOs.htm (visited on 11/13/2024).

[52] Orcina Ltd. *Winches*. Orcina Ltd. 2024. URL: https://www.orcina.com/webhelp/OrcaFlex/Content/html/Winches.htm.

[53] Otto Candies, LLC. *M/V Wyatt Candies*. 2024. URL: https://ottocandies.com/us-flagged/dive-support-vessels/mv-wyatt-candies/.

[54] A. Pillai et al. "Anchor loads for shallow water mooring of a 15 MW floating wind turbine—Part II: Synthetic and novel mooring systems". In: *Ocean Engineering* 266 (2022), p. 112619. ISSN: 0029-8018. DOI: https://doi.org/10.1016/j.oceaneng.2022.112619.

[55] R. G. Sargent. "Verification and validation of simulation models". In: *Proceedings of the 2010 Winter Simulation Conference*. 2010, pp. 166–183. DOI: 10.1109/WSC.2010.5679166.

[56] J. Serraris and J. Cozijn. "DP Stationkeeping Accuracy: a Calculation Approach, Integration in DP plots and Results of a Case Study". In: *Dynamic Positioning Conference*. Marine Technology Society. Houston, Oct. 2017. URL: https://dynamic-positioning.com/proceedings/dp2017/Performance%20-%20Cozjin%20-%20paper.pdf.

[57] Sinay. *Offshore vs. Floating: Key Differences in Energy Infrastructure*. 2024. URL: %5Curl%7Bhttps://sinay.ai/en/offshore-vs-floating-understanding-the-key-differences-in-energy-infrastructure/%7D (visited on 12/02/2024).

[58] B. Singh. *Features, Applications, and Limitations of Anchor Handling Tug Supply Vessels (AHTS)*. URL: https://www.marineinsight.com/types-of-ships/features-applications-and-limitations-of-anchor-handling-tug-supply-vessels-ahts/ (visited on 03/19/2019).

[59] R. Singh. "Chapter Six - Offshore Structures". In: *Corrosion Control for Offshore Structures*. Ed. by R. Singh. Boston: Gulf Professional Publishing, 2014, pp. 57–88. ISBN: 978-0-12-404615-3. DOI: https://doi.org/10.1016/B978-0-12-404615-3.00006-1. URL: https://www.sciencedirect.com/science/article/pii/B9780124046153000061.

[60] T. Stenlund. "Mooring System Design for a Large Floating Wind Turbine in Shallow Water PROJECT THESIS IN MARINE TECHNOLOGY SPRING 2018 FOR STUD.TECHN. Tiril Stenlund Mooring system design for a large floating wind turbine in shallow water". MA thesis. Norwegian University of Science and Technology, 2018. URL: https://ntnuopen.ntnu.no/ntnu-xmlui/handle/11250/2564461.

[61] V. Sykes, M. Collu, and A. Coraddu. "A Review and Analysis of the Uncertainty Within Cost Models for Floating Offshore Wind Farms". In: *Renewable and Sustainable Energy Reviews* 186 (2023), p. 113634. ISSN: 1364-0321. DOI: https://doi.org/10.1016/j.rser.2023.113634.

[62] F. Tech. *BTC Kraken and Mariner: Case Study*. 2024. URL: https://flint-tech.com/case-studies/btc-kraken-and-mariner/ (visited on 12/11/2024).

[63] TU Delft open course ware. *Validation & Verification*. PowerPoint Slides. URL: https://ocw.tudelft.nl/wp-content/uploads/Validation-verification.pdf.

[64] Vicinay Connectors. *Embedded Payedy*. Vicinay Connectors. 2021. URL: https://vicinayconnectors.com/product/embedded-payedy/ (visited on 12/06/2024).

[65] Vicinay Connectors. *Rope to Chain*. Vicinay Connectors. 2021. URL: https://vicinayconnectors.com/product/rope-to-chain/ (visited on 12/06/2024).

[66] J. C. Ward et al. "Comparison of FEED Level Design and Performance of Chain Catenary and Synthetic Mooring Systems for a 10+ MW Floating Offshore Wind Turbine". In: vol. Day 3 Wed, May 08, 2024. OTC Offshore Technology Conference. May 2024, D031S002R005. DOI: 10.4043/35194-MS.

[67] C. M. Webb and M. v. Vugt. "Offshore Construction – Installing the World's Deepest FPSO Development". In: vol. Day 2 Tue, May 02, 2017. OTC Offshore Technology Conference. May 2017, D021S025R002. DOI: 10.4043/27655-MS.

[68] S. Weller et al. "Synthetic mooring ropes for marine renewable energy applications". In: *Renewable Energy* 83 (2015), pp. 1268–1278. ISSN: 0960-1481. DOI: https://doi.org/10.1016/j.renene.2015.03.058.

[69] Y. Wu et al. "Mooring Tensioning Systems for Offshore Platforms: Design, Installation, and Operating Considerations". In: vol. Day 1 Mon, April 30, 2018. OTC Offshore Technology Conference. Apr. 2018, D011S004R004. DOI: 10.4043/28720-MS.

[70] K. Xu et al. "Design and comparative analysis of alternative mooring systems for floating wind turbines in shallow water with emphasis on ultimate limit state design". In: *Ocean Engineering* 219 (2021), p. 108377. ISSN: 0029-8018. DOI: https://doi.org/10.1016/j.oceaneng.2020.108377.

[71] S. Xu. "Mooring Design and Analysis for Offshore Platforms and Wave Energy Converters". PhD thesis. UNIVERSIDADE DE LISBOA INSTITUTO SUPERIOR TÉCNICO, Sept. 2021.

[72] Z.-M. Yuan, A. Incecik, and C. Ji. "Numerical study on a hybrid mooring system with clump weights and buoys". In: *Ocean Engineering* 88 (2014), pp. 1–11. ISSN: 0029-8018. DOI: https://doi.org/10.1016/j.oceaneng.2014.06.002.

A

Results of load cases for UTC effective tension

The results of the maximum tension in the UTC for the load cases described in Section 4.3.2 are presented in Section A.1, with range graphs of the tension along the UTC presented in Section A.2.

A.1. Maximum effective tension

Case 1

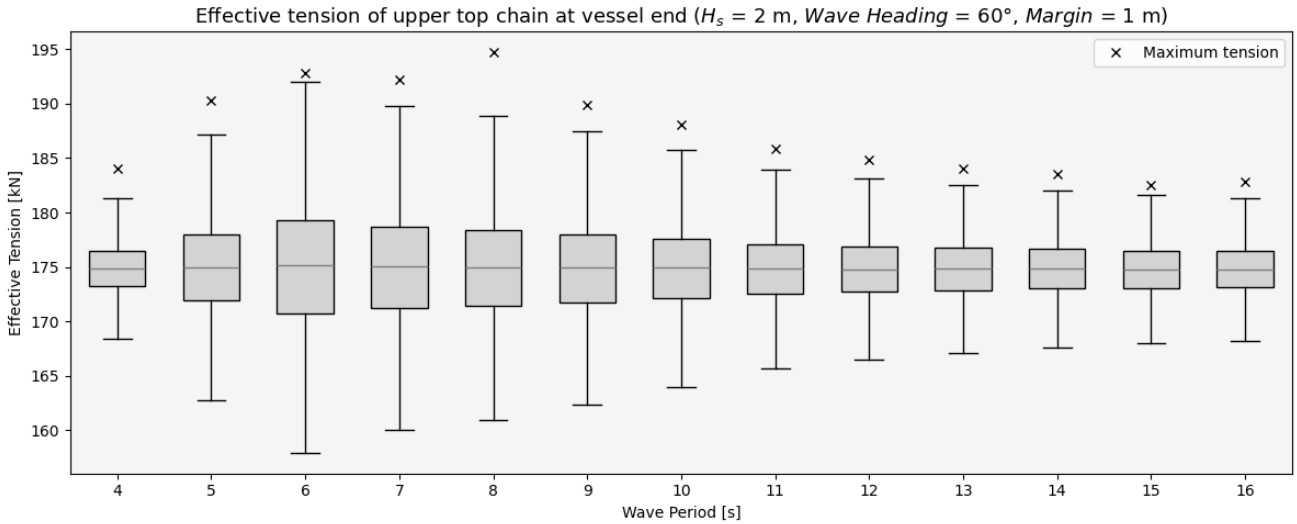

Figure A.1: Effective tension at the vessel end of the UTC, with a starting distance of 20 metres, a margin of 1 metre, an UTC length of 32.4 metres and a connection to the floater at the bottom

Case 2

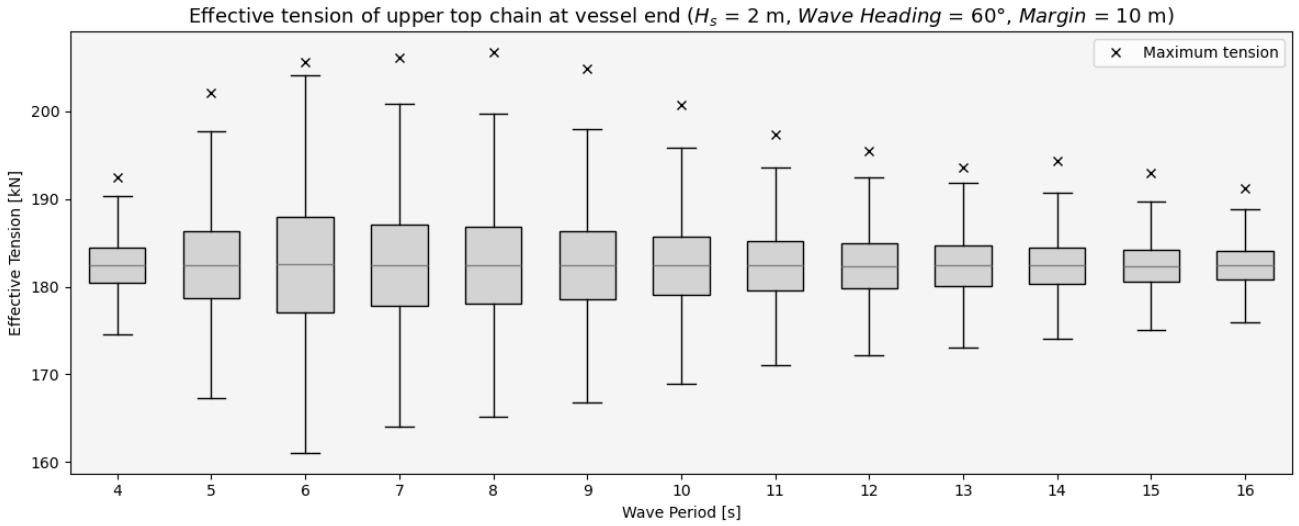

Figure A.2: Effective tension at the vessel end of the UTC, with a starting distance of 20 metres, a margin of 10 metres, an UTC length of 39.3 metres and a connection to the floater at the bottom

Case 3

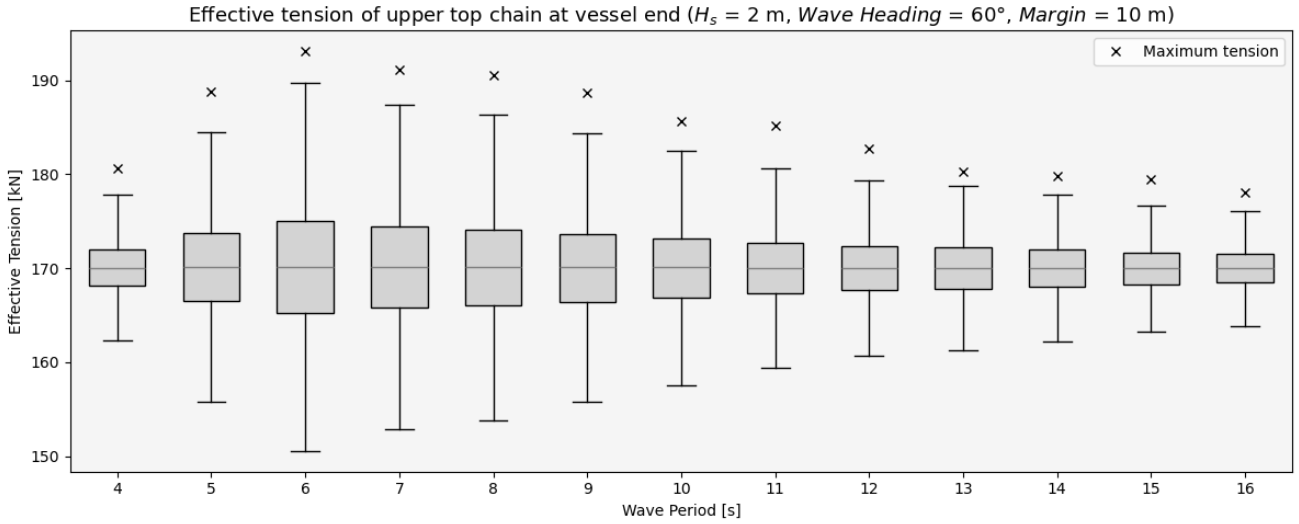

Figure A.3: Effective tension at the vessel end of the UTC, with a starting distance of 15 metres, a margin of 10 metres, an UTC length of 35.4 metres and a connection to the floater at the bottom

Case 4

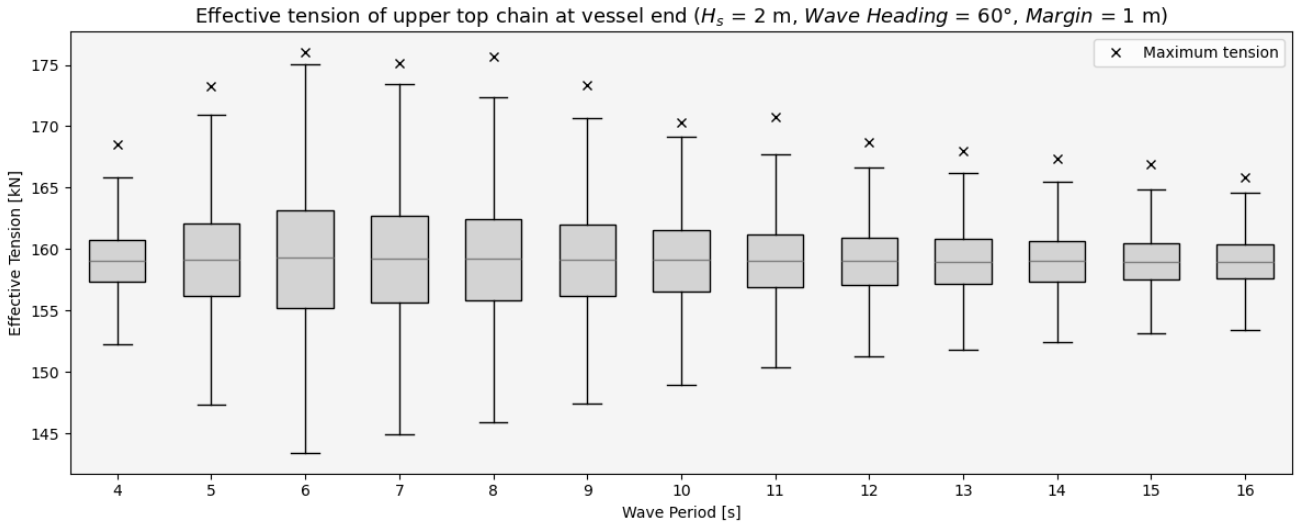

Figure A.4: Effective tension at the vessel end of the UTC, with a starting distance of 15 metres, a margin of 1 metre, an UTC length of 29.1 metres and a connection to the floater at the bottom

Case 5

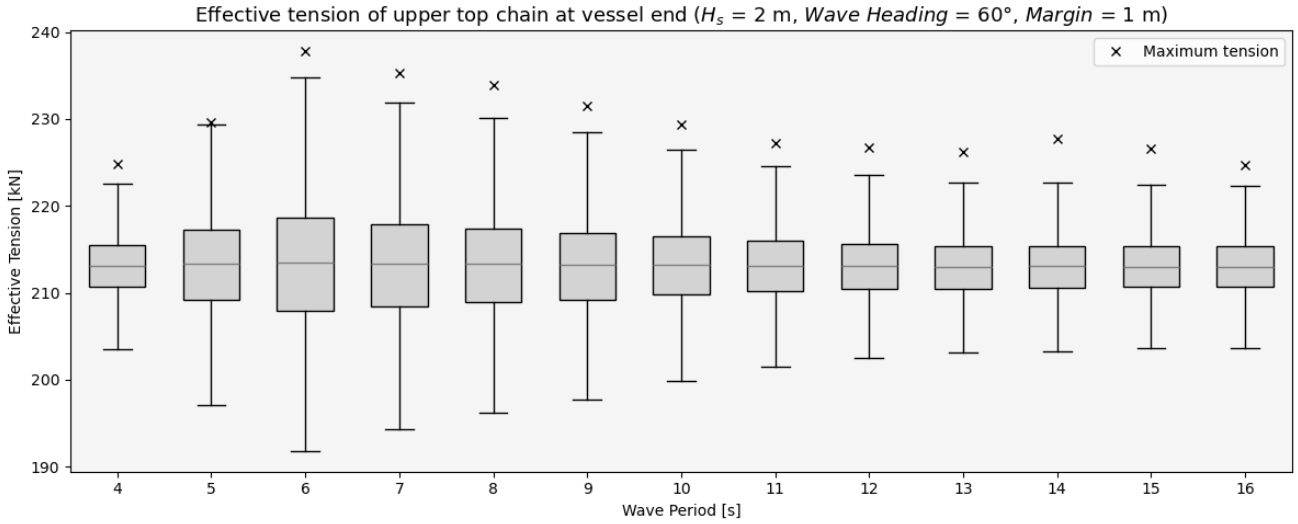

Figure A.5: Effective tension at the vessel end of the UTC, with a starting distance of 30 metres, a margin of 1 metre, an UTC length of 40.1 metres and a connection to the floater at the bottom

Case 6

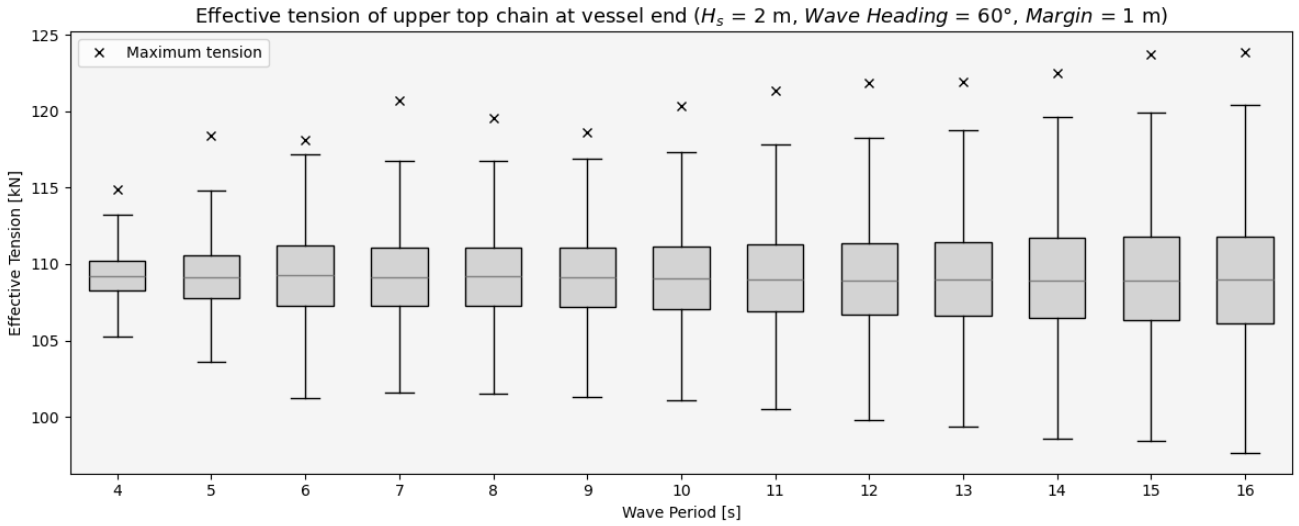

Figure A.6: Effective tension at the vessel end of the UTC, with a starting distance of 20 metres, a margin of 1 metre, an UTC length of 23.4 metres and a connection to the floater at the same height as the connection to the vessel

Case 7.1

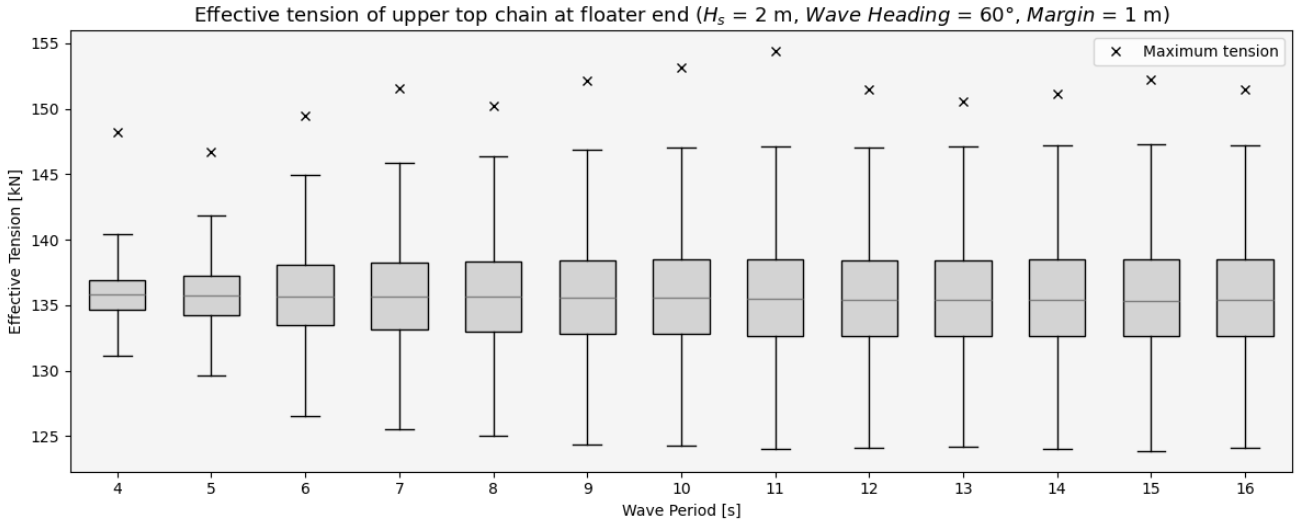

Figure A.7: Effective tension at the floater end of the UTC, with a starting distance of 20 metres, a margin of 1 metre, an UTC length of 28.5 metres and a connection to the floater at the top

Case 7.2 with adjusted chain length per T_p value

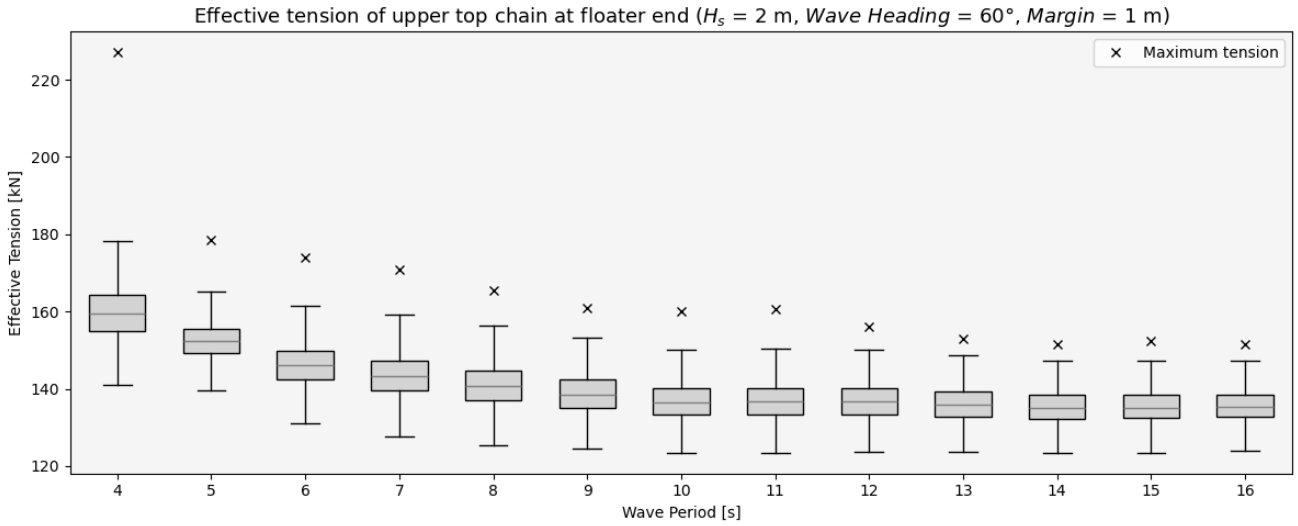

Figure A.8: Effective tension at the floater end of the UTC, with a starting distance of 20 metres, a margin of 1 metre and a connection to the floater at the top, with varying chain length per T_p

Case 8

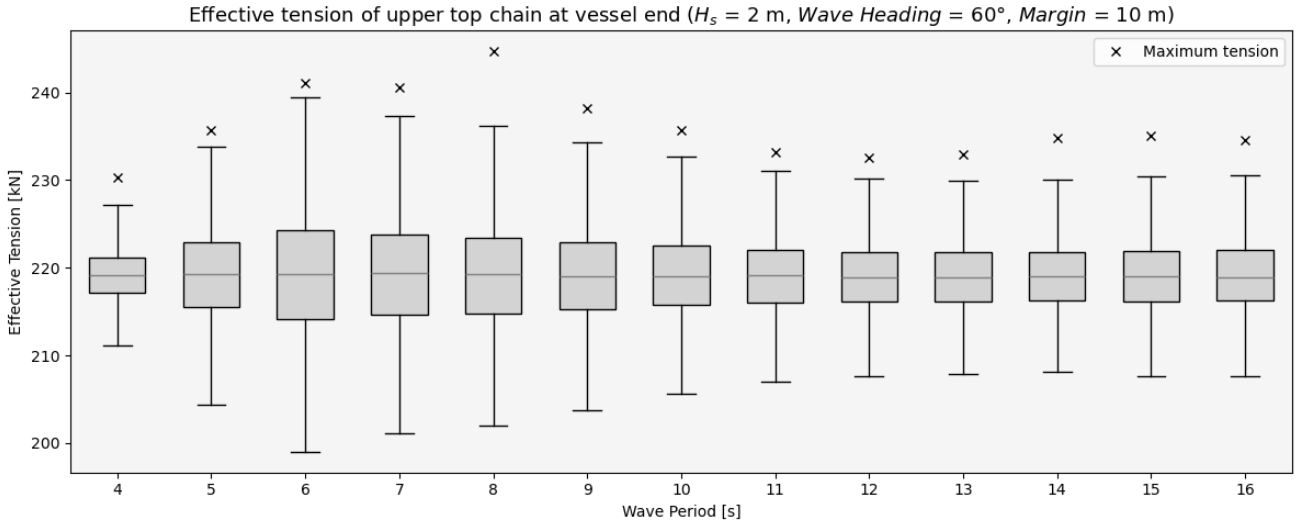

Figure A.9: Effective tension at the vessel end of the UTC, with a connection to the floater at the bottom and a margin of 10 added to both the UTC length and the starting distance, resulting in a starting distance of 30 metres and an UTC length of 39.3 metres

Case 9

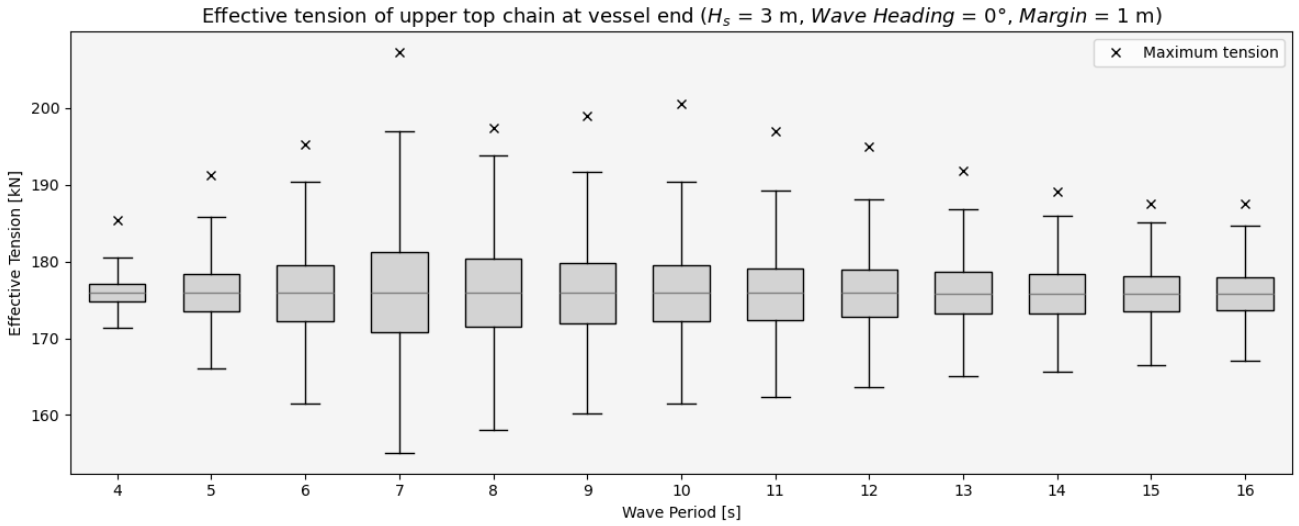

Figure A.10: Effective tension at the vessel end of the UTC, with a starting distance of 20 metres, a margin of 1 metre, an UTC length of 35.9 metres and a connection to the floater at the bottom

Case 10

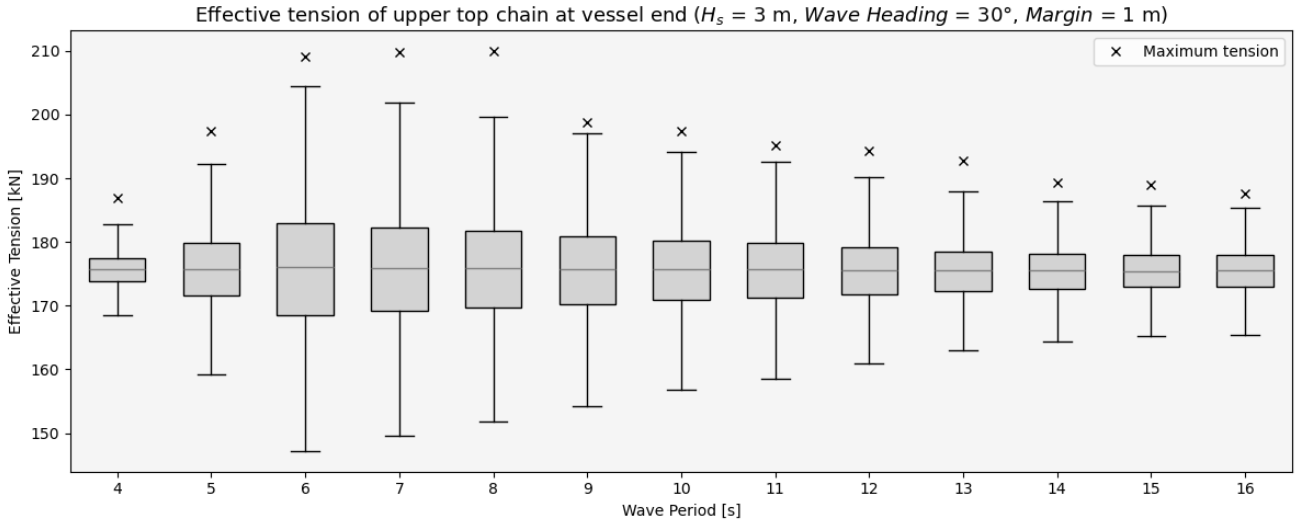

Figure A.11: Effective tension at the vessel end of the UTC, with a starting distance of 20 metres, a margin of 1 metre, an UTC length of 35.5 metres and a connection to the floater at the bottom

Case 11

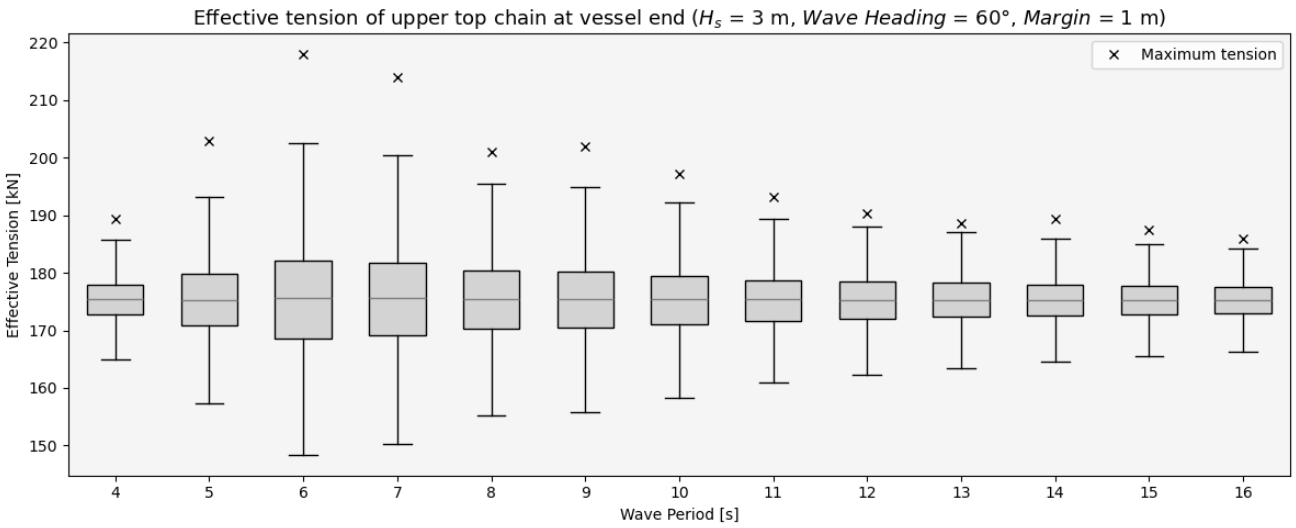

Figure A.12: Effective tension at the vessel end of the UTC, with a starting distance of 20 metres, a margin of 1 metre, an UTC length of 34.4 metres and a connection to the floater at the bottom

A.2. Range graph of effective tension

Top connection height

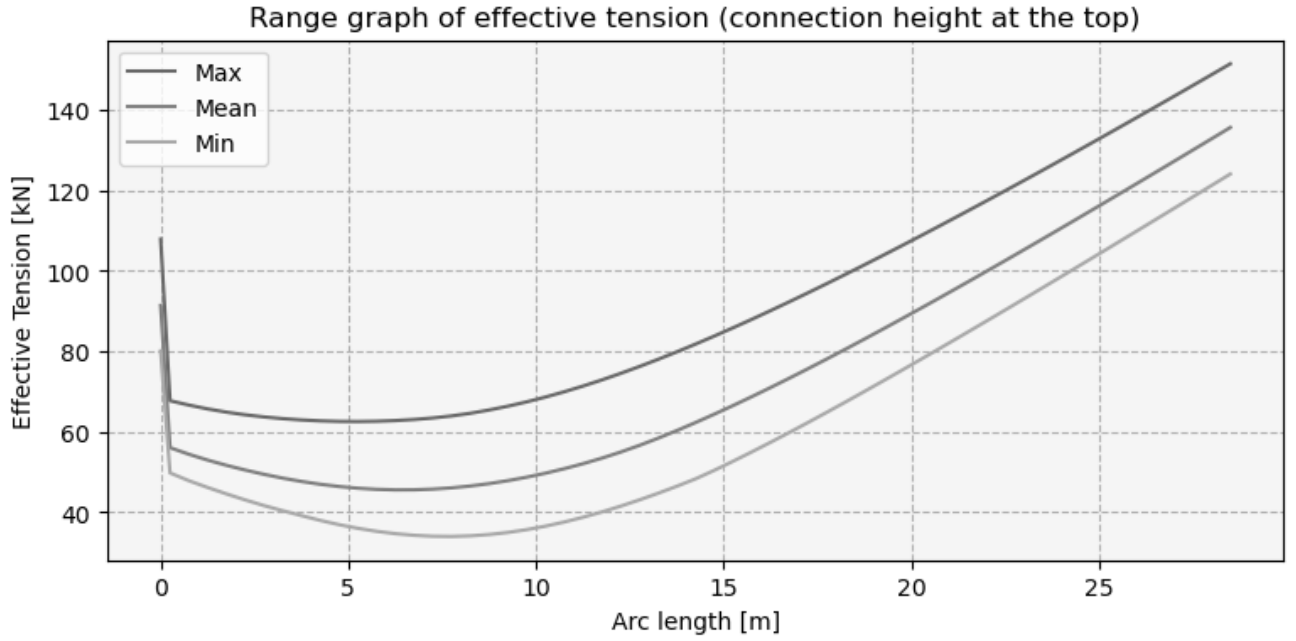

Figure A.13: Range graph of the effective tension along the UTC, with vessel end on the left and floater end on the right (connection height at the top), for Case 7.1

Middle connection height

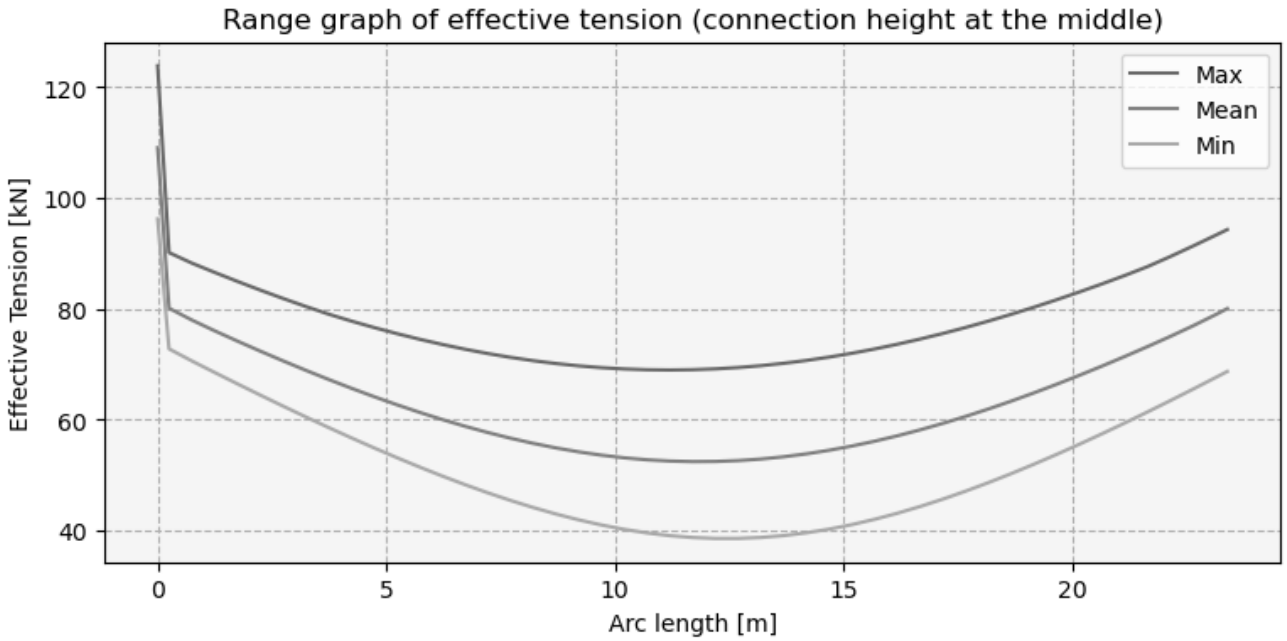

Figure A.14: Range graph of the effective tension along the UTC, with vessel end on the left and floater end on the right (connection height at the middle), for Case 6

Bottom connection height

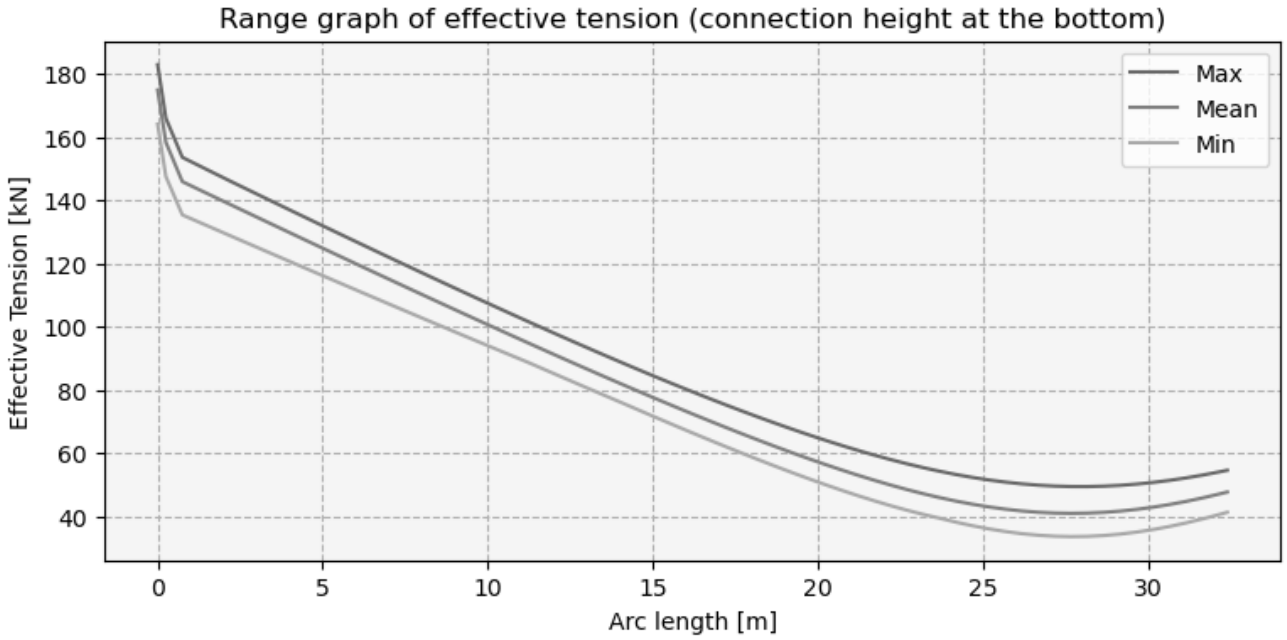

Figure A.15: Range graph of the effective tension along the UTC, with vessel end on the left and floater end on the right (connection height at the bottom), for Case 1

B

UTC length results

The table in this appendix presents the UTC length results, calculated according to the proposed approach, for all combinations of the described sea states, along with the lower and upper margins, for AHTS 1.

Table B.1: Upper top chain length for all considered combinations of sea states and both the lower and upper limit margin, for AHTS 1 and a connection to the FOWT at the bottom

Wave Heading [°]	Hs [m]	Margin [m]	4	5	6	7	8	9	10	11	12	13	14	15	16
0	2	1	28.8	29.1	29.8	30.5	31.1	31.6	32.1	32.4	32.7	32.9	33.1	33.3	33.5
		10	35.9	36.2	36.8	37.4	38.0	38.5	39.0	39.3	39.6	39.9	40.1	40.3	40.5
	2.5	1	28.9	29.3	30.0	31.0	31.7	32.4	32.9	33.3	33.7	34.0	34.2	34.4	34.7
		10	36.0	36.3	37.0	37.9	38.6	39.2	39.8	40.2	40.6	40.9	41.1	41.4	41.7
	3	1	28.9	29.4	30.2	31.6	32.5	33.1	33.8	34.3	34.7	35.0	35.3	35.6	35.9
		10	36.0	36.4	37.2	38.4	39.3	39.9	40.6	41.1	41.6	41.9	42.2	42.5	42.9
	3.5	1	28.9	29.5	30.5	32.1	33.3	34.0	34.6	35.2	35.7	36.1	36.4	36.8	37.2
		10	36.0	36.5	37.4	38.9	40.0	40.7	41.4	42.0	42.5	43.0	43.3	43.7	44.1
30	2	1	28.9	29.4	30.2	30.7	31.3	31.7	32.0	32.3	32.5	32.7	32.8	33.0	33.2
		10	36.0	36.4	37.1	37.7	38.1	38.5	38.9	39.2	39.4	39.6	39.8	40.0	40.2
	2.5	1	28.9	29.6	30.6	31.4	31.9	32.4	32.8	33.2	33.5	33.7	33.9	34.1	34.4
		10	36.0	36.6	37.5	38.2	38.7	39.3	39.7	40.0	40.3	40.6	40.8	41.1	41.3
	3	1	29.0	29.7	31.1	32.1	32.7	33.2	33.7	34.1	34.5	34.7	35.0	35.2	35.5
		10	36.1	36.7	37.9	38.8	39.5	40.0	40.5	40.9	41.3	41.6	41.9	42.1	42.5
	3.5	1	29.1	29.9	31.5	32.7	33.5	34.0	34.6	35.0	35.4	35.8	36.0	36.3	36.7
		10	36.1	36.9	38.3	39.4	40.2	40.8	41.3	41.8	42.2	42.6	42.9	43.2	43.6
60	2	1	29.0	29.6	30.3	30.7	31.0	31.3	31.5	31.7	31.9	32.0	32.1	32.2	32.4
		10	36.1	36.6	37.2	37.5	37.9	38.2	38.4	38.6	38.8	38.9	39.0	39.2	39.3
	2.5	1	29.1	29.8	30.8	31.3	31.6	32.0	32.3	32.5	32.7	32.8	33.0	33.2	33.4
		10	36.2	36.8	37.6	38.1	38.4	38.8	39.1	39.3	39.5	39.7	39.9	40.1	40.3
	3	1	29.2	30.1	31.3	31.9	32.3	32.7	33.0	33.3	33.5	33.7	33.9	34.1	34.4
		10	36.2	37.0	38.0	38.7	39.1	39.4	39.8	40.1	40.3	40.6	40.8	41.0	41.2
	3.5	1	29.3	30.3	31.7	32.6	33.1	33.4	33.8	34.1	34.4	34.6	34.8	35.1	35.4
		10	36.3	37.2	38.5	39.3	39.7	40.1	40.5	40.9	41.2	41.4	41.7	41.9	42.2
90	2	1	29.1	30.1	30.8	30.9	31.1	31.2	31.3	31.4	31.4	31.5	31.6	31.6	31.8
		10	36.2	37.0	37.6	37.7	37.9	38.0	38.1	38.2	38.3	38.4	38.4	38.5	38.7
	2.5	1	29.3	30.5	31.5	31.6	31.7	31.9	32.0	32.1	32.2	32.3	32.3	32.5	32.6
		10	36.3	37.3	38.2	38.4	38.5	38.6	38.8	38.9	39.0	39.1	39.2	39.3	39.5
	3	1	29.4	30.8	32.2	32.3	32.4	32.5	32.7	32.8	32.9	33.0	33.1	33.3	33.5
		10	36.4	37.6	38.8	39.0	39.1	39.3	39.4	39.6	39.7	39.8	39.9	40.1	40.3
	3.5	1	29.5	31.2	32.8	33.0	33.1	33.2	33.4	33.6	33.7	33.8	34.0	34.1	34.4
		10	36.5	38.0	39.4	39.6	39.7	39.9	40.1	40.3	40.4	40.6	40.7	40.9	41.2

120	**2**	**1**	29.1	30.0	30.7	31.0	31.3	31.5	31.7	31.8	32.0	32.1	32.2	32.3	32.4
		10	36.2	36.9	37.6	37.9	38.1	38.4	38.6	38.7	38.9	39.0	39.1	39.2	39.4
	2.5	**1**	29.2	30.3	31.4	31.7	32.0	32.3	32.5	32.7	32.8	33.0	33.1	33.2	33.4
		10	36.3	37.2	38.2	38.5	38.8	39.1	39.3	39.5	39.7	39.8	40.0	40.1	40.3
	3	**1**	29.4	30.6	32.0	32.5	32.7	33.0	33.3	33.5	33.7	33.9	34.0	34.2	34.4
		10	36.4	37.5	38.7	39.2	39.5	39.7	40.0	40.3	40.5	40.7	40.9	41.1	41.3
	3.5	**1**	29.5	31.0	32.6	33.3	33.5	33.8	34.1	34.4	34.6	34.8	35.0	35.2	35.5
		10	36.5	37.8	39.3	39.9	40.2	40.5	40.8	41.1	41.3	41.6	41.8	42.0	42.3
150	**2**	**1**	29.0	29.7	30.6	31.1	31.5	31.9	32.2	32.4	32.6	32.8	32.9	33.1	33.3
		10	36.1	36.7	37.5	38.0	38.4	38.8	39.1	39.3	39.5	39.7	39.9	40.0	40.2
	2.5	**1**	29.1	30.0	31.2	31.9	32.3	32.7	33.1	33.4	33.6	33.8	34.0	34.2	34.4
		10	36.2	37.0	38.0	38.6	39.1	39.5	39.9	40.2	40.5	40.7	40.9	41.1	41.4
	3	**1**	29.2	30.3	31.8	32.6	33.1	33.6	34.0	34.4	34.6	34.9	35.1	35.3	35.6
		10	36.3	37.2	38.5	39.3	39.8	40.3	40.8	41.1	41.5	41.7	42.0	42.2	42.5
	3.5	**1**	29.3	30.6	32.3	33.4	34.0	34.5	34.9	35.3	35.7	35.9	36.2	36.5	36.8
		10	36.4	37.4	39.0	40.1	40.6	41.1	41.6	42.1	42.4	42.8	43.0	43.4	43.7
180	**2**	**1**	29.0	29.7	30.3	30.9	31.4	31.9	32.3	32.6	32.8	33.0	33.2	33.4	33.6
		10	36.1	36.6	37.2	37.8	38.3	38.8	39.1	39.5	39.7	39.9	40.1	40.3	40.5
	2.5	**1**	29.1	29.9	30.8	31.6	32.1	32.7	33.2	33.6	33.9	34.1	34.3	34.5	34.8
		10	36.2	36.9	37.6	38.4	39.0	39.5	40.0	40.4	40.7	41.0	41.2	41.5	41.8
	3	**1**	29.2	30.2	31.2	32.2	33.0	33.6	34.1	34.5	34.9	35.2	35.5	35.7	36.0
		10	36.3	37.1	38.0	39.0	39.7	40.3	40.9	41.3	41.7	42.1	42.4	42.6	43.0
	3.5	**1**	29.3	30.4	31.6	32.9	33.8	34.4	35.0	35.5	36.0	36.3	36.6	36.9	37.3
		10	36.4	37.3	38.4	39.6	40.5	41.1	41.7	42.3	42.7	43.1	43.5	43.8	44.2

C RAOs

C.1. Rotational RAOs of AHTS 1

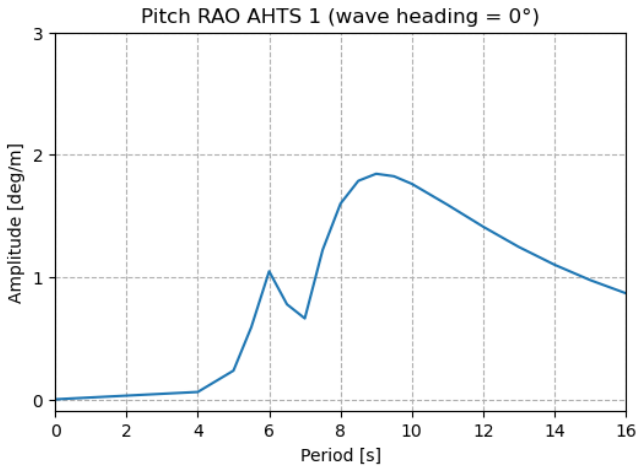

Figure C.1: Pitch RAO of AHTS 1 for a wave heading of 0 degrees

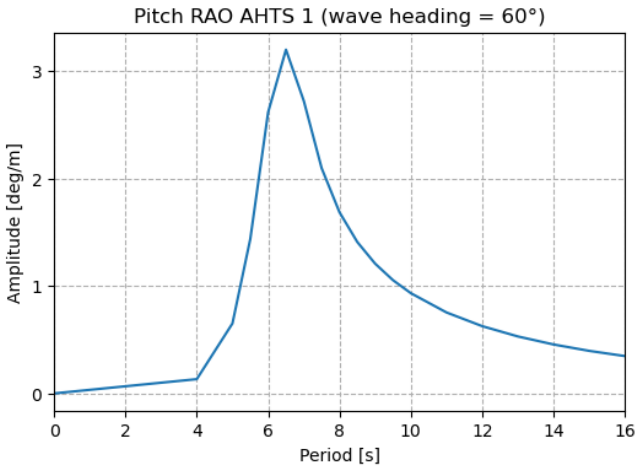

Figure C.2: Pitch RAO of AHTS 1 for a wave heading of 60 degrees

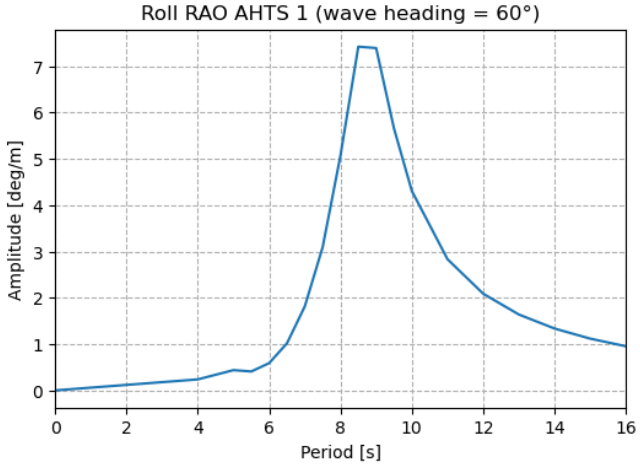

Figure C.3: Roll RAO of AHTS 1 for a wave heading of 60 degrees

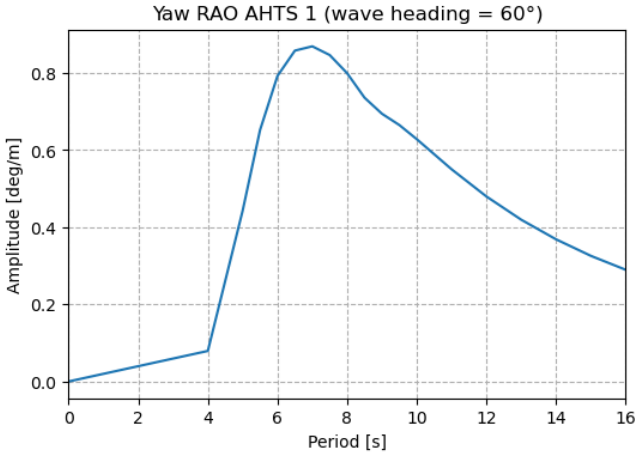

Figure C.4: Yaw RAO of AHTS 1 for a wave heading of 60 degrees

C.2. Translational RAOs of AHTS 1

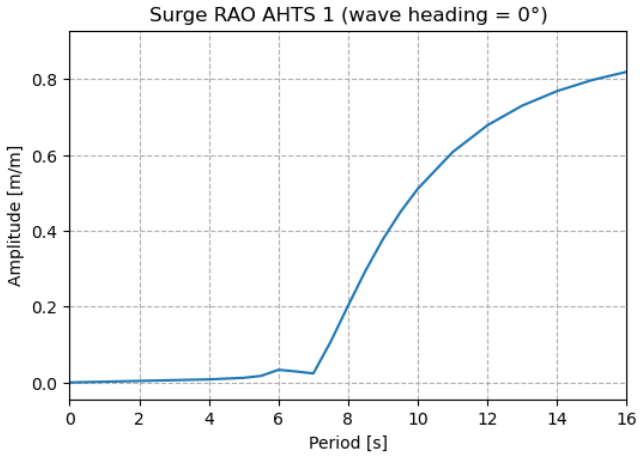

Figure C.5: Surge RAO of AHTS 1 for a wave heading of 0 degrees

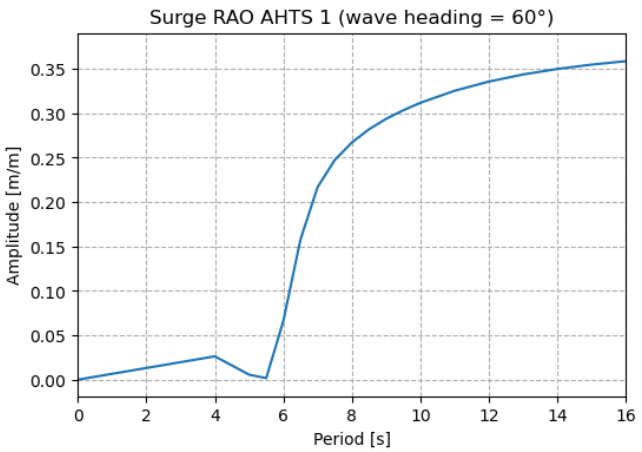

Figure C.6: Surge RAO of AHTS 1 for a wave heading of 60 degrees

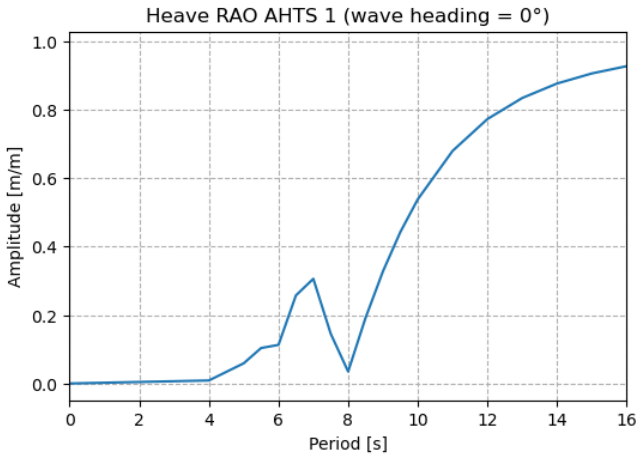

Figure C.7: Heave RAO of AHTS 1 for a wave heading of 0 degrees

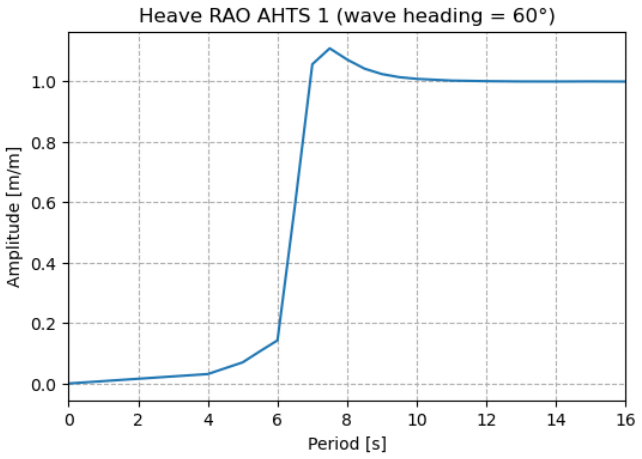

Figure C.8: Heave RAO of AHTS 1 for a wave heading of 60 degrees

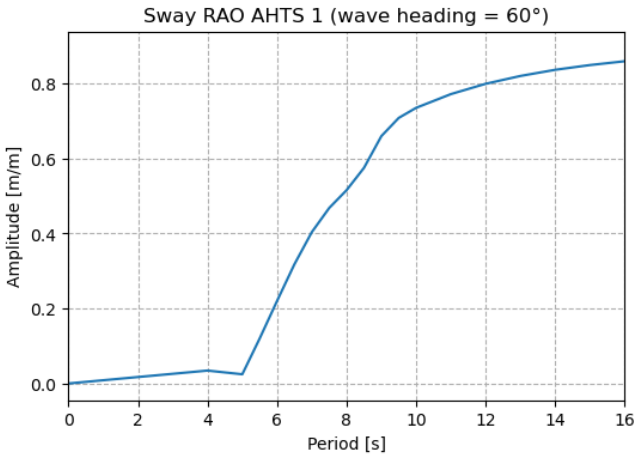

Figure C.9: Sway RAO of AHTS 1 for a wave heading of 60 degrees

C.3. Rotational RAOs of the FOWT

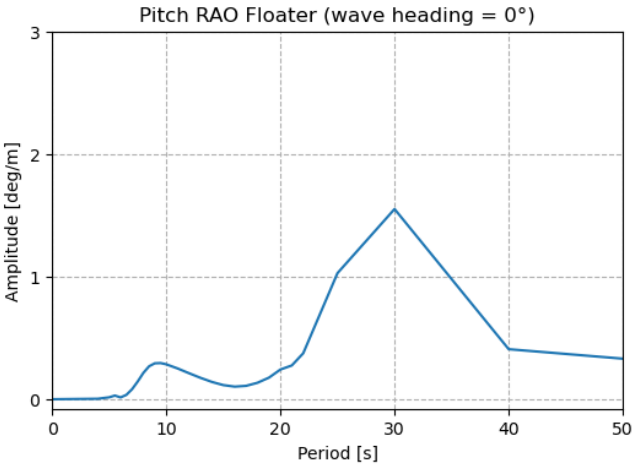

Figure C.10: Pitch RAO of FOWT for a wave heading of 0 degrees

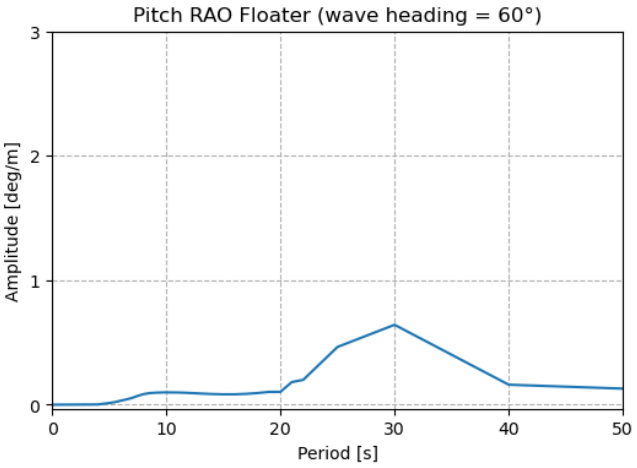

Figure C.11: Pitch RAO of FOWT for a wave heading of 60 degrees

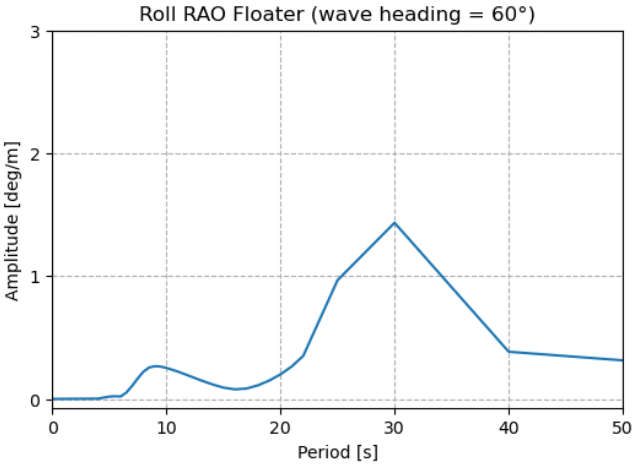

Figure C.12: Roll RAO of FOWT for a wave heading of 60 degrees

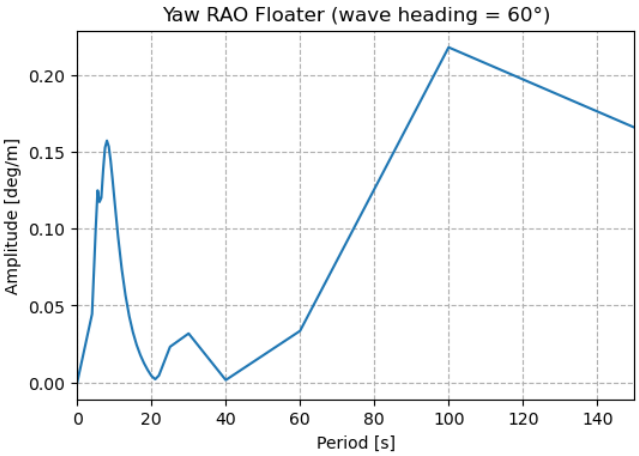

Figure C.13: Yaw RAO of FOWT for a wave heading of 60 degrees

C.4. Translational RAOs of the FOWT

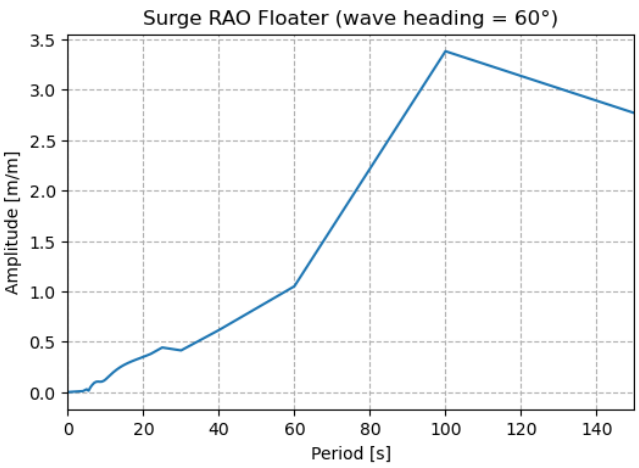

Figure C.14: Surge RAO of FOWT for a wave heading of 60 degrees

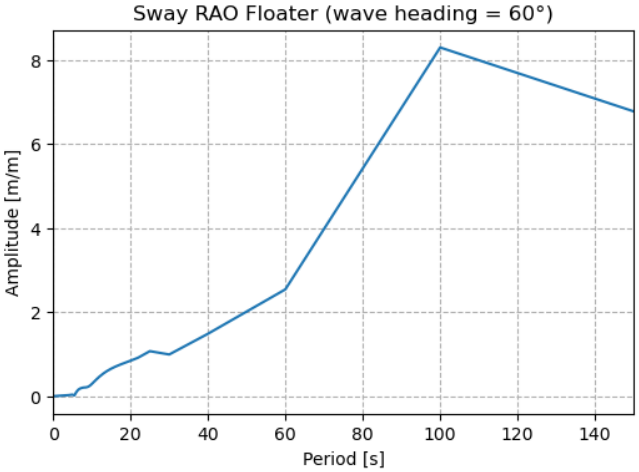

Figure C.15: Sway RAO of FOWT for a wave heading of 60 degrees

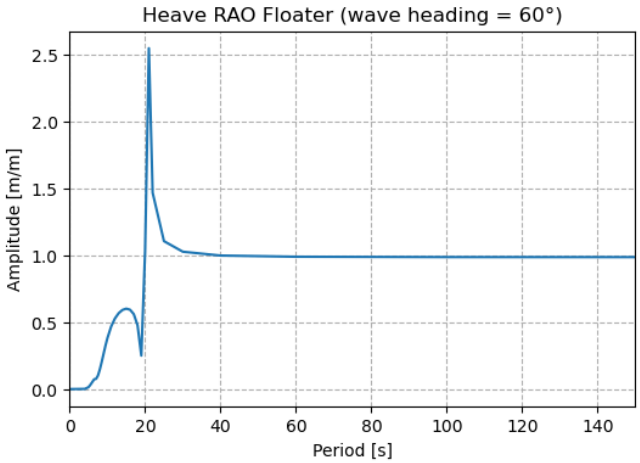

Figure C.16: Heave RAO of FOWT for a wave heading of 60 degrees

D

AHTS positioning during hook-up operation

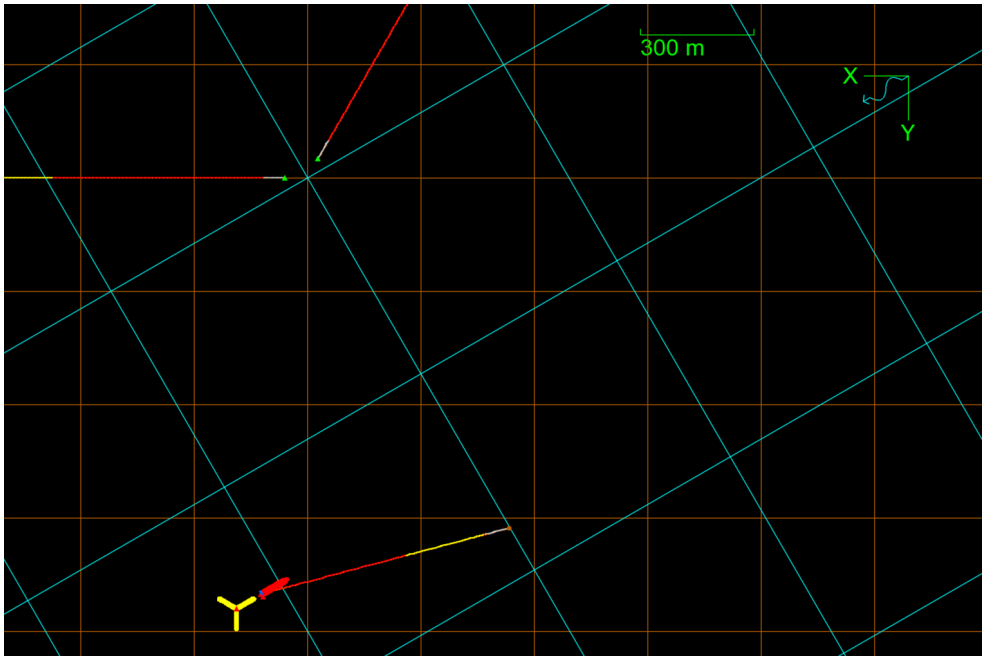

Figure D.1: Example of positioning flexibility for the first connected line, with the wave direction indicated in the top right corner

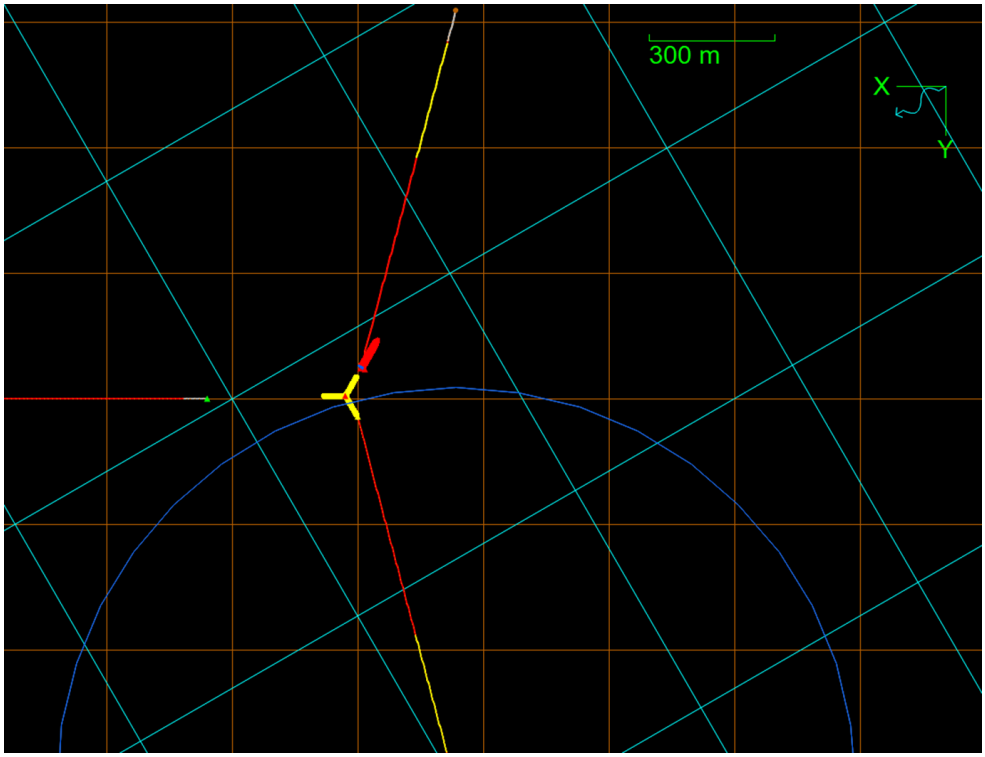

Figure D.2: Positioning restrictions caused by the first mooring line already connected, with the blue circle representing its stretch length

E

Tow line tension

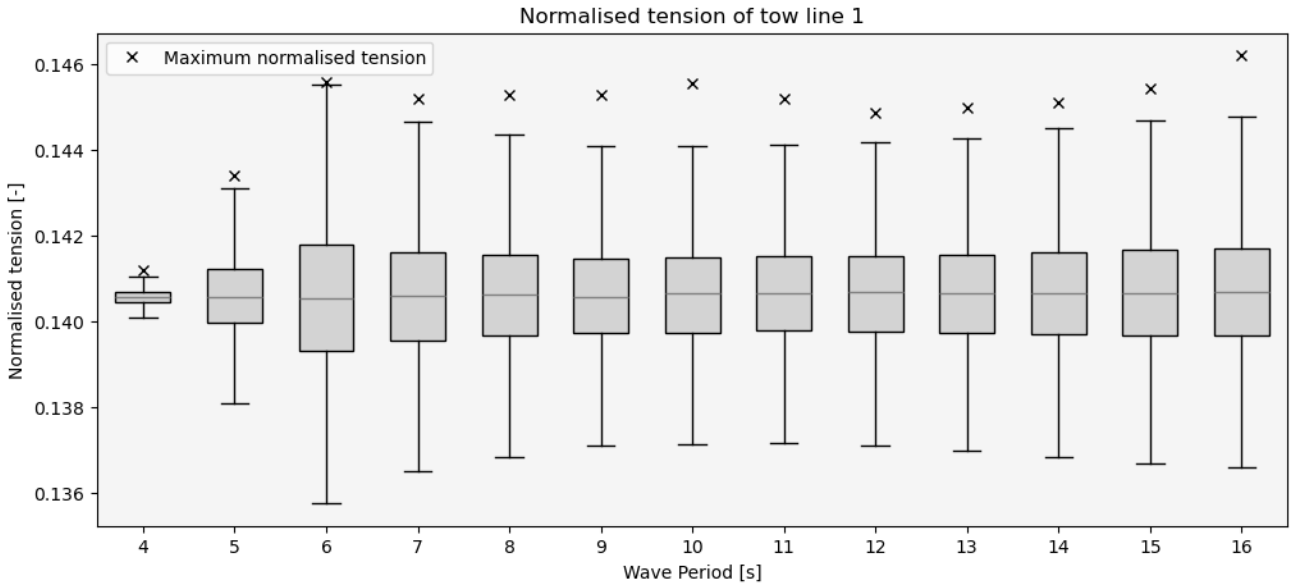

Figure E.1: Normalised tension of tow line 1 for H_s = 2 m, wave heading = 60° and a range of T_p values

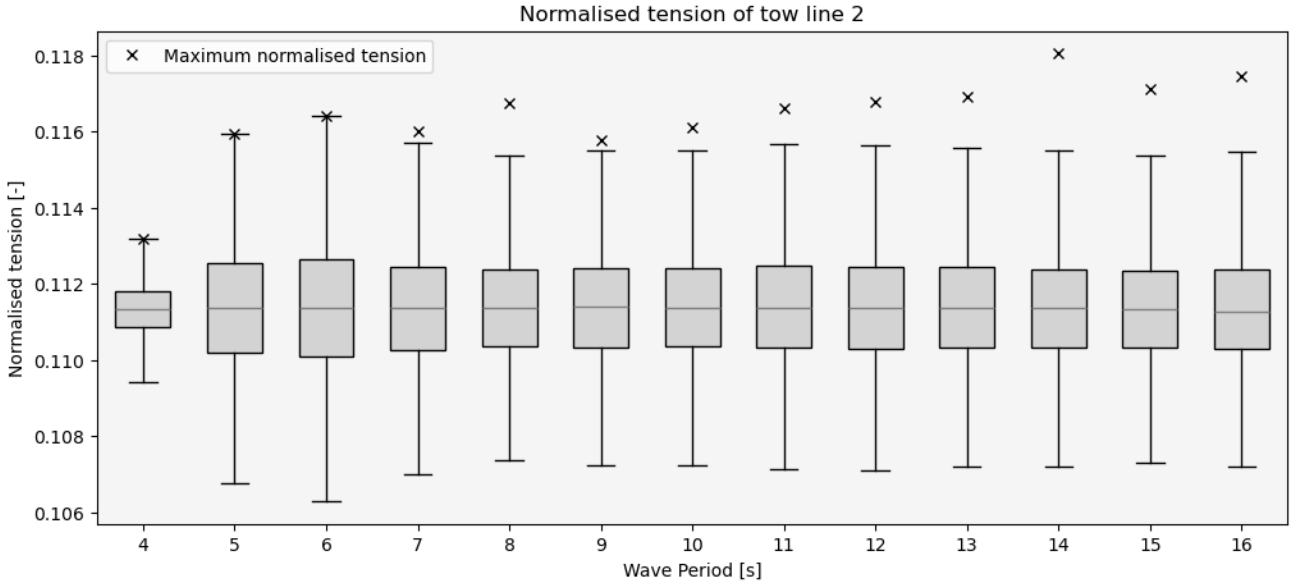

Figure E.2: Normalised tension of tow line 2 for H_s = 2 m, wave heading = 60° and a range of T_p values